12-1999

Enhancement of the properties of polymer blends by hydrogen bonding and transesterification

Bijan Radmard

To the Graduate Council:

I am submitting herewith a dissertation written by Bijan Radmard entitled "Enhancement of the properties of polymer blends by hydrogen bonding and transesterification." I have examined the final electronic copy of this dissertation for form and content and recommend that it be accepted in partial fulfillment of the requirements for the degree of Doctor of Philosophy, with a major in Chemistry.

Mark D. Dadmun, Major Professor

We have read this dissertation and recommend its acceptance:

Roberto S. Benson, Spiro D. Alexandratos, Jeff D. Kovac

Accepted for the Council:

Carolyn R. Hodges

Vice Provost and Dean of the Graduate School

(Original signatures are on file with official student records.)

To the Graduate Council:

I am submitting herewith a dissertation written by Bijan Radmard entitled "Enhancement of the Properties of Polymer Blends by Hydrogen bonding and Transesterification."
I have examined the final copy of this dissertation for form and content and recommend that it be accepted in partial fulfillment of the requirements for the degree of Doctor of Philosophy, with a major in Chemistry.

Mark D. Dadmun, Major Professor

We have read this dissertation
and recommend its acceptance:

Accepted for the Council

Associate Vice Chancellor and
Dean of the Graduate School

ENHANCEMENT OF THE PROPERTIES OF POLYMER BLENDS BY HYDROGEN BONDING AND TRANSESTERIFICATION

A Dissertation

Presented for the

Doctor of Philosophy

Degree

The University of Tennessee, Knoxville

Bijan Radmard

December 1999

ACKNOWLEDGMENTS

I would like to thank Professor Mark D. Dadmun for his excellent guidance and friendship, which were an impetus for accomplishing this work. I would like to thank Professors Spiro D. Alexandratos, Roberto S. Benson, and Jeff D. Kovac for their work as members of my committee. I would also like to thank Eric Eastwood and Phil Britt for their help in obtaining the GPC data and Scott Clingman and Chris Ober in developing the synthesis of the polyethers, particularly DHMS. Special thanks are due to Gary Lynn, Sudha Chidambaran, Dano Martineau, John Chaney, Sriram Viswanathan, and Dwayne Wilson for their sincere friendship. I am also thankful to my family for their support and encouragement during my study. Finally, I would like to thank the University of Tennessee, Department of Chemistry, National Science Foundation for financial support and East Tennessee Section of American Chemical Society for a graduate fellowship.

ABSTRACT

The importance of polymer rigidity on the extent of intermolecular hydrogen bonding in the blends of copolymers of 4-vinylphenol and styrene (PS-*co*-PVPh) and polyethers has been studied utilizing FT-IR spectroscopy. A series of polyethers containing mesogens with different rigidity including a liquid crystalline poly ether (LCP) are synthesized using phase-transfer polyetherification and blended with PS-*co*-PVPh. The extent of intermolecular hydrogen bonding between the hydroxyl group of PS-*co*-PVPh and the ethereal oxygen is correlated to the rigidity of polyethers.

The results of this study indicate that extent of intermolecular hydrogen bonding in blends increases as the flexibility of polyethers increases, causing a shift in the frequency of the hydrogen bonded hydroxyl band towards lower frequency. The rigidity of the polyethers inhibits the formation of intermolecular hydrogen bonds, however this effect is not dramatic. It must be recognized that the LCP utilized in this study can not be considered as a rod-like LCP, as it contains flexible aliphatic spacers. Therefore, the result shows that the rigidity of LCP does not dramatically affect the formation of intermolecular hydrogen bonds is only applicable to non-rodlike LCP. The data also show that a lower concentration of the polyether in the blends induces better mixing and higher extent of intermolecular hydrogen bonding due to better dispersion of polyether in PS-*co*-PVPh. This suggests that a one-phase system may exist in the region of the phase diagram of the blends that are rich in PS-*co*-PVPh.

The result also shows that the extent intermolecular hydrogen bonding between PS-*co*-PVPh and polyethers decreases at the higher temperatures. The concept of functional group accessibility of hydroxyl groups for intermolecular hydrogen bonding is also examined

in these blends. The amount of intermolecular hydrogen bonds increases with an increase in spacing between the hydroxyl groups.

The transesterification reaction between poly(carbonate) (PC) and thermoplastic liquid crystalline poly (hydroxy benzoate)-poly(ethylene terephthate) (PHB-PET) and its consequences on the blend morphology and mechanical properties of the blend has also been investigated. The transesterification reaction between PC and PHB-PET upon annealing at 260 °C is characterized and quantified by ^{13}C NMR spectroscopy , showing peaks at 120.9 ppm, 148.3 ppm, and 165.9 ppm corresponding to bisphenol-A terephthalate and bisphenol-A oxybenzoate diads, respectively. These peaks are the result of the initial formation of block copolymer and eventual formation of random copolymer at the interface as the mole fraction of corresponding diads increases. Polarized optical microscopy and tensile measurements reveal that there is a direct correlation between the loss of liquid crystallinity character and mechanical properties of the blend to the extent of transesterification reaction. The results of this study indicate a trade-off between the loss of liquid crystallinity of the blend and its strength resulting from transesterification upon annealing.

TABLE OF CONTENTS

CHAPTER PAGE

LIST OF TABLES

TABLE

PAGE

LIST OF FIGURES

FIGURE

PAGE

Chapter 1

The Effect of Rigidity on Intermolecular Hydrogen Bonding in Polymer Blends

1.1 Introduction

The field of polymer blends has emerged as an active area of polymer science research in recent years.[1] The primary advantage of utilizing polymeric blends is that mixing two polymers is more cost effective than producing entirely new polymeric materials. Additionally, blending may produce materials with combinations of properties superior to those of single polymers.[2] This has led to an increase in the interest in the use of blends in the polymer industry over the past several years, as well as a growing rise in the understanding of the science of blends. [3] Thus, the combination of two or more commercially available polymers through blending opens up an inexpensive method to produce polymeric materials with a range of desirable properties over a shorter development period.

The growth in polymeric blends consumption has historically outpaced the overall growth of the plastics Industry.[4] During the late 1980's the annual growth of the plastics industry was between 2 to 4%. At the same period, polymer blends have shown a 9 to 11% growth rate, while the growth for blends utilizing engineering thermoplastic polymers has been 13 to 17%. It is estimated that more than 30% of all polymers are sold as a mixture of two or more polymers. These blends are used in a variety of applications ranging from high tech applications such as optical disk devices, to polymer additives used solely for the purpose of cost reduction. In addition, a significant number of commercial polymer products that are commonly used are based on polymer blend technology. For instance, the blend of

polystyrene and poly(2,6-dimethyl-1,4-phenylene oxide) (PPO)is marketed by General Electric under the trade name of Noryl®, and a blend of butadiene -acrylonitrile copolymers and polyesters is used as a permanent plasticizer for poly(vinyl chloride).

Blend composition, viscoelastic properties of the components, and interfacial adhesion at the biphasic interface are important parameters that affect the final properties of a polymer mixture.[5] In particular, the interface can be a weak point in a polymer blend. The strength of the interface is very important in determining the properties of a biphasic polymer blend. Strong interactions across phase boundaries may promote good adhesion and result in efficient stress transfer between two phases. Thus, the size and morphology of the phases and the nature of the interface between two phases in an immiscible polymer blend are important determinants of how a blend will respond to stress and its mechanical properties.

Most polymer pairs are incompatible and form two phases when mixed.[6] This is because of the inherently low entropy of mixing two long polymer chains. The immiscibility leads to a weak interface with large interfacial tension in the blend. This in turn, results in a system with poor interfacial adhesion in the solid state and inferior mechanical properties. One method by which the properties of a biphasic blend can be improved is by inducing specific interactions between polymers at interface. These specific interactions can be in the form of strong covalent interactions such as transreactions and ionic bonding or non-bonding weak interactions such as hydrogen bonding, ion-dipole, dipole-dipole, and donor-acceptor interactions.[7]

In this thesis, we will explore hydrogen bonding as a method to improve the properties and phase behavior of polymer blends . To do so, an understanding of the thermodynamics

of mixing in polymer blends and the effect of hydrogen bonding on the alteration of the phase behavior in polymer blends will be useful.

1.2. Thermodynamics of Mixing in polymer blends

The earliest model that describes the thermodynamics of mixing long chain molecules was presented by Flory[6] and Huggins[8]. In this model, the entropy of mixing was assumed to be purely combinatorial in origin and was obtained by calculating the number of arrangements for polymer molecules on an imaginary lattice. For polymer blends, the Flory-Huggins formalism for the Gibbs free energy of mixing is given as in equation (1.1):

$$\frac{\Delta G_m}{RT} = \frac{\Phi_A}{N_A}\ln\Phi_A + \frac{\Phi_B}{N_B}\ln\Phi_B + \chi\Phi_A\Phi_B \qquad (1.1)$$

Where N_i and Φ_i represent the degree of polymerization and volume fraction of the *i*th species, and χ_{AB} is the Flory-Huggins interaction parameter which represents a measure of the interaction energy between the A and B components. The Flory-Huggins expression for the free energy of mixing has gained widespread recognition, mainly due to its algebraic simplicity and similarity to experiment. In the original form, the χ_{AB} parameter was considered entirely enthalpic and independent of composition and molecular weight. However, a number of later studies could only by explained by employing a χ_{AB} parameter which varies with these variables.[9, 10] In essence, the χ_{AB} parameter has evolved from a fundamental interaction energy term to an excess free energy function that incorporates all of the model inaccuracies. Another limitation of this theory comes from the assumption that the two species mix

randomly which is only true when one is dealing with athermal mixtures. This assumption is not valid in the presence of strong intermolecular interactions such as hydrogen bonds, as strong interactions will force polymer chains in to non-random configuration. The effect of volume changes upon mixing is also neglected in Flory-Huggins theory. The experimental observation of a lower critical solution temperature (LCST) in non-polar polymer solutions can not be predicted by the simple Flory-Huggins theory. Therefore, this theory has obvious limitations which prevents its use a general predictive tool.

Despite the shortcomings of Flory-Huggins theory, it still provides an intuitive understanding of the factors which affect blend miscibility. Many attempts have been made to overcome these limitations. Typical examples are Flory's equation of state theory[11, 12, 13], Sanchez and Lacombe[14] fluid lattice model which takes into account unoccupied sites or holes in a lattice and Coleman and Painter's association model[15, 16] which considers specific interactions in hydrogen bonded polymer blends.

The association model of Coleman and Painter is of particular interest for the work in this dissertation.[17] It describes the thermodynamics of mixing polymers which possess functional groups capable of hydrogen bonding. The theoretical free energy expression can be written:

$$\frac{\Delta G_m}{RT} = \frac{\Phi_A}{N_A}\ln\Phi_A + \frac{\Phi_B}{N_B}\ln\Phi_B + \chi\Phi_A\Phi_B + \frac{\Delta G_H}{RT} \qquad (1.2)$$

Where R, T, Φ_i and N_i have the same meaning as in the original Flory-Huggins Theory. However, this expanded model consists of three contributions rather than two : The

combinatorial entropy (first two terms), unfavorable "physical" interactions represented by χ_{AB} and favorable specific (or chemical) interactions represented by the $\Delta G_H/RT$ term that reflects the changes in the free energy that results from the change in the distribution of hydrogen bonds. The mathematical expressions for the first two contributions are simply those derived by Flory[6] and Huggins[8]. The effects of hydrogen-bonded associations are incorporated in the ΔG_H term, which reflects the hydrogen-bonding contribution to the overall free energy. The χ_{AB} term is evaluated by accounting for non-specific dispersive interactions by employing cohesive energy density or solubility parameters.

Based on a rule of thumb, if the difference between the solubility parameters of the components in a polymer blend is less than a critical value of 2.5 $(\text{cal cm}^{-3})^{0.5}$, then hydrogen bonding may induce miscibility in the blend.[18] The calculated values for the solubility parameters of the polymers used in this study are:[19] poly(vinyl phenol) (PVPh), 10.6 $(\text{cal cm}^{-3})^{0.5}$, poly(styrene-*co*-vinylphenol) (PS-*co*-PVPh), 10.18 $(\text{cal cm}^{-3})^{0.5}$; dihydroxy-methylstilbene copolyether (DHMS-7,9), 9.1 $(\text{cal cm}^{-3})^{0.5}$; methylene copolyether (Methylene-7,9), 9.16 $(\text{cal cm}^{-3})^{0.5}$; ethylidene copolyether (Ethylidene-7,9), 9.12 $(\text{cal cm}^{-3})^{0.5}$ and bisphenol-A-copolyether (Bisphenol-A-7,9), 8.96 $(\text{cal cm}^{-3})^{0.5}$. Because the difference in solubility parameters between PS-*co*-PVPh and 7,9-copolyethers is in the acceptable range of less than 2.5 $(\text{cal cm}^{-3})^{0.5}$, therefore the possibility of finding a miscible system for their blends can be predicted. The χ parameters for the blends of PS-*co*-PVPh/7,9-copolyethers are also calculated based on equation (1.3) and found to be around 0.34.[20]

$$\chi = 0.34 + \frac{V_r}{RT}\left(\delta_1 - \delta_2\right)^2 \qquad (1.3)$$

Assuming V_r = 100 Cm^3 mol^{-1} as a reference volume , δ_1 and δ_2 the solubility parameters of polymers, R is the ideal gas law constant and T= 298 °K. The value of χ parameter also predicts miscibility for these blends. However, in the presence of strong forces such hydrogen bonding, these predictions may not be accurate.

The contribution from favorable interactions such as hydrogen bonding is widely accepted as one of the most important causes of miscibility in certain polymer blends. This association model has provided an important tool in the estimation of the phase behavior of polymer blends by successfully predicting miscibility windows and maps for binary copolymers blends involving hydrogen bonds. A complete understanding of the relationship between phase behavior and intermolecular hydrogen bonding in polymer blends can only be found when the extent of hydrogen bonding that forms between the polymers in a blend can be accurately determined experimentally. An important fact related to this is that hydrogen bonds are dynamic and are continuously breaking and reforming under the influence of thermal motion and they exist at any instant as a distribution of free (non-hydrogen bonded) and hydrogen bonded species in the system at a given temperature. The hydrogen bonds formed at any temperature are in a state of dynamic equilibrium which must be characterized by an appropriate equilibrium constant. For example, poly vinyl phenol (PVPh) or its copolymer with styrene (PS-*co*-PVPh) are amorphous polymers which are capable of forming hydrogen bonds with itself (self-association) or other polymers (inter-association), with the hydroxyl group acting as a proton donor as is shown in Figure 1.[17]

The self-association of the hydroxyl groups in PVPh can be probed by infrared spectroscopy.[21] The stretching vibrations of "free" non-hydrogen bonded and self-associated

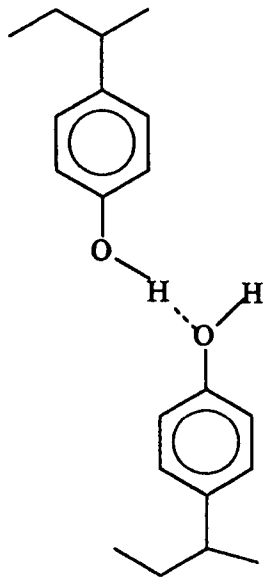

Intra molecular Hydrogen Bonding
in PVPh

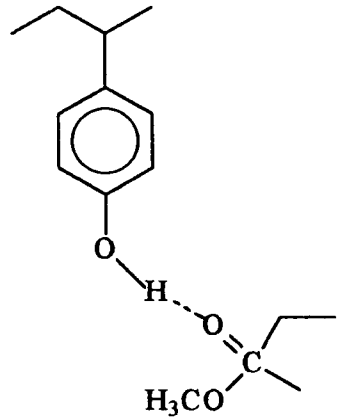

Inter molecular Hydrogen Bonding Between
the Hydroxyl of PVPh and the Carbonyl of PMMA

Figure 1. Intra molecular and Intermolecular Hydrogen bonding in PVPh

hydrogen bonded hydroxyl groups in PVPh can be observed at 3525 cm^{-1} and 3370 cm^{-1}, respectively. The self-association of hydroxyl containing polymer B like PVPh can be described as:[22]

$$B_1 + B_1 \xleftrightarrow{K_2} B_2 \tag{1.4}$$

$$B_n + B_1 \xleftrightarrow{K_B} B_{n+1} (n \geq 2) \tag{1.5}$$

Where K_2 and K_B are equilibrium constants for the formation of dimers and chain-like multimers and can be defined as:

$$K_2 = \frac{\Phi_{B_2}}{\Phi_{B_1}^2}\left(\frac{1}{2}\right) \tag{1.6}$$

$$K_B = \frac{\Phi_{B_{n+1}}}{\Phi_{B_n}\Phi_{B_1}}\left(\frac{n}{n+1}\right) \tag{1.7}$$

Where $\Phi_{B_1}, \Phi_{B_2}, \Phi_{B_n}$ and $\Phi_{B_{n+1}}$ are the volume fraction of monomer, dimer, *n*-mer and *n+1* mer of B. The term n/(n + 1) in equation (1.7) results from the conversion of molar concentration of species involved in equilibrium to their volume fractions. For flexible, strongly hydrogen bonded polymers like PVPh, the self-association equilibrium constants can be estimated from the self-association of corresponding small molecule analogs by scaling to the polymer repeat unit after correcting for molar volume differences.[23]

A similar expression can be derived for a blend consisting of a proton acceptor polymer A (which cannot self-associate) and a proton donor polymer B. Assuming that in a binary blend of a proton acceptor polymer A and a proton-donor polymer B, polymer A makes no distinction between forming a hydrogen bond to a dimer or *n*-mer, the intermolecular hydrogen bonding between A and B and inter-association equilibrium constant (K_A) can be written as:

$$B_i + A \xleftrightarrow{K_A} B_i A \qquad (1.8)$$

$$K_A = \frac{\Phi_{B_i A}}{\Phi_{B_i}\Phi_{0A}}\left(\frac{ir}{i+r}\right) \qquad (1.9)$$

Where $r = V_A/V_B$. Φ_{0A} is the volume fraction of non-hydrogen bonded polymer A. V_A and V_B are molar volume of A and B, respectively. The term ir/(i+r) in equation (1.9) accounts for the difference in volume when B_i is added to B_1 to form B_{i+1} or to A to form B_iA. The total volume fraction of all B units present in the mixture is given by:

$$\Phi_B = \Phi_{B_1} + \sum_{n=2}^{\infty}\Phi_{B_n} + \sum_{i=1}^{\infty}\Phi_{B_i A}\left(\frac{i}{i+r}\right) \qquad (1.10)$$

For the formation of dimer, trimer, ..., *n*-mer, according to the above equations we have

$$\Phi_{B_2} = 2K_2\Phi_{B_1}^2 \tag{1.11}$$

$$\Phi_{B_3} = \tfrac{3}{2}K_B\Phi_{B_2}\Phi_{B_1} \tag{1.12}$$

$$\Phi_{B_{n-1}} = \frac{n-1}{n-2}K_B\Phi_{B_{n-2}}\Phi_{B_1} \tag{1.13}$$

$$\Phi_{B_n} = \frac{n}{n-1}K_B\Phi_{B_{n-1}}\Phi_{B_1} \tag{1.14}$$

By successive substitution of $\Phi_{B_{n-1}}, \Phi_{B_{n-2}}, \ldots, \Phi_{B_2}$, we obtain

$$\Phi_{B_n} = nK_B^{n-2}\Phi_{B_1}^{n-2}K_2\Phi_{B_1}^2 \tag{1.15}$$

By multiplying and dividing the right side of (1.15) with K_B^2, we can obtain:

$$\Phi_{B_n} = \frac{K_2}{K_B^2}n\left(\Phi_{B_1}K_B\right)^n \tag{1.16}$$

The sum of Φ_{B_n} in equation (1.16) can be written as:

$$\sum_{n=2}^{\infty}\Phi_{B_n} = \frac{K_2}{K_B^2}\sum_{n=2}^{\infty}n\left(\Phi_{B_1}K_B\right)^n \tag{1.17}$$

Using the following binomial expansions:

$$\sum_{n=1}^{\infty} x^{n-1} = (1-x)^{-1} = 1 + x + x^2 + x^3 + \cdots \tag{1.18}$$

$$\left(\sum_{n=1}^{\infty} x^{n-1}\right)^2 = \sum_{n=1}^{\infty} n x^{n-1} = (1-x)^{-2} \tag{1.19}$$

So we can write for $K_B \Phi_{B_1}$:

$$\sum_{n=1}^{\infty} n(\Phi_{B_1} K_B)^{n-1} = \frac{1}{(1-K_B \Phi_{B_1})^2} \tag{1.20}$$

We can also consider the sum of $K_B \Phi_{B_1}$ in equation (1.17) as:

$$\sum_{n=2}^{\infty} n(K_B \Phi_{B_1})^n = K_B \Phi_{B_1} \sum_{n=1}^{\infty} n(K_B \Phi_{B_1})^{n-1} - 1(K_B \Phi_{B_1})^1 \tag{1.21}$$

Combining equations (1.21) and (1.17), one can rewrite equation (1.17) as:

$$\sum_{n=2}^{\infty} \Phi_{B_n} = \frac{-K_2}{K_B} \Phi_{B_1} K_B \sum_{n=1}^{\infty} n(\Phi_{B_1} K_B)^{n-1} - \frac{K_2}{K_B^2} 1(\Phi_{B_1} K_B)^1 \tag{1.21}$$

Using equation (1.20) for the sum of $K_B \Phi_{B_1}$ in equation (1.22) gives:

$$\sum_{n=2}^{\infty} \Phi_{B_n} = -\frac{K_2}{K_B} \Phi_{B_1} + \frac{K_2}{K_B} \Phi_{B_1} \left[\frac{1}{(1-K_B \Phi_{B_1})^2} \right] \tag{1.23}$$

From equation (1.9) we have:

$$\Phi_{B_iA} = \frac{K_A \Phi_{B_i} \Phi_{0A}(i+r)}{ir}$$

The third term in equation (1.10)can be written as:

$$\sum_{i=1}^{\infty} \Phi_{B_iA}\left(\frac{i}{i+r}\right) = \frac{K_A \Phi_{0A}}{r} \sum_{i=1}^{\infty} \Phi_{B_i} = \frac{K_A \Phi_{0A}}{r}\left[\Phi_{B_1} + \sum_{n=2}^{\infty} \Phi_{B_n}\right] \qquad (1.24)$$

We can rearrange equation (1.10) and substitute its two summation terms with corresponding values in equations (1.23) and (1.24) as:

$$\Phi_B = \Phi_{B_1}\left[\left(1 - \frac{K_2}{K_B}\right) + \frac{K_2}{K_B}\left(\frac{1}{\left(1 - K_B \Phi_{B_1}\right)^2}\right)\right]\left[1 + \frac{K_A \Phi_{0A}}{r}\right] \qquad (1.25)$$

The total volume fraction of all A units present in the mixture is given by:

$$\Phi_A = \Phi_{0A} + \sum_{i=1}^{\infty} \Phi_{B_iA}\left(\frac{r}{i+r}\right) \qquad (1.26)$$

Using the expansion term in equation (1.18), one can obtain equation (1.27):

$$\sum_{n=1}^{\infty} (K_B \Phi_{B_1})^{n-1} = \frac{1}{1 - K_B \Phi_{B_1}} \qquad (1.26)$$

Combining equations (1.23), (1.24) and (1.27) into the summation term in equation (1.26)

gives:

$$\Phi_A = \Phi_{0A} + K_A \Phi_{0A} \Phi_{B_1} \left[\left(1 - \frac{K_2}{K_B} \right) + \frac{K_2}{K_B} \left(\frac{1}{1 - K_B \Phi_{B_1}} \right) \right] \quad (1.28)$$

Infrared spectroscopy can be utilized quantitatively for probing hydrogen bonding interactions in blends of PVPh and a carbonyl containing polymer which allows one to determine the number of hydrogen bonded and free carbonyl groups. The carbonyl stretching band in the IR spectrum splits to two peaks corresponding to free and hydrogen bonded carbonyl groups, as a consequence of the hydrogen bonding interaction between the hydroxyl and the carbonyl groups. The area of each peak can be quantified by a least-squares curve-fitting procedure of FT-IR data using Guassian functions. The fraction of carbonyl groups that are involved in the hydrogen bonding with PVPh can then be calculated as:

$$f_{HB}^{C=O} = \frac{1}{1 + a_r \left(\frac{A_F}{A_B} \right)} \quad (1.28)$$

Where A_B and A_F are the areas corresponding to the hydrogen-bonded and free carbonyl groups, respectively and a_r is the absorptivity ratio, which takes into account the difference between the absorptivities of hydrogen bonded and free carbonyl groups. The total absorbance of carbonyl groups (free and hydrogen bonded) in a blend can be described by the Beer-Lambert Law as follows:

$$A_{total} = A_F + A_B = a_F b C_F + a_B b C_B \quad (1.30)$$

Where A_F, A_B are the absorbances (peak areas) of the free and hydrogen bonded

carbonyl groups, respectively. A_{total} is the absorbance of the total carbonyl groups. a_F and a_B are the absorptivity coefficients of free and hydrogen bonded carbonyl groups, and C_F and C_B are the concentration of free and hydrogen bonded carbonyl groups in the blend. b is the sample thickness. The total concentration of carbonyl groups in the blend, C, can be written as:

$$C = C_F + C_B \qquad (1.31)$$

Using equations (1.30) and (1.31), The total concentration of carbonyl group at temperature T_1 can be described as:

$$C = \frac{(A_B)_{T_1}}{ba_B} + \frac{(A_F)_{T_1}}{ba_F} \qquad (1.32)$$

Similarly, the total concentration of carbonyl groups at temperature T_2 can be written as:

$$C = \frac{(A_B)_{T_2}}{ba_B} + \frac{(A_F)_{T_2}}{ba_F} \qquad (1.33)$$

Note that the left side of both equations (1.32) and (1.33) are equal, as the total concentration of carbonyl groups (free and hydrogen bonded) stay the same in the blend, regardless of temperature. The areas (or absorbances) of the free and hydrogen bonded carbonyl peaks in the blend are temperature dependent. However, the increase in the area of free carbonyl peak must equal the decrease in the area of hydrogen bonded carbonyl peak with rising temperature. Thus, using equations (1.32) and (1.33), one can write:

$$a_B\left[(A_F)_{T_1} - (A_F)_{T_2}\right] = a_F\left[(A_B)_{T_2} - (A_B)_{T_1}\right] \qquad (1.34)$$

We can obtain the absorptivity ratio from equation (1.34) as the following:

$$a_r = \frac{a_B}{a_F} = \frac{(A_B)_{T_2} - (A_B)_{T_1}}{(A_F)_{T_1} - (A_F)_{T_2}} \qquad (1.35)$$

In practice, the absorptivity ratio is calculated by obtaining the areas of free and hydrogen bonded carbonyl peaks of as-cast and annealed blends, using equation (1.35). Using equations (1.24) and (1.27), the fraction of hydrogen bonded carbonyl groups, $f_{HB}^{C=O}$, can be written as:

$$f_{HB}^{C=O} = 1 - \frac{\Phi_{0A}}{\Phi_A} = 1 - \left(\frac{1}{\left\{ 1 + K_A \Phi_{B_1} \left[\left(1 - K_2/K_B \right) + \left(K_2/K_B \right)\left(1/1 - K_B \Phi_{B_1} \right) \right] \right\}} \right) \qquad (1.35)$$

Where Φ_A and Φ_{0A} are the volume fractions of hydrogen bonded and non-hydrogen bonded carbonyl groups, respectively. Knowing K_2 and K_B for PVPh (21 and 66.8, respectively) and the fraction of hydrogen bonded carbonyl groups (obtained from experimental FT-IR data), the inter association equilibrium constant (K_A) can be determined in the blend. The K_A values at different temperatures can be obtained using van't Hoff relationship (linearity of ln K_A vs 1/T). The van't Hoff relationship describes the temperature dependence of the equilibrium

constant in chemical reactions.

$$\left(\frac{\partial \ln K_{eq}}{\partial T}\right)_p = \frac{\Delta H^o}{RT^2} \qquad (1.37)$$

Where K_{eq} is the equilibrium constant, T is temperature in Kelvin, ΔH^o is the reaction enthalpy and R is the ideal gas law constant. The integration of equation (1.37) gives the equation (1.38) which shows a linear relationship between ln K_{eq} as a function of 1/T. In practice, a straight line is obtained by plotting ln K_{eq} against 1/T.

$$\ln K_{eq} = -\frac{\Delta H^o}{R}\frac{1}{T} + I_K \qquad (1.38)$$

Where I_K is an integration constant.

The frequency shift observed in the spectra of the blends containing carbonyl and hydroxyl functional groups can be confidently assigned to intermolecular interactions because these vibrations are essentially localized modes and are not coupled to the vibrational modes of substituents attached to the carbonyl group.[24] However, In blends of PVPh and polyethers, the C-O-C stretching vibration for the polyether which occurs in 1000-1300 Cm^{-1} region is not a localized mode and is conformationally sensitive to the vibrational modes of the substituents in both sides of the ether linkage. Therefore, the frequency shifts of this stretching mode observed in blends can not be assigned specifically to intermolecular interactions with the same degree of confidence as those of carbonyl and hydroxyl stretching vibration modes. Furthermore, unlike the carbonyl group, the C–O–C stretching mode does not separate in to bands that can be attributed to "free" and hydrogen bonded ether groups.

As a result, a quantitative analysis of the fraction of hydrogen-bonded ether groups and inter-association equilibrium constant in PVPh/polyether blends can not be obtained directly from FT-IR spectroscopy. However, an indirect quantitative analysis of the fraction of hydrogen-bonded ether groups and inter-association equilibrium constant in PVPh/polyether blends may be feasible by the formation of a miscible ternary blend of PVPh, polyether and a carbonyl containing polymer.[17]

1.3 Literature Review

The growing history of polymer blend science and technology has been documented in a number of review books and monographs.[25, 26] One of the most referenced blends, believed to be miscible via hydrogen bonding is poly (vinyl chloride) (PVC)/poly (ε-caprolactone), (PCL). One of the first studies on this system utilized inverse gas chromatography and indicated a negative interaction parameter, χ, which may imply an intermolecular hydrogen bonding between the oxygen of the carbonyl group in PCL and the α-hydrogen (CH) in PVC.[27]

Prud'homme[28, 29] mentioned that PCL is miscible with a variety of chlorinated polymers (e.g., poly(chlorostyrene) and poly (vinylidene chloride)) which do not contain α-hydrogens and proposed that dipole-dipole interactions may be responsible for the observed miscibility. Another widely studied polymer where hydrogen bonding prominently appears in its miscibility in blends is poly (hydroxyether Bisphenol- A) (phenoxy). Phenoxy is miscible with many polymers containing proton accepting groups (e.g., poly (butylene terephthalate),[30] poly (ethylene oxide)[31] (PEO), poly (vinyl methyl ether)[14](PVME), aliphatic polyesters[32], poly

(vinyl pyrrolidone)[33], and poly (ethyl oxazoline).[34]) An FT-IR study of phenoxy/PCL and phenoxy/PEO blends showed evidence of hydrogen bonding interactions[35], as did an additional study of phenoxy/PVME.[36] Pearce and coworkers[37,38] have shown the importance of hydrogen bonding interactions in blends of styrene-vinyl phenyl hexafluorodimethyl carbinol copolymers with various proton acceptor polymers. Strong hydrogen bonding between acidic and basic water soluble polymers yields, in many cases, water insoluble, miscible blends (e.g., poly (acrylic acid)/poly (ethylene oxide)).[39,40] Polyelectrolyte complexes constitute an extreme case of specific interactions where proton transfer occurs and an organic salt results.[41, 42] This interaction can be classified as an acid-base interaction. Of course, hydrogen bonding is a subset of acid-base interaction to the extent that the proton-donor polymer acts as an acid and proton-acceptor polymer acts as a base.

The blend of polystyrene and poly (2,6-dimethyl-1,4 phenylene oxide) (PPO) is another widely studied blend. The nature of miscibility of this system has not been clearly elucidated in the literature. Negative heat of mixing[43] and melting point depression data suggested the existence of specific interactions between PPO and polystyrene. Wellinghoff and coworkers used ultra violet spectroscopy (UV) to study this system, focusing on the $A_{1g} \rightarrow B_{2u}$ ($\pi \rightarrow \pi^*$) transition band of the phenyl ring in PPO which is sensitive to conformational changes of PPO in the blend which could result in a change in the extent of conjugation between the π-electrons of the phenyl ring and lone pairs of ethereal oxygen in PPO. They concluded a strong dispersive interaction exists between the phenyl groups of the two polymers in the blend.[44] Djordjevic and Porter[45] utilized ^{13}C nuclear magnetic resonance spectroscopy (NMR) to study the potential interactions for this blend and concluded a π-

hydrogen bond exists between the electron deficient methyl groups of PPO and π-electrons of polystyrene. Additionally, dipole-dipole interactions between the oxygen of the polarized C=O bond and the fluorine of the polarized C–F bond have been attributed to the miscibility of poly (vinylidene fluoride) with a large number of carbonyl containing polymers such as poly (methyl methacrylate) (PMMA), poly (vinyl acetate) (PVAc), and poly (vinyl methyl ketone).[46, 47, 48]

The miscibility maps for (PS-*co*-PVPh) and poly (ethylene-*co*-vinyl acetate) have been calculated based on the association model.[49] Theoretical calculations and experimental IR studies of this blend provided the equilibrium constants of the inter-association of phenolic hydroxyl groups and the enthalpy of hydrogen bond formation. The carbonyl stretching vibration shifts to lower frequency and broadens in the presence of phenolic hydroxyl in the blend from 1738 cm^{-1} to 1708 cm^{-1}, due to intermolecular hydrogen bonding. In a similar study Coleman *et al.* studied the blend of PS-*co*-PVPh and random poly(ethyl-*co*-methylacrylate).[50] Using FT-IR spectroscopy, the fraction of hydrogen-bonded carbonyl groups was obtained for the blend. Furthermore, the equilibrium constant describing the inter-association of phenolic hydroxyl groups to acetate carbonyl groups was obtained experimentally and was comparable with the calculated value based on the association model.

Ternary blend systems have not been as widely studied due to the complications in calculating of phase diagrams and the interpretation of experimental data.[51] However, the ternary blend of poly (vinyl acetate) (PVAc)/PVPh/styrene-*co*-methylacrylate (72% methylacrylate) is shown to be miscible by DSC measurements. The calculation of the miscibility maps and phase diagram for this system have been reported. The miscible ternary

blends of PVPh/PEO/PVAc and PVPh/PEO/PMMA have also been investigated by Coleman *et al* .[52] The fraction of hydrogen-bonded ether and carbonyl groups and inter association constant for PVPh/PEO and PVPh/PVAc were determined by a least-square curve-fitting of experimental IR data.

The phase diagrams and miscibility maps of the blends of PVPh/poly acrylates, PVPh/poly acetates, PVPh/poly lactones, PS-*co*-PVPh/poly (*n*-octyl methylacrylate) and PS-*co*-PVPh/poly(*n*-decyl methylacrylate) have been calculated and determined based on the association model. [53] FT-IR studies of PVPh and a series of poly (*n*-alkyl methylacrylates) provided the equilibrium constants of inter-association, the enthalpy of hydrogen bond formation and the fractions of hydrogen bonded carbonyl groups in these blends.[54] In another study[55], FT-IR was used to confirm the predictions that resulted from the calculation of miscibility windows and the phase diagram using solubility parameters in blends of PS-*co*-PVPh/poly (*n*-butyl methacrylate) (PBMA) and PS-*co*-PVPh/poly (*n*-hexyl methacrylate) (PHMA). Using various PS-*co*-PVPh copolymers, values of the self-association and inter-association equilibrium constants were determined spectroscopically using the least square procedure described for miscible blends with PBMA and PHMA.

The intermolecular hydrogen bonding between the hydroxyl groups of PVPh and the carbonyl of the acetate groups in PVPh/PVAc blend and PVPh/ethylene-vinyl acetate copolymer blends was investigated as a function of temperature, utilizing FT-IR spectroscopy.[56] The average overall strength of the intermolecular hydrogen bonding interaction between PVPh and PVAc decreases with increasing temperature. A quantitative analysis of the free and hydrogen bonded carbonyl of PVAc was also performed. The

stretching frequency of the carbonyl group decreased from 1739 cm^{-1} to 1714 cm^{-1} in the blend, showing a red shift, as the C=O bond becomes weaker due to inter molecular hydrogen bonding between PVPh and PVAc. The stretching frequency of the self-association of the hydroxyl group of PVPh shifts from 3360 cm^{-1} for pure PVPh to 3430 cm^{-1} for a blend of PVAc/PVPh (80/20) wt%. The results confirmed that the O–H bonds involved in intra molecular hydrogen bonding are weaker than those involved in intermolecular hydrogen bonding with PVAc. Thus, the PVPh hydroxyl-PVAc carbonyl interaction is weaker than the self-association interaction in PVPh. DSC also confirmed a single Tg for this miscible blend.

The blend of PVPh and Poly (vinyl pyrrolidone) (PVPr) has also been studied.[57] Again, the stretching frequency of the hydrogen bonded hydroxyl group of PVPh was red shifted from 3360 cm^{-1} for pure PVPh to 3230 cm^{-1} for 35/65 wt% of PVPh/PVPr blend. This also showed that PVPh hydroxyl-PVPr carbonyl interaction is stronger than the self-association interaction in PVPh. The blends of PVPh and poly (ϵ-caprolactone) (PCL) was also studied by FT-IR spectroscopy. The stretching frequencies of the carbonyl bands at 1734 cm^{-1} and 1708 cm^{-1} were assigned to the free and hydrogen bonded carbonyl of PCL in the blend. The relative intensity of the hydrogen bonded carbonyl band at 1708 cm^{-1} increases with an increase in the concentration of PVPh in the blend. Morever, the stretching frequency of the hydroxyl groups of PVPh was shifted from 3370 cm^{-1} for pure PVPh to 3420 cm^{-1} for the 50/50 (w/w%) blend. The shift of hydroxyl groups of PVPh to higher frequencies in the blend of PVPh and PCL suggests that the O–H bonds which are intermolecularly hydrogen bonded to carbonyl groups of PCL are stronger than those that are self-associated in PVPh.

1.4 Hydrogen-bonded Rod/coil Blends

The concept of a self-reinforcing molecular composite composed of a rigid rod-like polymer and a flexible- coil polymer was first proposed in 1975 by Helminiak and coworkers.[58] Such a blend on a molecular level is analogous to a fiber-reinforced matrix resin. The presence of rigid rod-like polymer dispersed on a molecular level can be advantageous to bring high modulus and strength to the blend because of the high aspect ratio of the rigid rod-like polymer. However, the miscibility of a blend between a rod-like polymer and a random-coil polymer to form a polymeric composite has been a difficult task due to the small entropy of mixing.[59] The extent of mixing between rigid rod-like and flexible polymers is a crucial factor in determining the overall strength and mechanical properties of the composite. In 1978, Flory predicted that a blend of rod-like polymers and random-coil polymers immersed in a solvent will separates into an anisotropic phase of rod-like polymers and an isotropic phase which consists mainly of a solution of the coiled polymer.[60]

However, it has been suggested by Ballauff [61] that the miscibility in a rod-like/coil polymer blend can be promoted by specific interactions such as hydrogen bonding or tailoring flexible side chains attached to rods. The phase behavior with hydrogen bonding windows of a rod-like/coil blend was calculated by Coleman et al.[62] They concluded that a single phase rod/coil blend can be reached in the presence of very strong specific interactions between a rod-like and random-coil polymers. Following the theoretical results, the phase behavior of lyotropic liquid crystal poly (γ-alkyl-L-glutamates) such as poly (γ-methyl-L-glutamate) (PMLG), poly (γ-butyl-L-glutamate) (PBLG), and poly (γ-ethyl-L-glutamate) (PELG) blended with PVPh were investigated.[63] The phase behavior of these blends were predicted

using an association model assuming a disorder index for the flexible coil polymer in the calculation of the chemical potentials.

It was also assumed that these rigid poly peptides retain their helical conformations in the blend upon hydrogen bonding between the hydroxyl group of PVPh and the ester functional group on the side chains of the poly peptides. This assumption turned out to be true, as the shape of amide band (responsible for helical structure in poly peptides via intra molecular hydrogen bonding) stayed unchanged in all blends during the experiments, as confirmed by FT-IR.[60] The calculation of the phase diagram in these blends predicted the formation of a single phase mixture with a very small biphasic gap between an isotropic and anisotropic phase in appropriate compositions. The formation of a single phase, miscible blend between PVPh and PELG was also confirmed by DSC and optical microscopy.

The observed phase behavior of PVPh/PELG and PVPh/PMLG blends using optical microscopy was consistent with the predicted phase behavior. The evidence for intermolecular hydrogen bonding between PVPh and the rigid poly peptides was obtained by FT-IR spectroscopy. The percentage of hydrogen bonded carbonyl groups of PELG and PMLG was also determined by FT-IR and was in agreement with predicted values. In contrast, the blend of PVPh/PBLG showed phase separation as confirmed by FT-IR spectroscopy. No change in the location and shape of carbonyl peaks in IR spectra of this blend at different compositions was observed even upon annealing.

1.5 Functional Group Accessibility in Polymer Blends

The accessibility of functional groups is an important concept in polymer blends which

incorporate specific interactions such as hydrogen bonding.[64] Factors such as chain connectivity and steric shielding or crowding can limit the number of intermolecular interactions that can form in hydrogen bonded blends. Thus, practically, not all functional groups of the polymer in a blend can be involved in intermolecular hydrogen bonding. In other words, less than 100 percent of functional groups in a polymer blend are "accessible" for interchain hydrogen bonding. Specifically, the accessibility of the carbonyl functional group in the blends of poly(2,3-dimethylbutadiene-*stat*-4-vinyl phenol) (24% vinyl phenol) (DBPVPh) with poly(*n*-alkyl acrylate) (PAA) with different side groups and poly(ethylene-*co*-vinyl acetate) (70,45, 25, 18 wt.% vinyl acetate) copolymers have been studied.[65] The inter-association equilibrium constant was obtained by the curve-fitting procedure of IR data for the carbonyl band. Using the van't Hoff relationship, the standard inter association equilibrium constant (K_A at 25 °C) was calculated. The magnitude of the standard inter association equilibrium constant was considered a measure for the accessibility of the carbonyl groups for intermolecular hydrogen bonding. The higher the K_A value, the more accessible the carbonyl groups are for intermolecular hydrogen bonding. This is because the higher K_A value favors more intermolecular hydrogen bonding between the carbonyl groups and hydroxyl of vinyl phenol as it shifts the equilibrium shown in equation (1.7) towards the right.

A decrease in the standard inter association equilibrium constant of the carbonyl group of PAA (lower accessibility) was observed for blends of DBPVPh/PAA with bulky side chains. The formation of hydrogen bonds require that specific segments be adjacent to one another and orient in a specific manner. Evidently, the bulky side groups of PAA could inhibit the formation of hydrogen bonds in blends. The standard inter association equilibrium

constant DBPVPh/poly(ethylene-*co*-vinylacetate) blends (or accessibility of acetate group) increases as the spacing between vinyl acetate groups in poly(ethylene-*co*-vinyl acetate) copolymer increases, until it reaches a maximum for poly(ethylene-*co*-vinyl acetate) copolymer with 18 wt.% vinyl acetate. The authors suggested that as the percentage of vinyl acetate groups in poly(ethylene-*co*-vinyl acetate) copolymer decreases, the average distance between vinyl acetate increases and therefore the possibility for intermolecular hydrogen bonding between the carbonyl of acetate groups and hydroxyl of DBPVPh increases, until it reaches to a maximum. This is because, a particular carbonyl group of ethylene-*co*-vinyl acetate may be adjacent to a phenolic hydroxyl group of DBPVPh, but because one or more of its nearest same chain neighbors are already hydrogen bonded to other phenolic hydroxyl group, it may not be able to orient itself in a proper way to form a hydrogen bond due to rotational bond angle restrictions. As the vinyl acetate groups are separated by more segments of ethylidene units, they gain their rotational freedom with respect to each other. At the point where the groups are freely rotating with respect to each other, the extent of intermolecular hydrogen bonding between the carbonyl of acetate group and the phenolic hydroxyl of the DBPVPh will be maximized.

The effect of chain connectivity and steric crowding on the extent of hydrogen bonding has been studied by Coleman *et al.* [66] in the solutions of poly(methyl methacrylate) (PMMA), poly(ethyl methacrylates) (PEMA), poly(*n*-butyl methacrylate) (PBMA), poly(*n*-hexyl methacrylate) (PHMA), poly(*n*-decyl methacrylate) (PDMA), poly(*n*-lauryl methacrylate) (PLMA), and poly(ethylene-*stat*-vinyl acetate) (70, 45, 40 wt.% vinyl acetate) in 4-ethyl phenol. An increase in the accessibility of a carbonyl group to form intermolecular

hydrogen bonds with the hydroxyl group of 4-ethyl phenol was observed as the spacing between acrylate groups increases in the poly(*n*-alkyl methacrylate). Using FT-IR spectroscopy, the fraction of hydrogen bonded carbonyl and inter-association equilibrium constant were also obtained. The results also showed the effect of steric crowding on the extent of hydrogen bonding in poly(*n*-alkyl methacrylate) and 4-ethyl phenol solutions. A decrease in K_A values was observed with increasing the length of alkyl group of poly(*n*-alkyl methacrylate) from PMMA to PLMA. This is due to the steric crowding of long chain alkyl group in PLMA which could lead to a decrease in the accessibility of the carbonyl group of PLMA for intermolecular hydrogen bonding with the hydroxyl group of 4-ethyl phenol.

1.6 Goals and Justifications

The main objective of the work in this thesis is to explore the effect of chain rigidity on the extent of intermolecular hydrogen bonding in blends of PS-*co*-PVPh and polyethers with different rigidities. The chain stiffness plays an important role in the phase behavior of polymer blends, as the rigid polymer tends to exclude the flexible-coil polymer from the mixture. Induced intermolecular hydrogen bonding between polymers favors the mixing of polymers in the blend. However, the formation of hydrogen bonds demands the proximity of functional groups in polymer chains and their orientation in a specific manner. Thus, the extent of interchain hydrogen bonding in polymer blends can vary with the polymer rigidity. Increasing the rigidity in polymer chains may cause a loss of internal rotational freedom in the polymer chains and improper orientation of functional groups involved in intermolecular hydrogen bonding. This can inhibit intermolecular hydrogen bonding between polymers in

the blend and affect the ultimate bulk properties of the blend. This rigidity effect has not been studied in depth for blends.

The concept of functional group accessibility for the phenolic hydroxyl group of PS-*co*-PVPh in these blends is also investigated. The copolymerization of 4-vinylphenol with styrene in different ratios of comonomer will produce PS-*co*-PVPh copolymers which have different spacing length between hydroxyl groups. The spacing between hydroxyl groups in PS-*co*-PVPh can play an important role in the accessibility of the hydroxyl group for intermolecular hydrogen bonding with polyethers. In this thesis, based on a qualitative approach, the extent of intermolecular hydrogen bonding in blends of PS-*co*-PVPh/polyethers with different rigidity as a function of temperature, blend composition, and PVPh content in PS-*co*-PVPh will be studied.

1.7 Experimental

Styrene, 4-acetoxy styrene, Hydrazine hydrate, phenol, chloroacetone, 1,7-dibromoheptane, tetrabutyl ammonium hydrogen sulfate (TBAHS) and 1,9-dibromonanone were purchased from Aldrich Chemical Company. Azobisisobutyronitrile (AIBN) was purchased from Dojac, Inc. 4,4'-dihydroxy diphenylmethane was provided by Lancaster Synthesis Incorporation and used as received. 4,4'-ethylidenebisphenol was purchased from TCI America, Inc. and used as received. Poly 4-vinyl phenol (PVPh) (M_w = 22,000g/mole) was purchased from Polyscience, Inc. The synthesized 7,9-copolyethers were characterized by nuclear magnetic resonance (NMR), differential scanning calorimetry (DSC) and gel permeation chromatography (GPC).

Proton NMR experiments were carried out on a 400 MHz Bruker NMR spectrometer using TMS as an internal standard. Differential scanning calorimetry (DSC) measurements was completed using a Mettler DSC 821 calibrated with Indium at the rate of 10 °C/min. Molecular weights of polymers was determined using a Waters gel permeation chromatography (GPC) equipped with Ultrastyragel columns with a refractive index detector. Tetrahydrofuran (THF) was used as the elution solvent and narrow dispersity polystyrene was used as calibration standards. The blends of poly (styrene-*co*-vinyl phenol) (PS-*co*-PVPh) and 7,9-copolyethers were prepared by dissolving appropriate amounts of the polymers in THF to form 2%(w/v) solutions of 15/85, 35/65, 50/50, 65/35, and 85/15 (w/w%) blends of the two polymers.

1.7.1 Synthesis of PS-*co*-PVPh (10% and 20% PVPh)

PS-*co*-PVPh copolymers (10% and 20% PVPh) were synthesized by free-radical polymerization of styrene and 4-acetoxy styrene using AIBN as the initiator and subsequent hydrolysis of the acetoxy groups to hydroxyl groups was completed using hydrazine hydrate, as shown in Figure 2.[67] The typical procedure for the synthesis of poly (styrene-*co*-acetoxy styrene) (10% acetoxy styrene) is:

2.7 mL of Styrene (23.56 mmole), 0.4 mL of 4-acetoxy styrene (2.62 mmole) and 0.0104 g of AIBN were transferred in to a 3-neck round bottom flask filled with 50 mL of dioxane under a mild flow of Argon. The flask, equipped with a water-jacketed condenser was heated at 60 °C for 18 hours. The solution was then poured into methanol to precipitate the poly(styrene-*co*-acetoxy styrene) as the product. The polymer was dried *in vacuo* for 24

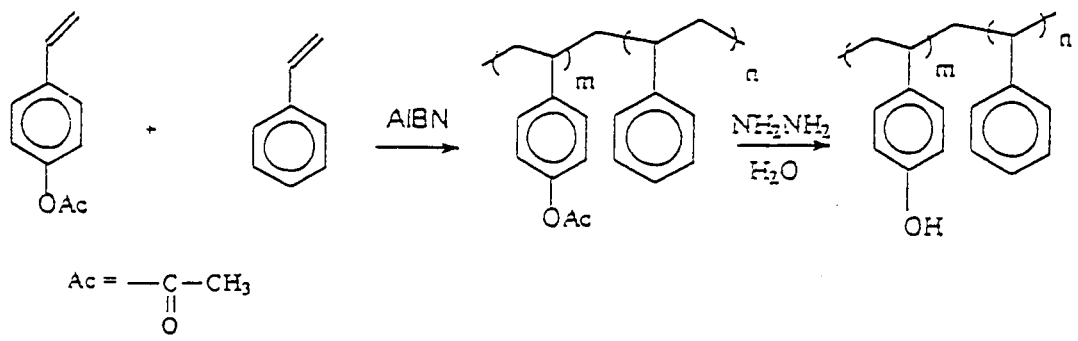

Figure 2. Synthesis of poly(styrene-*co*-vinylphenol) (10% and 20% vinylphenol)

hours. Proton NMR spectra of poly(styrene-*co*-acetoxy styrene) (10, 20% acetoxy styrene) are shown in Figure 3. Yield: 84%. ^{1}H NMR: 1.4 ppm (2H, d, CH_2); 1.7 ppm (1H, t, CH); 2.2 ppm (3H, s, CH_3); 6.2-7.2 ppm (9H, m, aromatic).

Acetoxy styrene groups are randomly distributed throughout the copolymer and the reactivity ratios of styrene and 4-acetoxy styrene are $r_1 = 0.8$ and $r_2 = 1.02$.[64] The hydrolysis of acetoxy groups to hydroxyl groups was carried out by the dissolution of 2 g of poly(styrene-*co*-acetoxy styrene) in 40 mL of dioxane in a round bottom flask.[68] Six mL of hydrated hydrazine was then added to this solution and stirred for 40 hours at room temperature. The polymer was precipitated into methanol and dried *in vacuo* for 24 hours. The completion of hydrolysis was verified by the disappearing of the methyl peak of acetoxy group at 2.2 ppm in ^{1}H NMR spectrum (see Figure 3).

The compositions of the copolymers were determined by ^{1}H NMR. The singlet peak at 2.2 ppm corresponds to the three protons of the methyl group of the acetoxy styrene repeating unit. Therefore the normalized area per proton corresponding to the acetoxy styrene repeating unit can be determined as:

$$A_{acetoxy} = \text{Area of 2.2 ppm peak} / 3$$

The broad peaks at 6.2-7.2 ppm correspond to the aromatic protons of styrene (5 hydrogens) and acetoxy styrene (4 hydrogens). Thus, the normalized area per proton corresponding to the styrene repeating unit can be calculated using:

$$A_{styrene} = [(\text{Total area of region from 6.2 to 7.2 ppm}) - 4\, A_{acetoxy}]/ 5$$

The percentage of acetoxy styrene repeating units can then be calculated from:

$$\% \text{ acetoxy styrene} = 100 \times A_{acetoxy} / (A_{styrene} + A_{acetoxy})$$

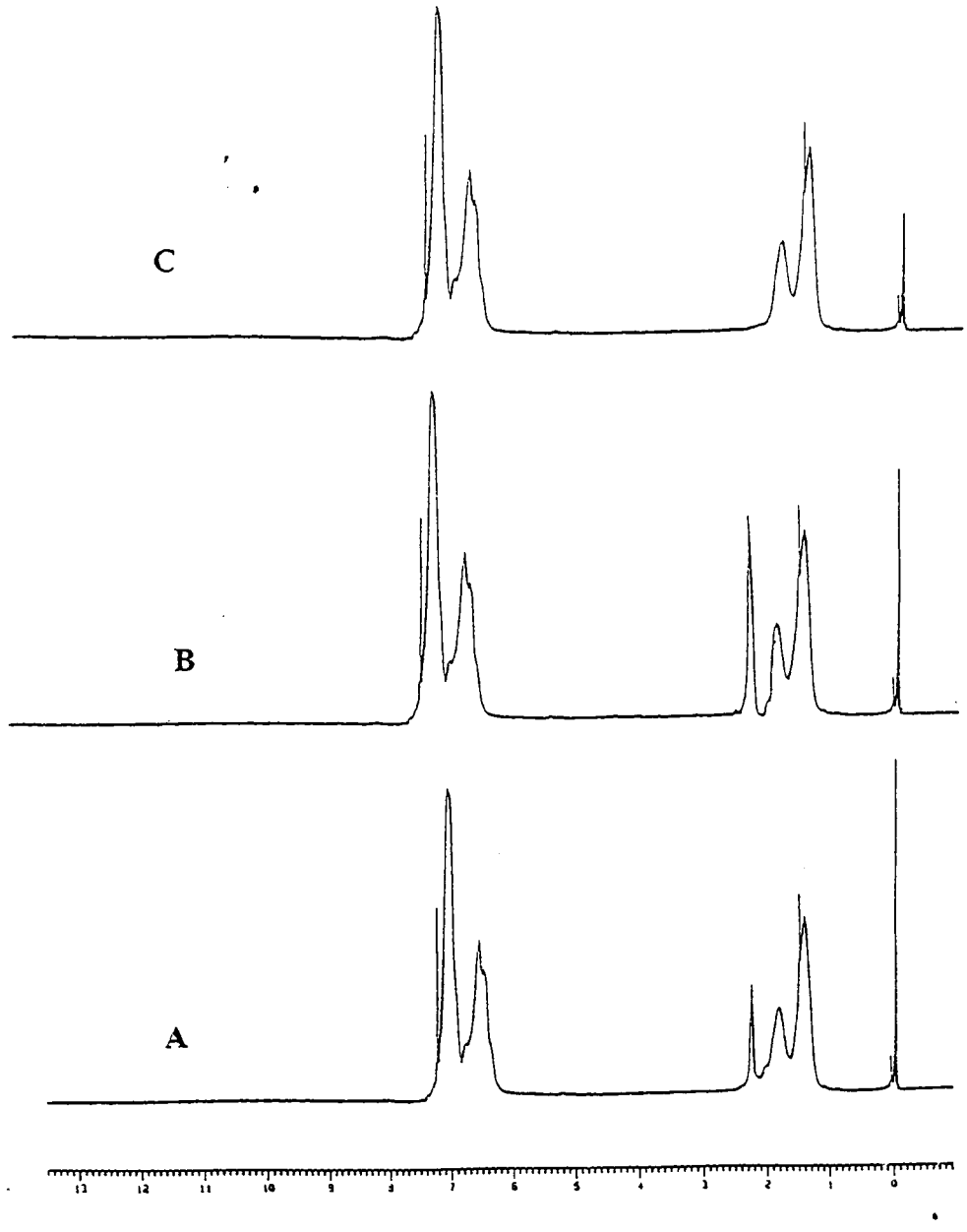

Figure 3. ^{1}H NMR spectra of (A) Poly(styrene-*co*-acetoxy styrene)(10% acetoxy styrene); (B) Poly(styrene-co-acetoxy styrene) (20% acetoxy styrene); (C) Poly (styrene-*co*-vinylphenol) (10% PVPh).

The percentage of acetoxy styrene in the synthesized PS-*co*-PVPh were calculated to be 9.98% and 19.9%. Yield: 72%. The PS-*co*-PVPh (10 and 20 %PVPh) had number average molecular weights of 24,000 g/mol (poly dispersity index P.D.I = 1.90) and 21,900 g/mol (P.D.I.=1.71), as determined by GPC. GPC data are available in Appendix. The DSC results of PS-*co*-PVPh (10% and 20% PVPh) exhibited the glass transitions at 83 °C and 91 °C, respectively (see Figure 4). The DSC thermogram of PVPh exhibits a glass transition of 147 °C (see Figure 4).

1.7.2 Synthesis of α,α'-dihyroxy methyl stilbene (DHMS)

DHMS was synthesized by the reaction of phenol and chloroacetone in presence of concentrated sulfuric acid, according to literature procedures with some modifications.[69, 70] (see Figure 5). The procedure as utilized is:

A three-neck 2 piece baffled reaction vessel equipped with thermometer, mechanical stirrer, addition funnel and dry nitrogen inlet, is placed in a dry-ice/ethylene glycol bath. Phenol (150 g, 1.59 mol) and chloroacetone (63 mL, 0.58 mol) were added and the mixture stirred and cooled to -5 °C. Conversion was followed via TLC using a 50/50 (v/v%)ethyl acetate/heptane eluent. When the reaction became too viscous for adequate stirring, the reaction was stopped by the addition of 300 mL of distilled water with continuous stirring over several hours until a thick slurry had formed. The crude product was filtered and washed several times with copious amounts of water. The crude was then recrystallized from ethanol twice. It was then added to a 50/50 ethyl acetate/heptane mixture and stirred to form a slurry. The product was purified by silica gel column chromatography using an ethyl acetate/heptane mixture (50:50,

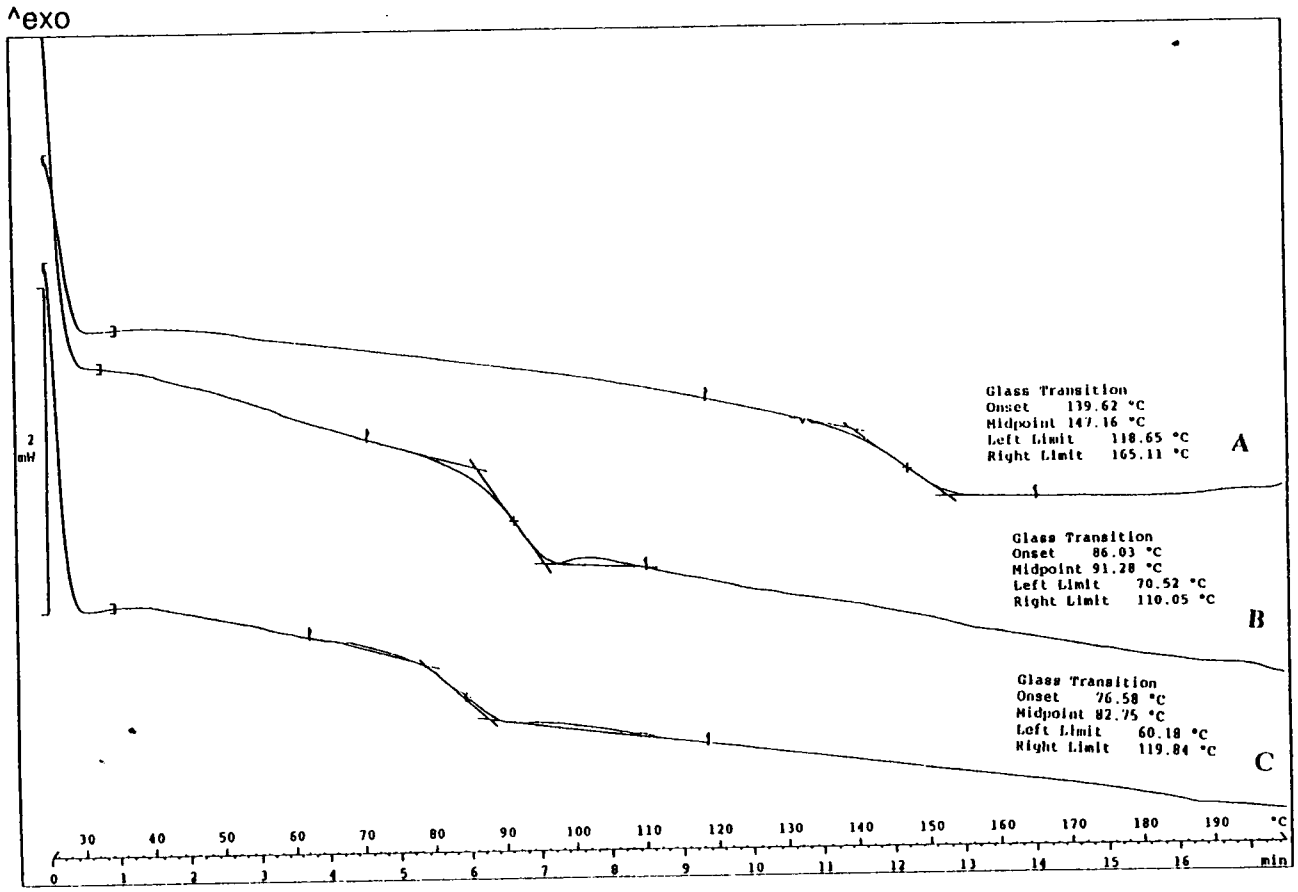

Figure 4. DSC curves of (A) PVPh; (B) PS-*co*-PVPh (20% PVPh); (C) PS-*co*-PVPh (10% PVPh)

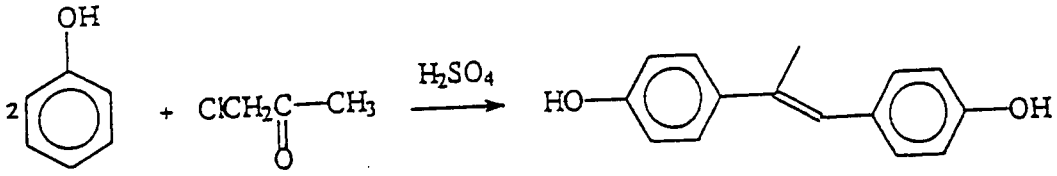

Figure 5. Synthesis of α,α′-dihydroxy methylstilbene (DHMS)

v/v%) as an eluent. Fractions which contain DHMS were collected, combined and rotary-evaporated before being redissolved in the same eluent. A second column produced pure DHMS powder which was then recrystallized from ethanol/water to obtain large crystals which where dried *in vacuo*. Yield: 10%; ^{1}H NMR (d_6-DMSO): 2.18 (3H, s, CH_3); 6.62 (1H, s, olefinic CH); 6.75 (4H, quartet, aromatic); 7.18 (2H, d, aromatic); 7.38 (2H, d, aromatic); 9.40, 9.41 (2H, s, OH) (See Figure 6). Melting point: 187 °C, DSC measurement (lit.[3] 185 °C) (see Figure 7).

1.7.3 Synthesis of DHMS-7,9 copolyether

DHMS-7,9 copolyether was synthesized by phase-transfer polyetherification of DHMS, 1,7-dibromoheptane, and 1,9-dibromonanoane, and TBAHS as a catalyst.[66, 67] (see Figure 8) Sodium hydroxide (25 g, 0.623 mol) was dissolved in distilled water (50 mL) and allowed to cool. DHMS (2 g, 0.00884 mol) and TBAHS (0.9 g, 0.00265 mol) were added to this solution and poured into a two piece reaction vessel equipped with a mechanical stirrer and nitrogen bubbler. A solution of 1,7-dibromoheptane (0.9 g, 2.1 mmol) and 1,9-dibromononane (0.84 g, 2.1 mmol) in o-dichloro benzene (50 mL) was added to the reaction vessel and the mixture was stirred for 8 hours under nitrogen at 80 °C. The reaction mixture was then washed with water (3 x 50 mL), dilute HCl solution (1 x 100 mL) and twice further with distilled water. The remaining organic phase was precipitated into methanol, redissolved in chloroform and reprecipitated into heptane. Further purification of the polymer was performed by dissolving it in hot toluene and reprecipitation in methanol. Yield: 65%.The synthesized DHMS-7,9 has a number average molecular weight (M_n) of 29,000 g/mol (P.D.I

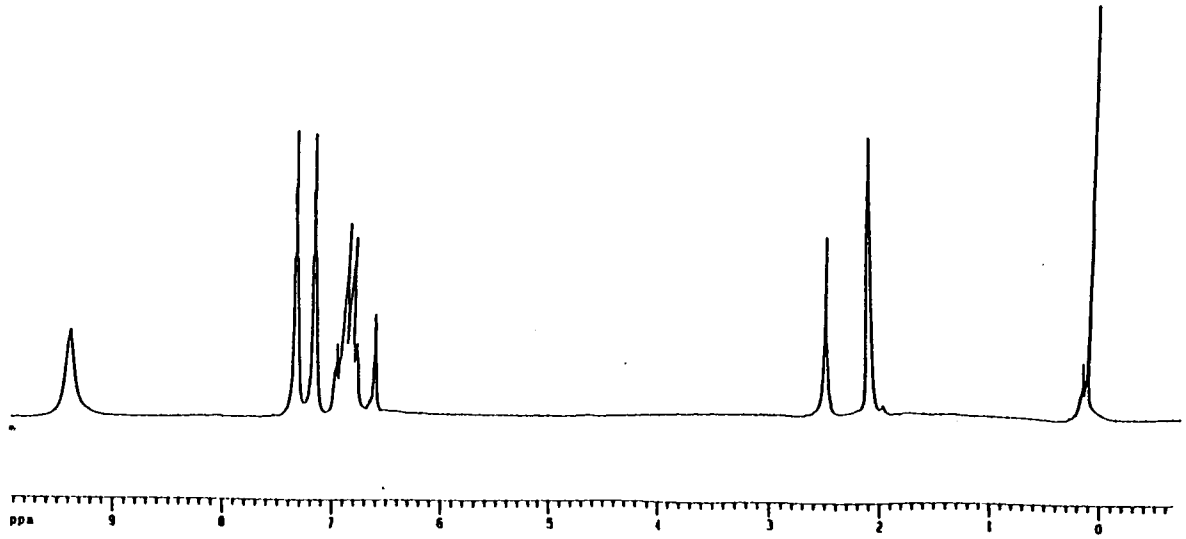

Figure 6. ^{1}H NMR Spectrum of DHMS

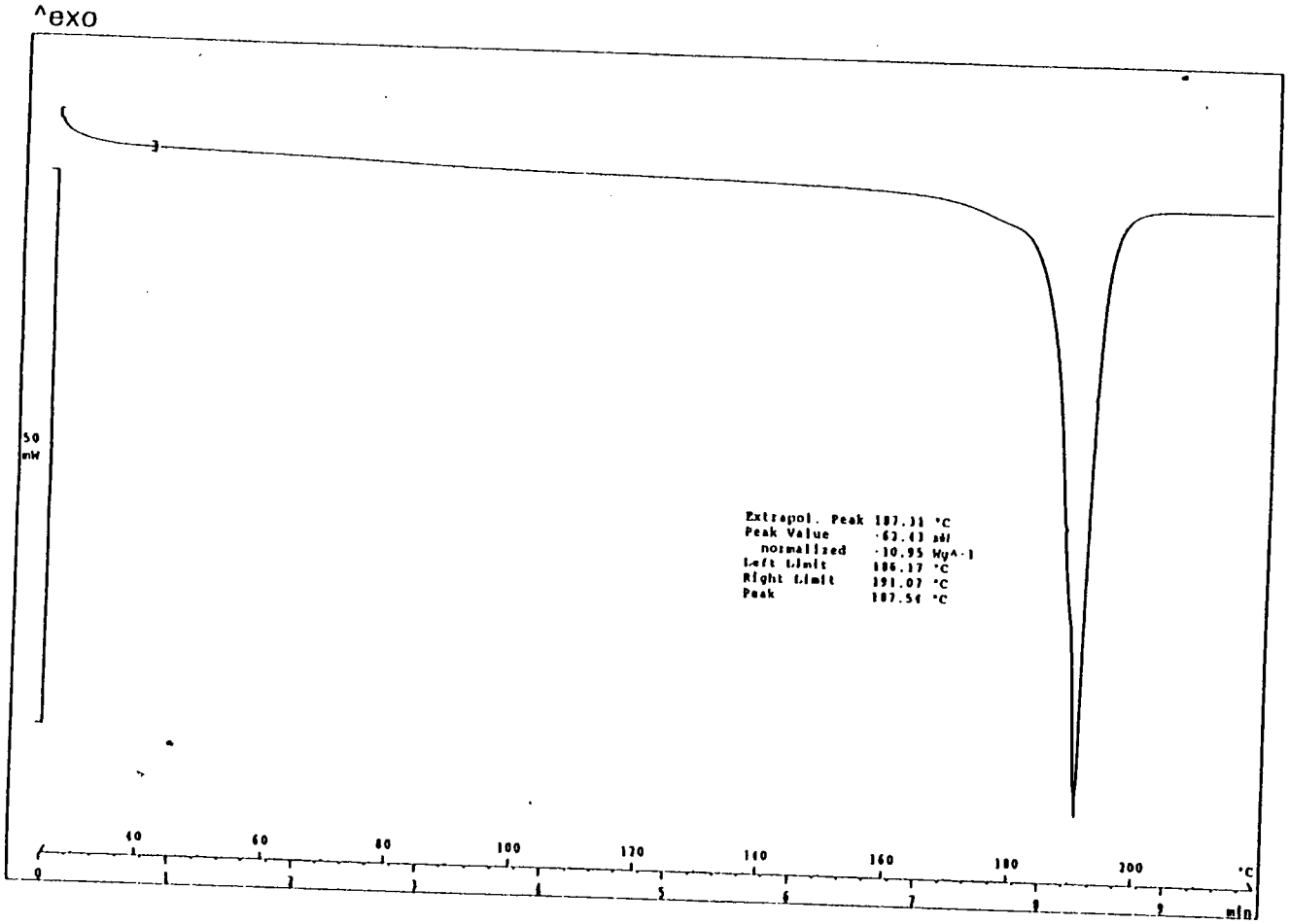

Figure 7. DSC curve of DHMS

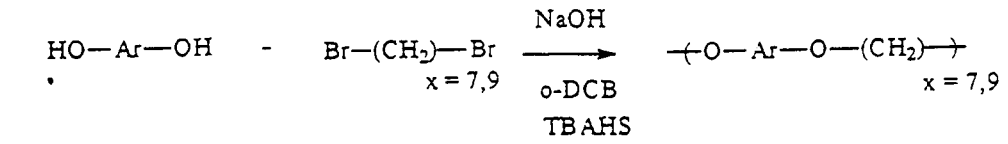

7,9-Copolyether	Ar
DHMS-7,9	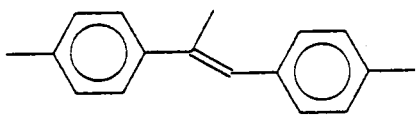
Methylene-7,9	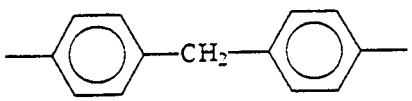
Ethylidene-7,9	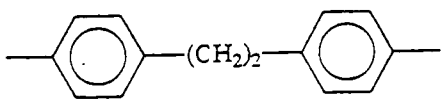
Bisphenol-A-7,9	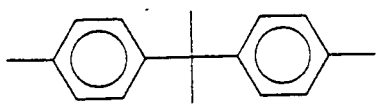

Figure 8. Synthesis of different 7,9-copolyethers

= 1.83), as determined by GPC. GPC data are available in the appendix. The thermal characterization of DHMS-7,9 copolyether includes a crystalline melting point at 90 °C, followed by transition, T_{xn} at 115 °C which likely corresponds to a transition from a smectic phase to a nematic phase.[4] The polymer also undergoes a nematic- isotropic transition, T_{ni} , at 186 °C. The DSC curve is shown in Figure 9. ^1H NMR ($CDCl_3$): 1.35, 1.42, 1.55 (10H, m, $-CH_2-$;1,79 (4H, m, $-CH_2$); 2.21 (3H, s, CH_3); 3,96 (4H, s, $-CH_2-O$); 6.70 (1H, s, olefinic CH); 6.91 (4H, d, aromatic); 7.22 (2H, d, aromatic); 7.42 (2H, d, aromatic) (see Figure 10).

1.7.4 Synthesis of Methylene-7,9 copolyether

Methylene-7,9 copolyether was synthesized by phase-transfer polyetherification of 4,4'-dihydroxy diphenylmethane, 1,7-dibromoheptane, and 1,9-dibromonanoane, using TBAHS as a catalyst in the same manner described for DHMS-7,9 copolyether (see Figure 8). The methylene-7,9 used in the blend study has a M_n of 30,900 g/mole (P.D.=1.85), as determined by GPC. GPC data are available in the appendix. Methylene-7,9 shows a crystalline melting point, T_m, at 88 °C (see Figure 11); Yield: 70% . ^1H NMR characterization of polymer in $CDCl_3$ is as follows :1.33, 1.43, 1.52 (10H, m, $-CH_2-$); 1.73 (4H, s, $-CH_2-$); 3.81(2H, s, Ar-CH_2-Ar) , 3.89 (4H, s, CH_2-O-); 6.76 (4H, d, aromatic); 7.02(4H, d, aromatic)(see Figure 12).

1.7.5 Synthesis of ethylidene-7,9 copolyether

The polyetherification of 4,4'-ethylidene bisphenol , 1,7-dibromoheptane and 1,9-dibromonanoane with TBAHS as a catalyst resulted in the formation of ethylidine-7,9 copolyether. This polymer was found to have a M_n of 22,100 g/mol (P.D.I =1.68) using size

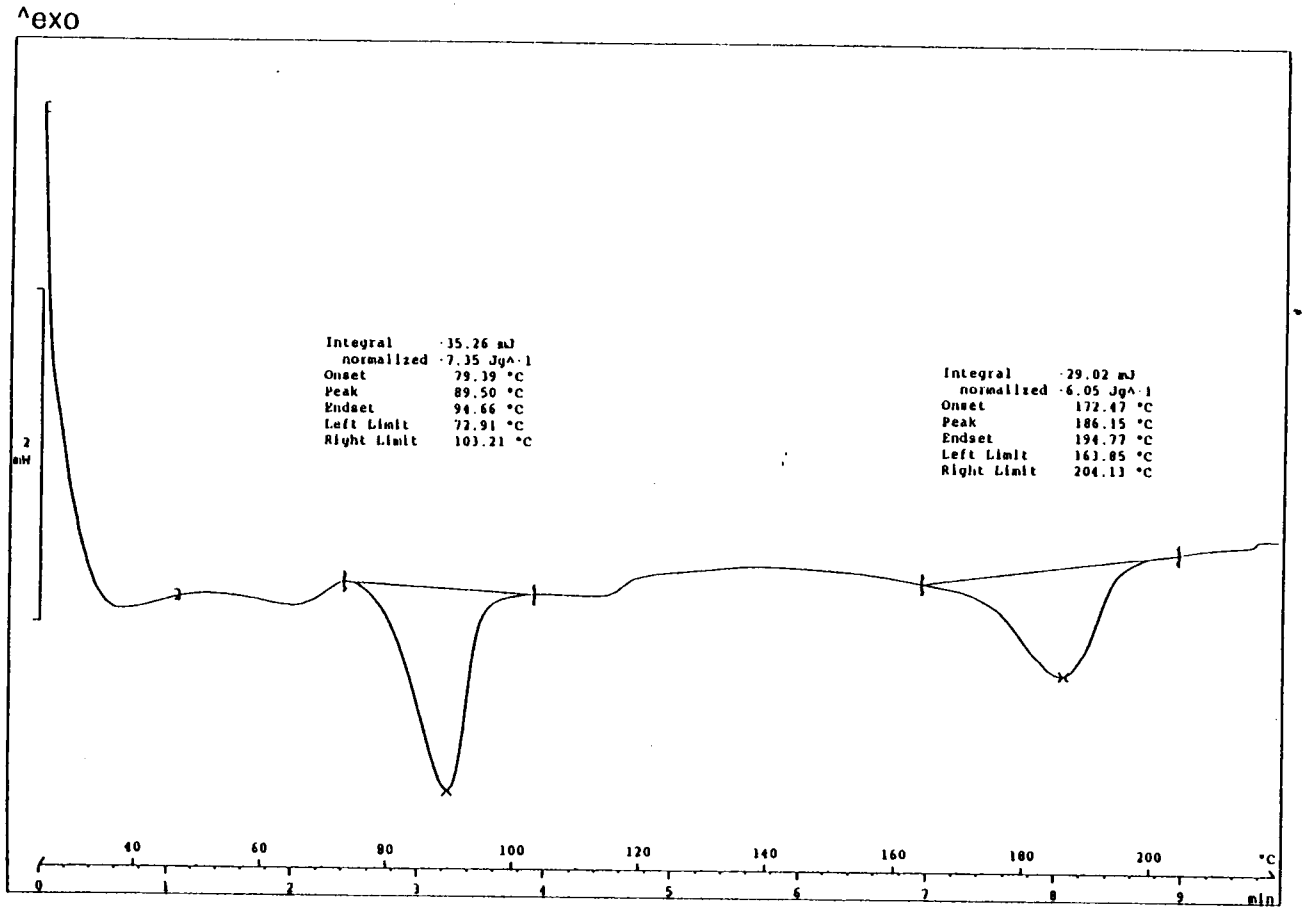

Figure 9. DSC curve of DHMS-7,9

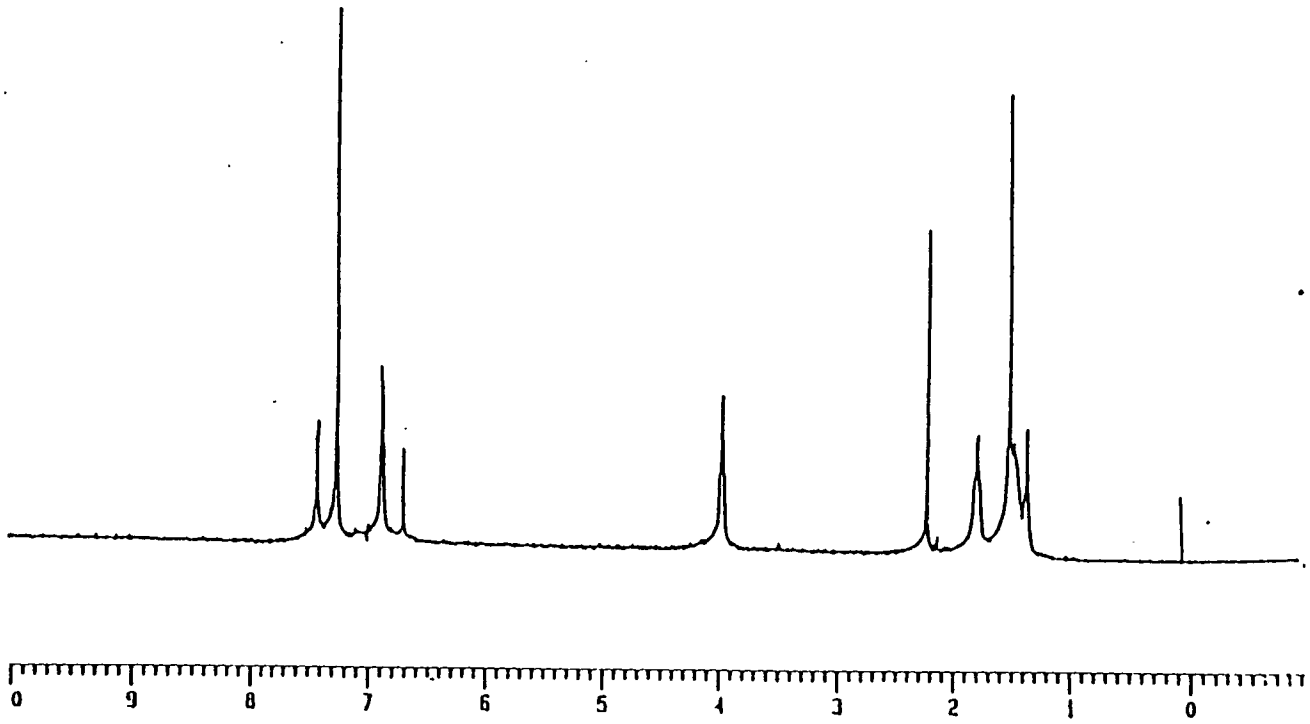

Figure 10 . ^{1}H NMR spectrum of DHMS-7,9

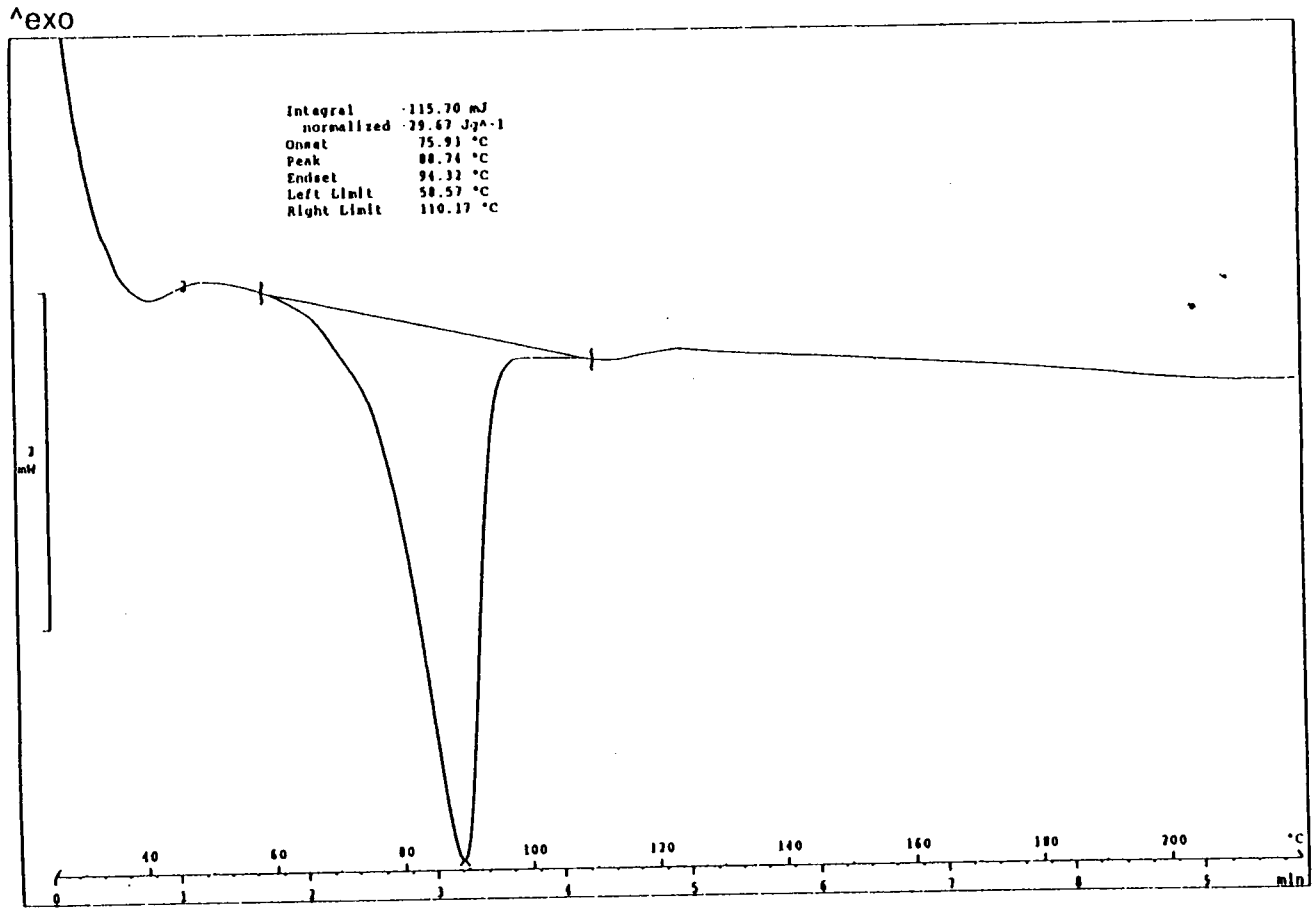

Figure 11. DSC curve of Methylene-7,9 copolyether

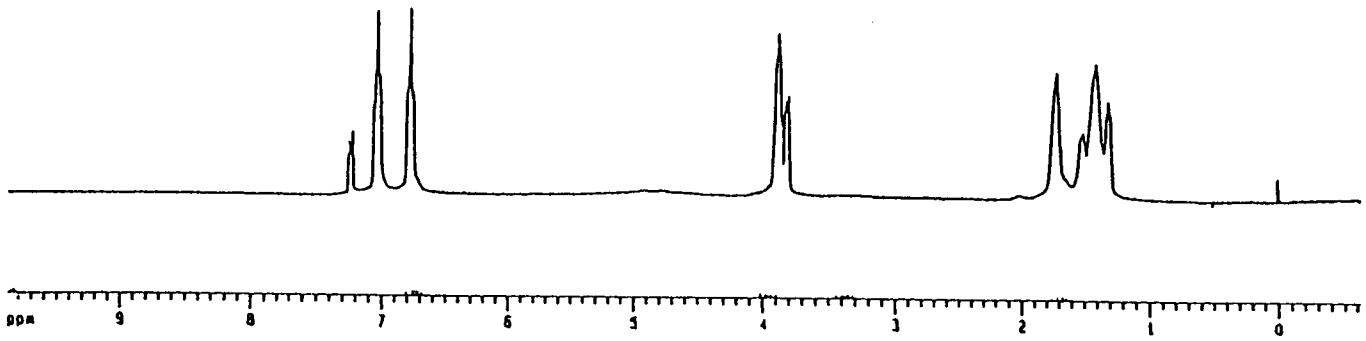

Figure 12. ^{1}H NMR spectrum of Methylene-7,9 copolyether

exclusion chromatography. The polymer shows a crystalline melting point, T_m, at 69 °C (see Figure 13); The ^1H NMR characterization of the polymer in $CDCl_3$ is as follows: 1.32, 1.43, 1.53,1.73 (14H, m, $-CH_2-$); 3.90 (4H, t, $-CH_2-O$); 6.70 (4H, d, aromatic); 7.1 (4H, d, aromatic)(see Figure 14).Yield: 62%.

1.7.6 Synthesis of bisphenol-A-7,9 copolyether

Bisphenol-A-7,9 copolyether was also synthesized using a phase transfer catalyzed polymerization of bisphenol-A, 1,7-dibromoheptane, 1,9-dibromonanoane and TBAHS. The bisphenol-A-7,9 copolyether exhibited no melting point as observed by DSC from 25 °C to 220 °C in Figure 15. The M_n of this polymer was found to be 16,800 g/mole (P.D.I = 1.95). GPC data are available in Appendix. The ^1H NMR assignment of bisphenol-A-7,9 copolyether in $CDCl_3$ as follows: 1.43, 1.45, 1.59, 1.64 (14H, m, $-CH_2-$; 1.53 (6H, s, CH_3); 3.89 (4H, t, $-CH_2-O$); 6.74 (4H, d, aromatic); 7.04 (4H, d, aromatic)(see Figure 16).Yield: 71%.

1.8 Infrared Spectroscopy

Sample preparation for completion of IR experiments consisted of solvent casting the blends on KBr disks at room temperature from THF. After a majority of the solvent had evaporated, the KBr disks were transferred to vacuum and kept there for two days to remove residual solvent. The average film thickness of the samples were 95 μm (with precision of ±25 μm) utilizing a height gauge, manufactured by Starrett Company, MA. Films prepared for this study were adequately thin to be within an absorbance range where the Beer-Lambert

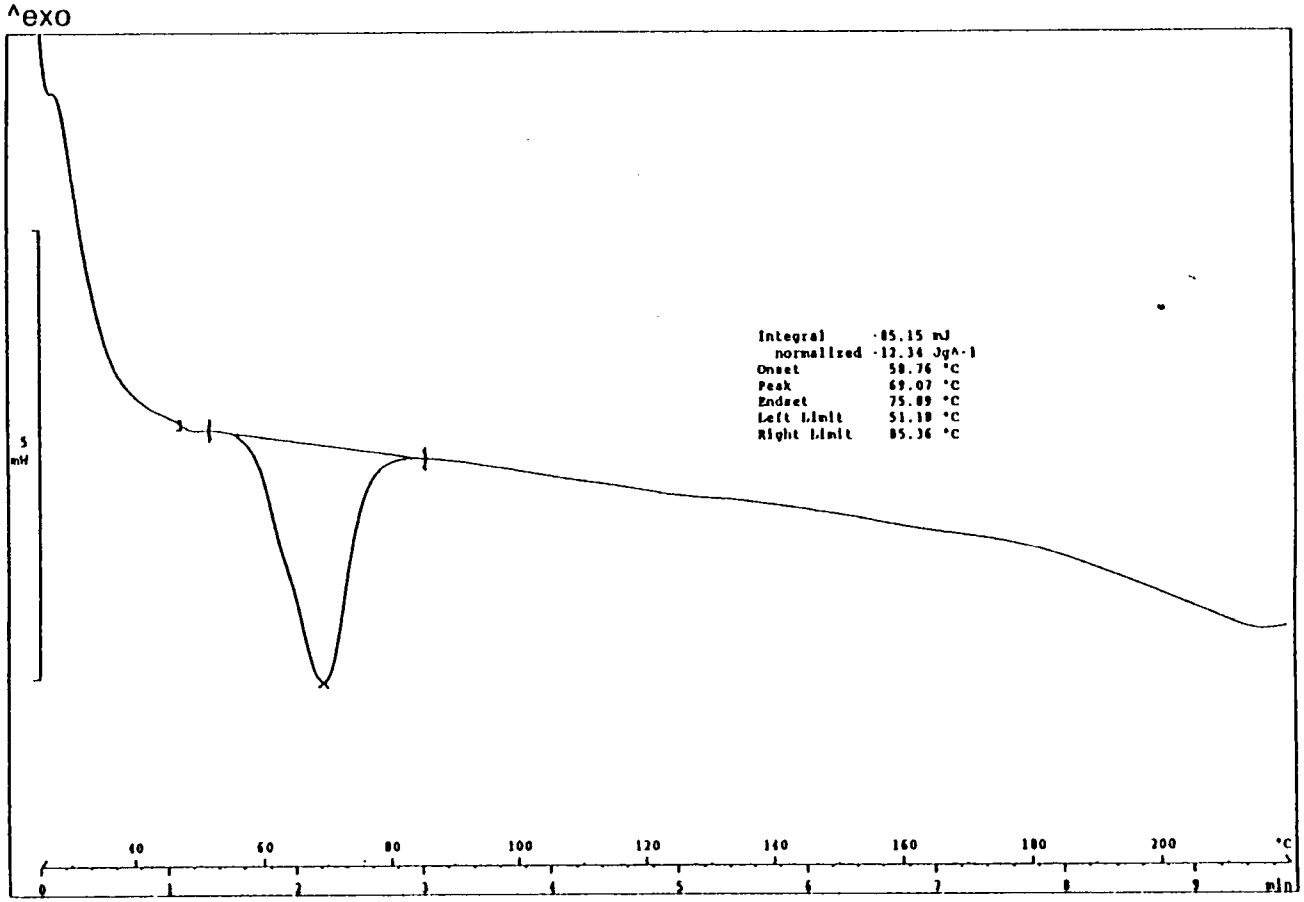

Figure 13. DSC curve of Ethylidene-7,9 copolyether

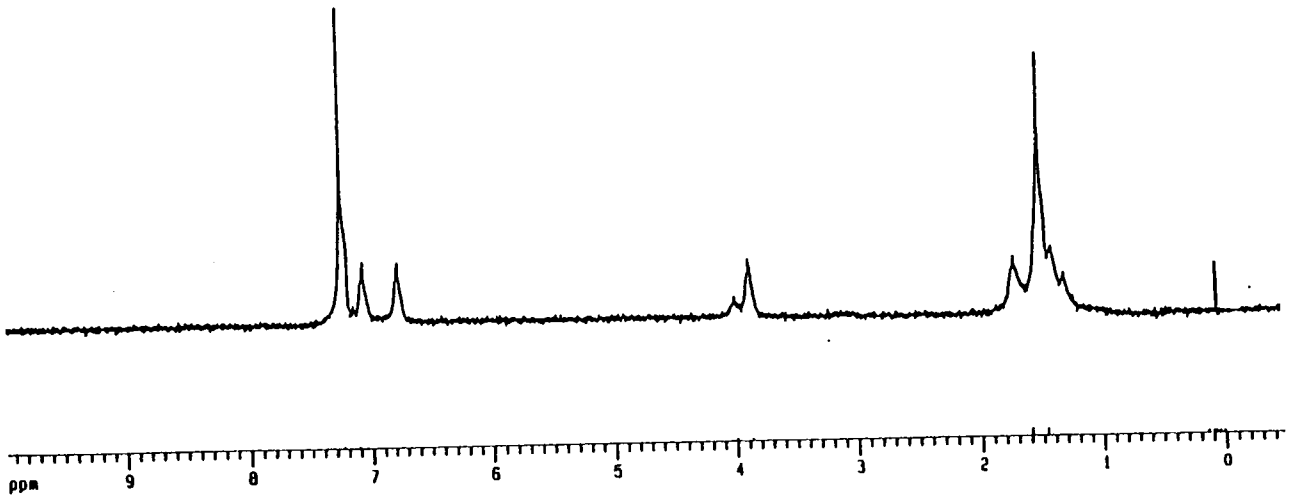

Figure 14. ^{1}H NMR spectrum of Ethylidene-7,9 copolyether

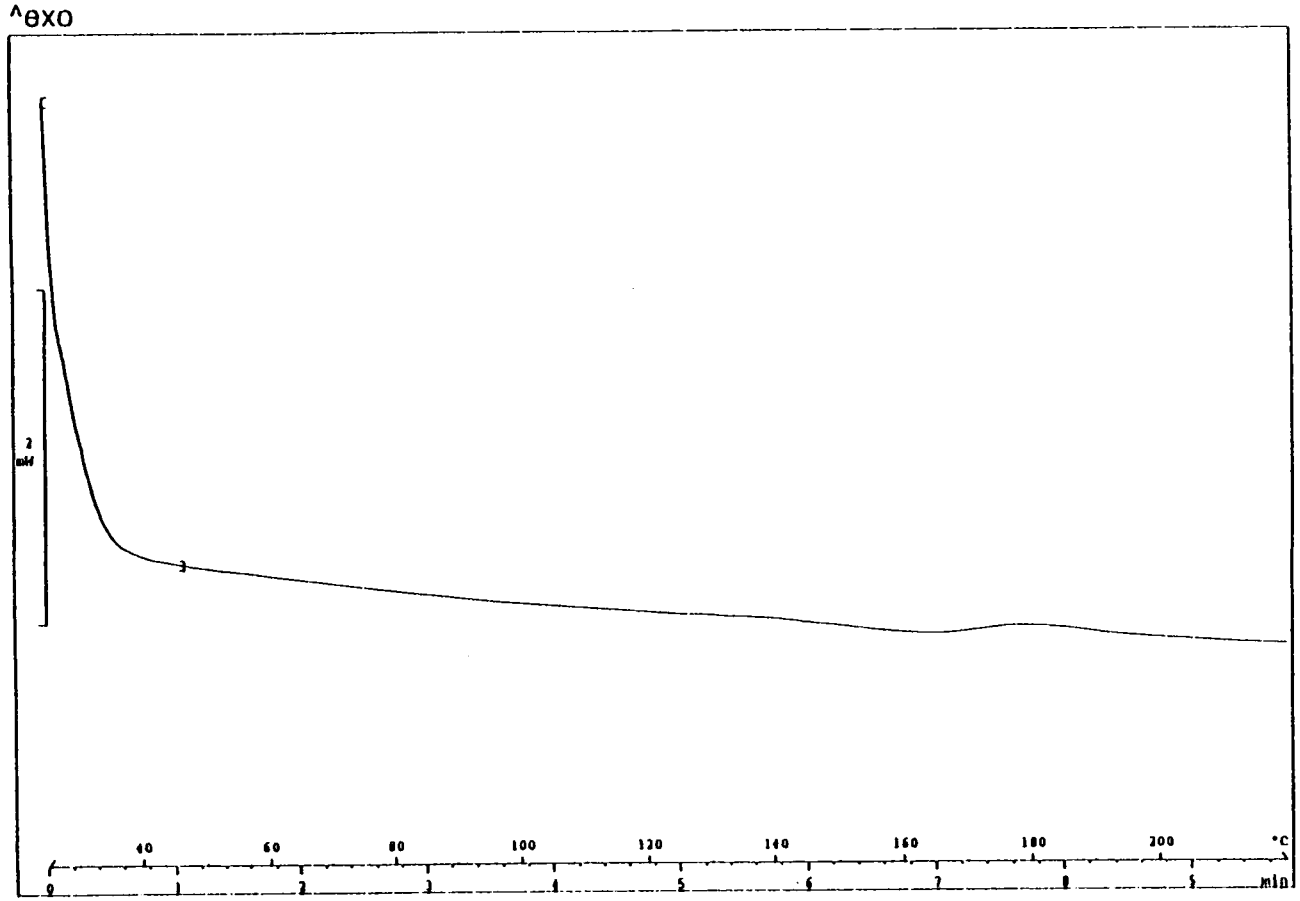

Figure 15. DSC curve of Bisphenol-A-7,9 copolyether

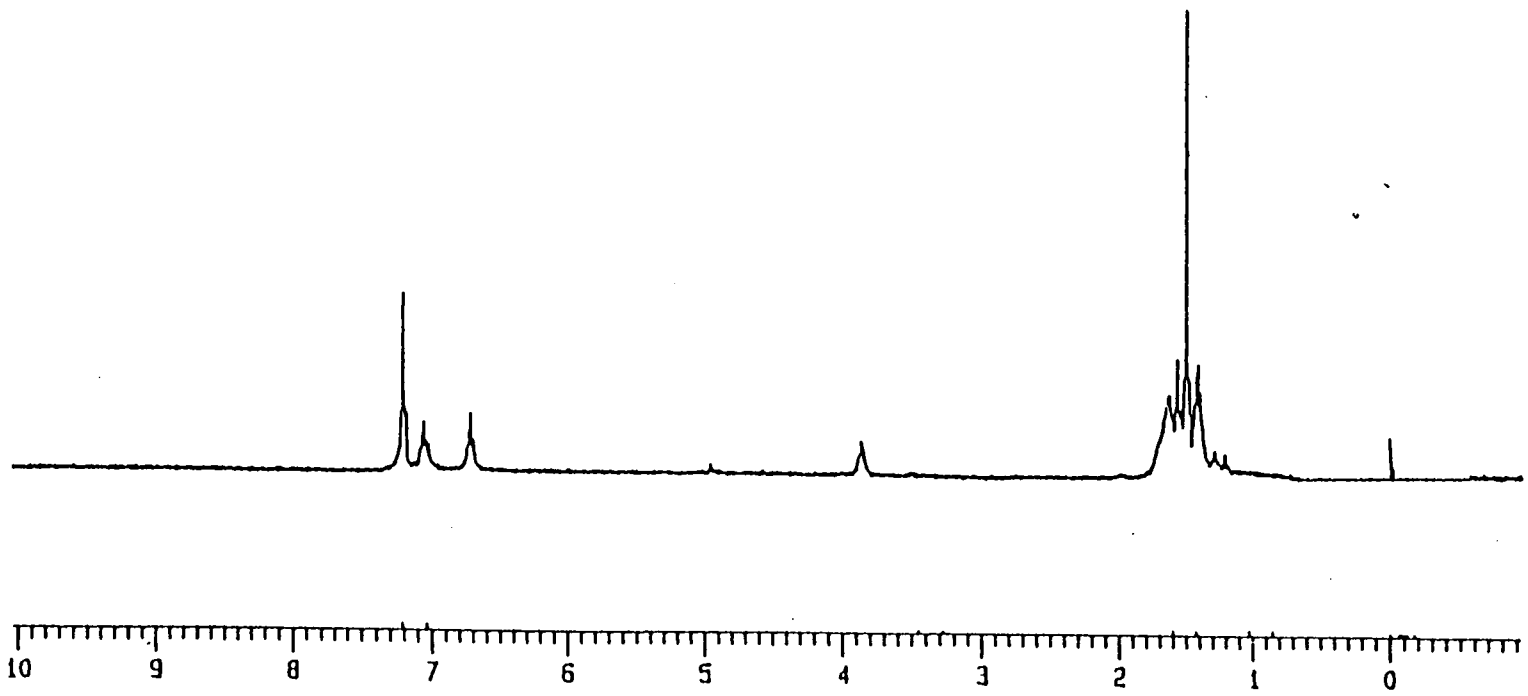

Figure 16. ^{1}H NMR spectrum of Bisphenol-A-7,9 copolyether

law is satisfied. The IR spectra were recorded on a FTS-60 Bio-Rad FT-IR purged with dried air. Sixty four scans at a resolution of 2 cm^{-1} were signal averaged and stored. The frequency scale was internally calibrated with a reference He-Ne to an accuracy of 0.2 cm^{-1} and externally with polystyrene. The curve-fitting of the absorbance IR peaks were performed by PeakFit software version 3.0, upon base-line correction of absorbance IR signals. A high temperature cell mounted in the spectrometer was employed to obtain elevated temperature spectra. The temperature was controlled to an accuracy of ±0.1 °C. For elevated temperature experiments, the temperature was kept constant for 30 minutes at a given temperature before taking the scans to ensure the samples reached thermal equilibrium. The samples which were heated from 25 °C to 40 °C and from 40 °C to 200 °C with 10 °C increment. The IR spectra of the samples were also recorded at 160 °C, 130 °C, 100 °C, 70 °C, 40 °C and eventually 25 °C in the cooling cycle. The IR spectra of samples were reproducible at any given temperature during heating or cooling cycle as long as the samples were not heated above 170 °C. This also means that the IR spectra were also reproducible for samples undergoing frequent heating or cooling process as long as the samples were not heated above 170 °C. This will be discussed further in section 1.11.

To produce a % transmittance IR spectrum, the sample single-beam spectrum is divided by the background single-beam spectrum and plotted from 0 to 100%. To make sure that the background single-beam spectrum at higher temperatures is not different from that at room temperature, the background single-beam spectra were recorded at 100 °C and 200 °C. Figure 17 shows the background single-beam spectra at 25 °C, 100 °C and 200 °C. For the sake of clarity in presentation, these spectra which were originally superimposed on each

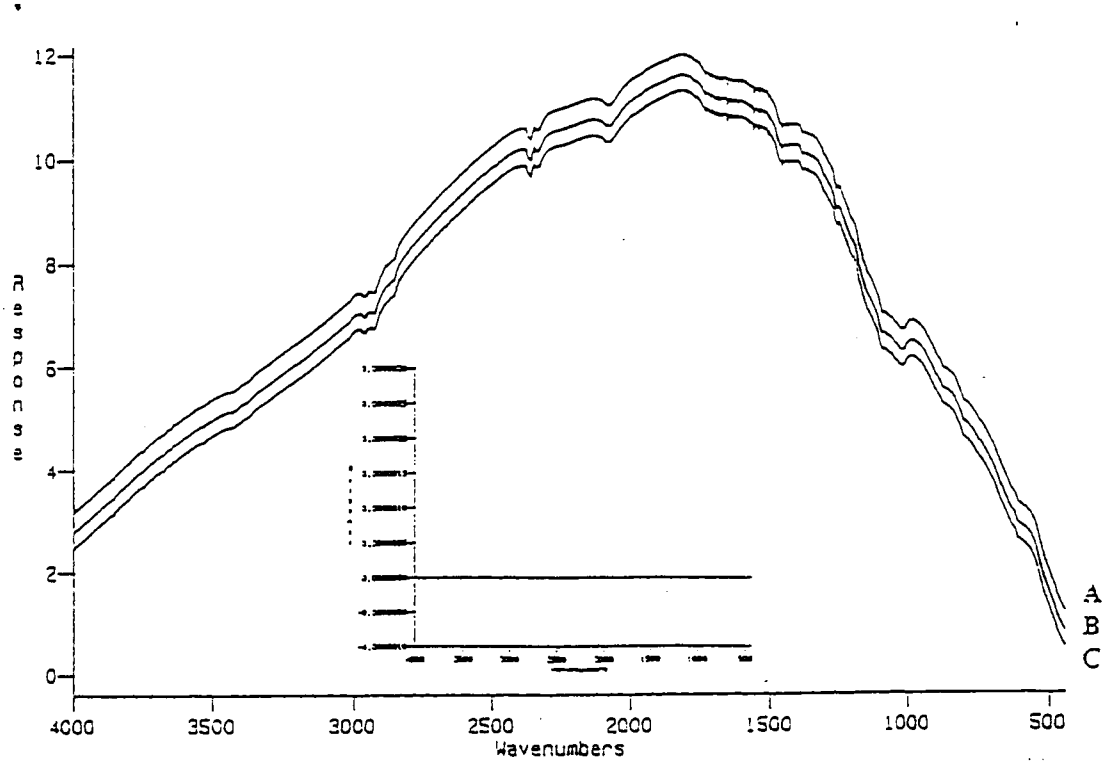

Figure 17. Single Beam background spectra at: (A) 25 °C; (B) 100 °C; (C) 200 °C. Inset is the subtractions of single beam background spectra at 100 °C and 200 °C from 25 °C.

other have been vertically separated. No significant difference was observed in the background single-beam spectra at room temperature and high temperatures. Moreover, the subtraction of single-beam spectra at 100 °C and 200 °C from 25 °C spectrum confirmed that all three spectra are identical, as shown in the inset of Figure 17. Thus, the background single-beam spectrum at 25 °C was used for both room temperature and high- temperature IR transmittance spectra.

To qualitatively determine the extent of intermolecular hydrogen bonding, the stretching band of the hydroxyl group in the region of 3000-3700 cm^{-1} is examined. Using infrared spectroscopy the stretching vibrations of "free" non-hydrogen bonded hydroxyl groups in pure PVPh can be observed at 3525 cm^{-1}, while the stretching vibration of hydroxyl groups that undergo hydrogen bonding to other –OH in pure PVPh can be found at 3370 cm^{-1}.[71] When the PS-*co*-PVPh is in a blend with a polyether, however, other possibilities occur; the hydroxyl hydrogen can form an intermolecular hydrogen bond to ethereal oxygen. In general, the ethereal oxygen in polyethers is more basic than the oxygen of an O–H in PVPh.[72] This statement can be supported by the comparison between the Pk_a values of phenol (- 8.0) and an alkyl phenoxide (- 6.5).[73] The lower Pka value of phenol compared to an alkyl phenoxide indicates that an alkyl phenoxide is more basic than phenol. This is due to the presence of electron-donating alkyl groups in an alkyl phenoxide. It is also known the basicity of a compound can be reduced by the presence of the steric hindrance of bulky substituents.[74] However, the Pka values of phenol and an alkyl phenoxide clearly shows that this is not the case here as the more hindered alkyl phenoxide is more basic than phenol which does not have a bulky alkyl substituent.

As a consequence, the intermolecular hydrogen bonding between a hydroxyl phenolic group and ethereal oxygen is stronger than that between the hydroxyl phenolic groups in pure PS-*co*-PVPh. Therefore, the O–H bonds involved in intermolecular hydrogen bonding with the ethereal oxygen become weaker than those involved in self-association among PS-*co*-PVPh molecules. This, in turn, impacts the frequency of the stretching of the O–H band. The IR band of the stretching of a hydroxyl group that participates in intermolecular hydrogen bonding will occur at a lower frequency (a red shift will occur) than that of a free or self-associated –OH group. This fact will be utilized in our analysis to determine the relative amount of intermolecular hydrogen bonding that occurs between the hydroxyl group of PS-*co*-PVPh and the ether oxygen of the polyether. The frequency of the stretching of the hydrogen bonded –OH will be correlated with the amount of intermolecular hydrogen bonding with a lower frequency equating to the formation of more intermolecular hydrogen bonds.

The frequency of the IR transmittance signals at the minimum of the peaks will be used as a measure of the frequency of the shift. Thus, the frequency of the stretching of hydrogen bonded –OH reported in the results section were determined by fitting the experimental data of the stretching vibration of the hydrogen bonded hydroxyl group between 3150 and 3630 cm^{-1} into Guassian functions. The curve fitting of the stretching hydroxyl signals were performed assuming both two bands (associated with free and hydrogen bonded –OH groups) and three bands (associated with free, intra molecular and intermolecular hydrogen bonded –OH groups). It is difficult to argue that the peak associated with the hydrogen bonded –OH groups should consist of two peaks rather than one, as the choice between these two options is not clear. However, it was found that there was no significant

differences in the trends described below when comparing the results of the two band and three band fits. As the purpose of the curve-fitting procedure is to determine a "frequency indicator" for hydrogen-bonded hydroxyl stretching vibration, we report the results for two bands in the curve-fitting process. The absorbance spectra were linearly base- line corrected from 3150-3630 cm^{-1} where there are minimal absorbances for all blends. The base line was fixed and not allowed to vary in the least squares procedure for all spectra. The frequency of the "free" hydroxyl band was fixed at 3525 $cm^{-1} \pm 1$ cm^{-1} as the strength of the free hydroxyl bond will remain the same in all blends.

1.9 Results and discussion

To verify that the observed red shift of hydrogen bonded hydroxyl band results solely from the intermolecular hydrogen bonding between hydroxyl group PVPh and with ethereal oxygen of 7,9-copolyethers, the blends of polystyrene (which does not have any suitable functional group for intermolecular hydrogen bonding with PVPh) and PVPh were examined in two different compositions (15/85, 40/60, w/w%) after annealing at 170 °C for 8 hours. The IR spectra of these blends are shown in Figure 18. The frequency of the hydrogen bonded hydroxyl band at 3370 cm^{-1} (obtained by curve-fitting) in the blends stayed the same as that of pure PVPh. Thus, the stretching frequency of the hydrogen bonded hydroxyl band was not shifted in polystyrene/PVPh blends in both compositions. This shows that more dilution does not affect the stretching frequency of hydroxyl band of vinylphenol and thus the changes described below are due to changes in the hydroxyl bond interactions in the blends.

It is known that the thermal phase transitions of polymers are strongly influenced by

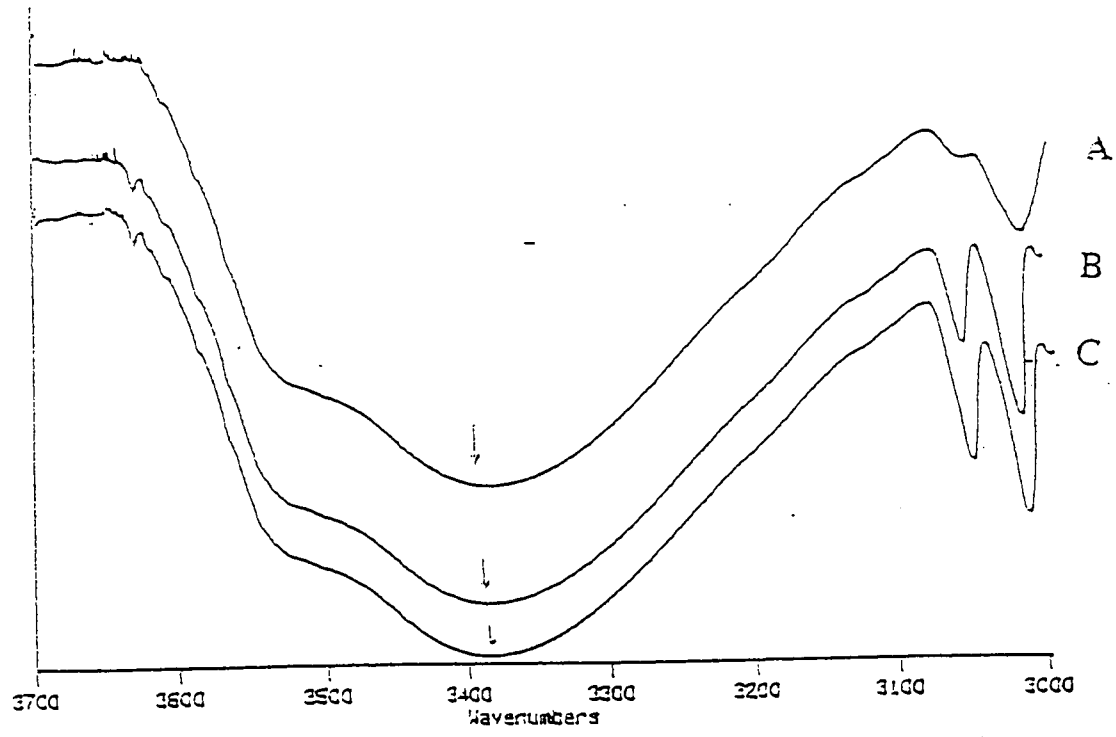

Figure 18. IR spectra of (A) Pure PVPh; (B) PS/PVPh (15/85 w/w%); (C) PS/PVPh (40/60 w/w%).

the flexibility of the polymer chain.[75] For example, poly (ethylene terephthalate) with a phenyl ring in its repeating units exhibits a glass transition of 69 °C and a crystalline melting point of 265 °C (see Figure 19). In contrast, poly (ethylene adipate) has a melting point of 50 °C. Poly (ethylene adipate) replaces the phenyl ring in PET with a C_4 aliphatic group. Though the C_4 aliphatic spacer has similar dimensions to the phenyl ring, the increased flexibility results in poorer packing of chains and a decrease in the crystalline melting point of the polymer. Similarly, it is well understood that a further increase in rigidity can result in the formation of a liquid crystalline phase as the polymer chain becomes more rodlike. For instance, if a phenyl group replaces the ethylene group in PET, the resulting polymer becomes very rigid as it has very little freedom of rotation about bonds in the chain backbone. This results in a compound that forms a liquid crystalline phase with a very high melting point (>600 °C). Thus, we will utilize the thermal phase behavior and crystalline melting point as a means to qualitatively rank DHMS-7,9, methylene-7,9, and ethylidene-7,9 in rigidity. This correlation is only possible because other important parameters that affect the melting point such as chain packing, molecular weight, and intermolecular interactions are very similar for these polymers.

The thermograms of the four 7,9-copolyethers were measured from 25 °C to 220 °C at 10 °C/min and are shown in Figure 20. These results and optical microscopy show that DHMS-7,9 exhibits a crystalline melting point at 90 °C and liquid crystalline phases between 90 °C and 190 °C. The presence of a liquid crystalline phase (and its absence for the other polymers) proves that this polymer is the most rigid of these polyethers. Replacement of the stiff methyl stilbene mesogen with a methylene group provides more rotational freedom about

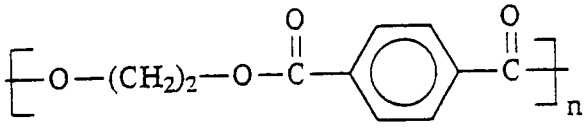

Poly (ethylene Terephthalate)

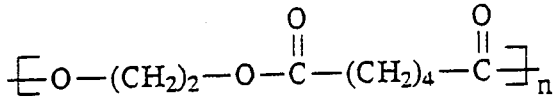

Poly (ethylene adipate)

Figure 19. The chemical structure of poly(ethylene terephthalate) and poly (ethylene adipate)

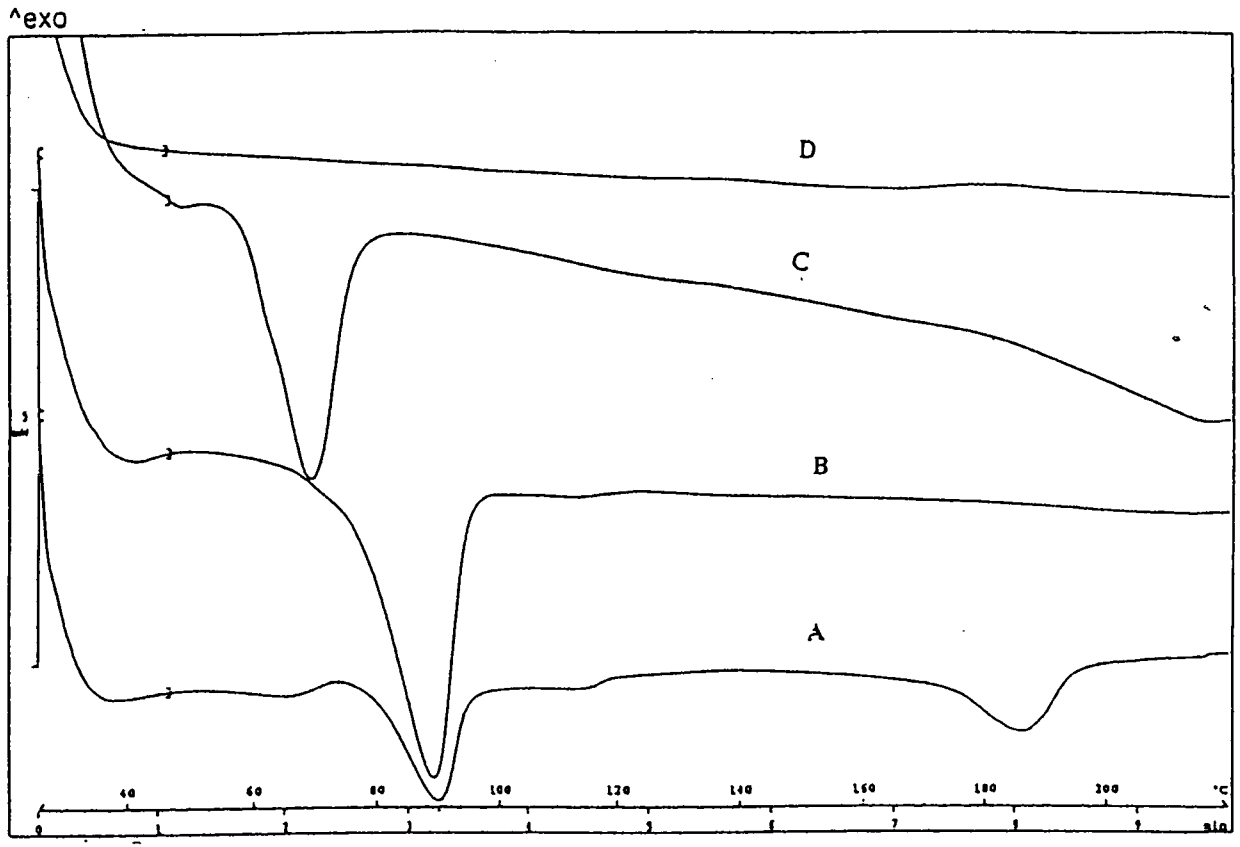

Figure 20. DSC of (A) DHMS-7,9-copolyether; (B) Methylene-7,9- copolyether; (C) Ethylidene-7,9-copolyether; (D) Bisphenol-A-7,9-copolyether

the polymer backbone. Thus, one would expect that this alteration will result in a polymer that is slightly more flexible than DHMS-7,9. The DSC results support this prediction, showing a compound that has lost liquid crystalline behavior and has a crystalline melting point that is very similar to that of DHMS-7,9. The addition of another methylene group to two phenols in ethylidene-7,9 should further increase the flexibility of polymer chain. This is born out by the DSC curve, which shows a decrease in the crystalline melting point of the polymer to 69 °C. Thus, the thermal phase behavior of these three polymers supports the prediction that the rigidity of the polymer chains decreases as one goes from DHMS-7,9 copolyether to ethylidene-7,9 copolyether in Figure 8. The rigidity of bisphenol-A-7,9 must be considered differently from the other 7,9-copolyethers in Figure 8. This is due to the fact that an additional parameter, chain packing, which alters the melting point and phase behavior of a polymer chain, is important in the comparison of bisphenol-A -7,9 with other three polyethers.

1.10 The Effect of Temperature on Intermolecular Hydrogen bonding

Hydrogen bonds are dynamic entities in that they are continuously breaking and reforming. This formation and breaking can be thought of as an equilibrium which can be characterized by an equilibrium constant at any given temperature.[76] It is expected that with increasing temperature, the hydrogen bonds will favor dissociation due to increased thermal energy. Therefore the average amount of intermolecular hydrogen bonding decreases with increased temperatures.

Thus, we are interested in determining the effect of temperatures above the glass transition temperature and melting point of both polymers on the amount of intermolecular

hydrogen that exists in blends of PS-*co*-PVPh and the 7,9-copolyethers. Figure 21 represents the hydroxyl region of the IR spectra in PVPh/DHMS-7,9 blend (65/35, w/w%) at various temperatures. The arrows in Figure 21 represent the minima in the stretching frequency of the hydrogen bonded hydroxyl group as determined by the curve fitting procedure. Examination of this figure shows that the stretching frequency of the free hydroxyl band remains near 3525 cm^{-1} regardless of temperature, due to the fact that strength of the free O–H bond is relatively independent of temperature. In contrast, the stretching frequency of the blend is 3375 cm^{-1} at 100 °C and 3433 cm^{-1} at 200 °C. Interpretation of these results leads to the conclusion that the amount of intermolecular hydrogen bonding does indeed decrease with an increase in temperature. Similar behavior was observed for blends of PVPh with all 7,9-copolyethers. This is shown in Figure 22 and Figure 23. Figure 22 shows a plot of the stretching frequency of the hydrogen bonded hydroxyl band versus temperature for blends of PVPh and DHMS-7,9 at various compositions, whereas Figure 23 shows the same parameters for blends of PVPh with all four polyethers for a composition of 65% PVPh and 35% polyethers. An increase in the strength of O–H bond of PVPh is observed as the amount of intermolecular hydrogen bonding between PVPh and 7,9-copolyethers decreases at elevated temperatures. Therefore, a higher υ_{OH} corresponds to less intermolecular hydrogen bonding between PVPh and 7,9-copolyethers.

Figure 22 shows that at any given temperature the amount of intermolecular hydrogen bonding changes with blend composition. This change suggests an increase in the number of intermolecular hydrogen bonds with an increase of PVPh content in the blends. This point will be discussed in more detail below. The interpretation of Figure 22 also reveals that the

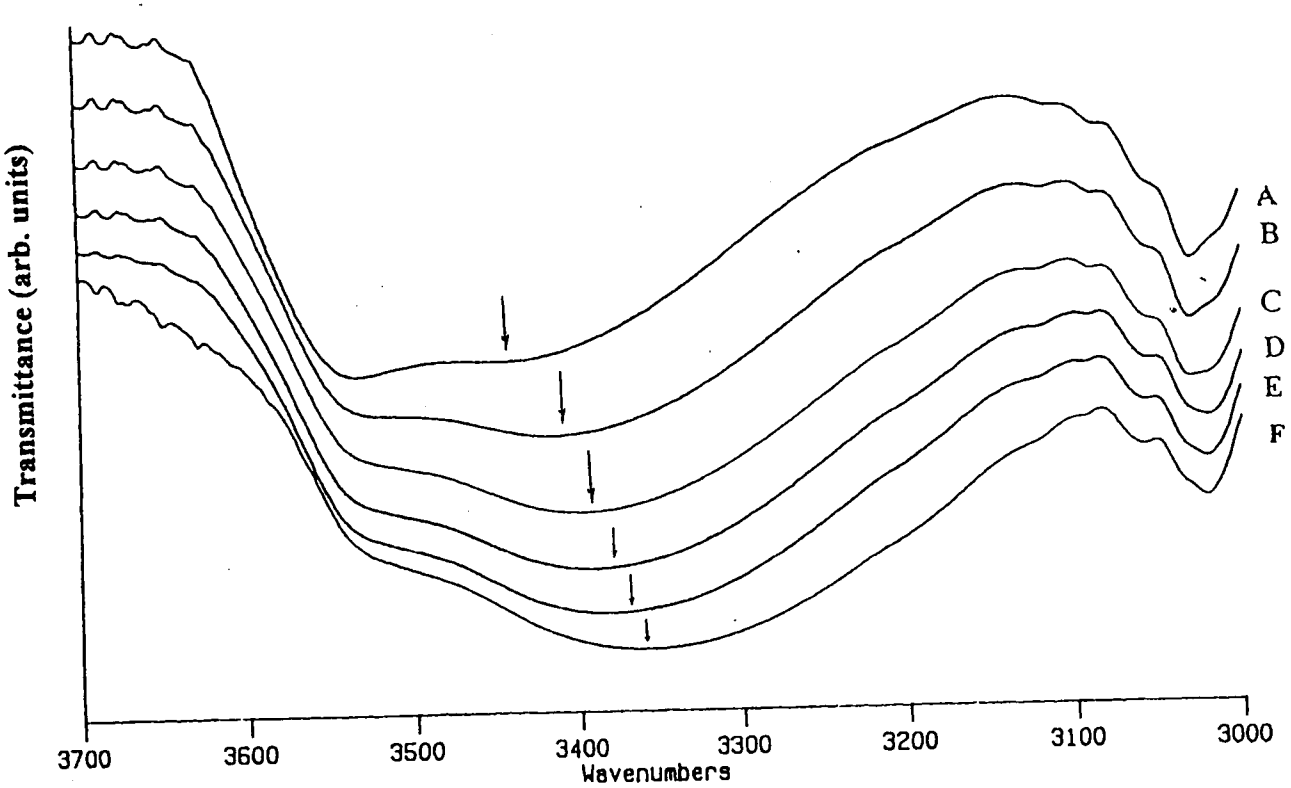

Figure 21. The IR spectra of the hydroxyl region of PVPh/DHMS-7,9 (65/35 w/w%) at various temperatures.(A) 200 °C; (B) 150 °C; (C) 120 °C; (D) 100 oC; (E) 70 °C ; (F) 25 °C.

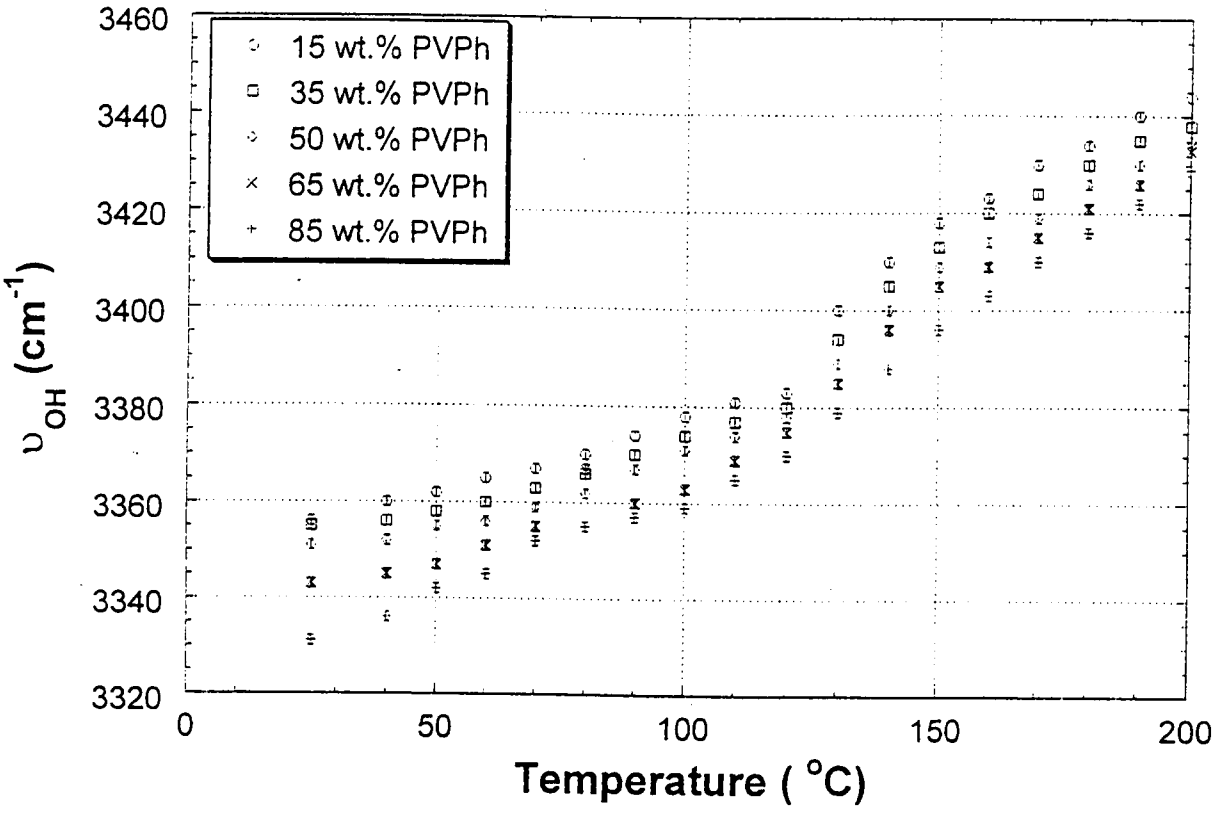

Figure 22. The plot of the stretching frequency of hydrogen bonded hydroxyl band in PVPh/DHMS-7,9 blends at various composition as a function of temperature.

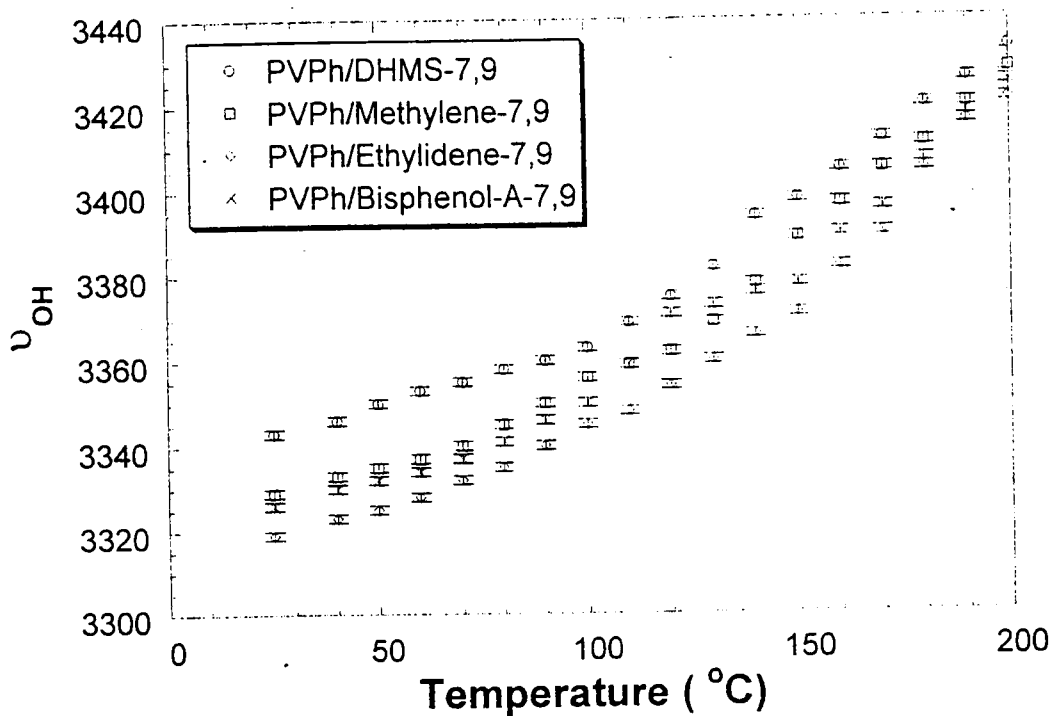

Figure 23. The plot of the stretching frequency of hydrogen bonded hydroxyl band in PVPh/7,9-copolyether blends (65/35, w/w%) as a function of temperature.

temperature dependence of υ_{OH} exhibits two distinct regimes; one at low temperatures, where the change in the amount of intermolecular hydrogen bonding shows a smaller temperature dependence and the other at high temperatures, where the change in intermolecular hydrogen bonding is more sharply dependent on temperature. The transition temperature depends on blend composition indicating that the existence of these two regimes is most likely due to the thermal transitions of PVPh and DHMS-7,9. One or both polymers are relatively immobile at low temperatures and therefore any changes in intermolecular hydrogen bonding in this regime are due to segmental (local) motions. It should be noted that at temperatures below the glass transition of the polymers, the thermal energy of the blend is not sufficient to overcome the rotational and hydrogen bonding energy barriers of the polymers. This results in low mobility of the polymers at these temperatures. However, at higher temperatures, with an increase in the thermal energy of the blend, the polymers overcome the rotational and hydrogen bonding energy barriers. Thus, the mobility of the polymer chains increases as the DHMS-7,9 melts and the PVPh undergoes a glass transition. DHMS-7,9 is nematic above 120 °C. It is also known that at temperatures above 120 °C DHMS-7,9 flows rather easily in the nematic phase suggesting an increase in the polymer chain mobility.[77] Thus, at high temperatures the rate of loss of intermolecular hydrogen bonds increases due to both rotational motions and global motions. In other words, the increased chain mobility and rotational freedom in this regime facilitates the breaking of intermolecular hydrogen bonds.

Figure 23 provides evidence of the effect of rigidity on intermolecular hydrogen bonding. For any given composition, the amount of intermolecular hydrogen bonding increases as the flexibility of the 7,9-copolyether increases. This figure suggests a similar trend

for the temperature dependence of υ_{OH} in two distinct regimes (around 100 °C) for other PVPh/7,9-copolyether blends. This figure also shows that the temperature dependence discussed above for the DHMS-7,9 blend is also evident for the other 7,9-copolyether blends, i.e. a temperature around 100 °C approximately delineates a change in slope in the plot. This is surprising as one might expect that the different melting and glass transition temperatures of the 7,9-copolyethers would result into different delineation temperatures. A possible explanation for this behavior is that the reduction of glass transition temperature of PVPh in these blends could increase the mobility of PVPh at temperatures lower than Tg of pure PVPh (147 °C). Examination of the thermal behavior of these blends provides supporting evidence for this explanation.

Figures 24 shows the DSC curves for the blends of PVPh with DHMS-7,9, methylene-7,9 and ethylidene-7,9 (65/35, w/w%). As shown in this Figure, the Tg of PVPh is lowered to ca. 112 °C in PVPh/DHMS-7,9 blend, to ca.103 °C in PVPh/methylene-7,9 blend and to ca. 95 °C in PVPh/ethylidene-7,9 blend. These reductions are probable due to the plasticizing effect of 7,9-copolyethers on the Tg of PVPh. Thus, in the DHMS-7,9 blend, both polymers become mobile above 112 °C. This transition occurs at 103 °C for the methylene-7,9 blend and 95 °C for the ethylidene-7,9 blend. Comparing of this data to Figure 22 shows that these temperatures are in the general region of the delineation temperatures in Figure 22, where the transition from a shallow to a sharper temperature dependence occurs. Thus, these data support the interpretation that the change in slope at delineation temperatures is due to a change in polymer mobility in the blends.

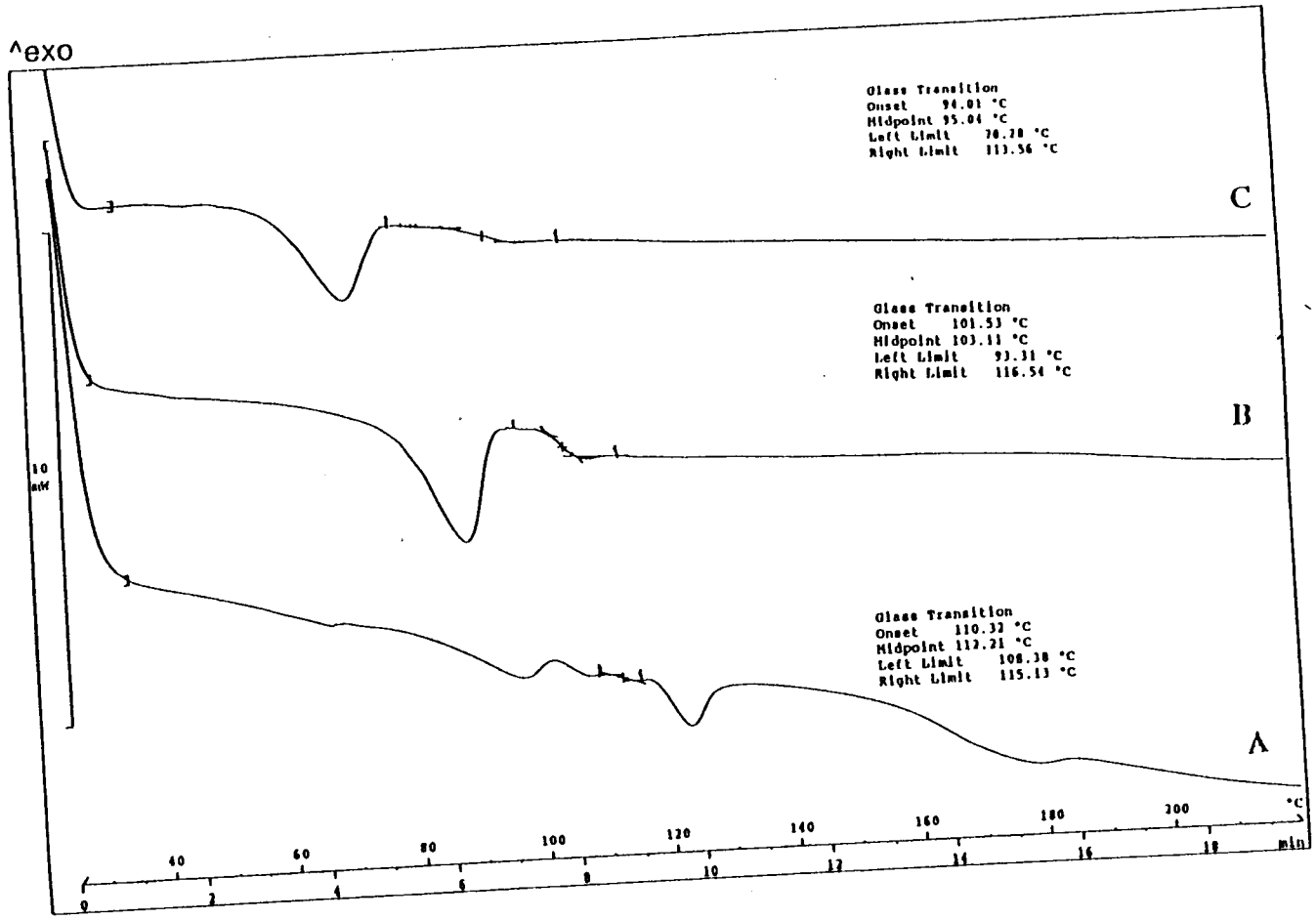

Figure 24. DSC curves of (A)PVPh/DHMS-7,9 (65/35 w/w%); (B) PVPh/Methylene-7,9 (65/35, w/w%); (C) PVPh/Ethylidene (65/35, w/w%).

1.11 Effect of High- Temperature Annealing on Intermolecular Hydrogen Bonding

It is well known that blends that are formed by solution casting are often not equilibrium structures due to varying solvent-polymer interactions among the blend constituents. Thus, we have sought to determine the effect of thermal annealing above T_g of both polymers to ascertain the equilibrium structure of these blends. Pursuant to this, each of the PS-*co*-PVPh/7,9-copolyether blends was annealed at temperatures above the glass transition or crystalline melting point of all the polymers up to 200 °C for 8 hours and then cooled to room temperature. This annealing procedure will allow the polymers to relax to their equilibrium conditions. The IR spectra were thus obtained and analyzed before and after the annealing procedure.

The results for the 50/50 (w/w%) blends of PVPh and each 7,9-copolyether after 8 hours of annealing at 170 °C are shown in Table 1. Interpretation of Table 1 shows that the stretching frequency of the hydrogen bonded hydroxyl band (υ_{OH}) is identical before and after annealing temperatures up to 170 °C. This is somewhat surprising as the previous results demonstrate that at 170 °C the amount of intermolecular hydrogen bonding is less than at room temperature. Additionally, 170 °C is in the temperature range where the amount of intermolecular hydrogen bonding is decreasing rapidly with temperature. One might expect that the increased slope at higher temperatures in Figure 22 might correspond to an irreversible process, such as change in the dispersion of the blend or phase separation. These results demonstrates that this is not the case. These results demonstrate that bringing the sample to a temperature up to 170 °C does not alter the amount of hydrogen bonding that occurs at room temperature, i.e. the breaking and reforming of hydrogen bonds is reversible.

Table 1

Effect of High Temperature Annealing on the Hydrogen Bonded Stretching Frequency (υ_{OH})

	DHMS-7,9 Blends (cm^{-1})	Methylene-7,9 Blends (cm^{-1})	Ethylidene-7,9 Blends (cm^{-1})	Bisphenol-A-7,9 Blends
As Cast	3351	3343	3327	3330
Annealed 170°C, 8 hours	3351	3343	3327	3330

More importantly, they also show that the blends that are formed from solution casting are similar to the equilibrium structure.

In Figure 25, the difference in stretching frequency of the hydrogen bonded hydroxyl band before and after annealing ($\Delta\upsilon_{OH}$) in the PVPh/7,9-copolyether blends (85/15, w/w%) is plotted at different annealing temperatures. The magnitude of $\Delta\upsilon_{OH}$ can be considered as a measure of decrease in the amount of intermolecular hydrogen bonding in the blends due to irreversible breaking and reforming of hydrogen bonds upon annealing. The annealing of blends at temperatures higher than 170 °C show a decrease in the amount of intermolecular hydrogen bonding of the blends after annealing. The magnitude of the difference in the stretching frequency of the hydrogen bonded hydroxyl group before and after annealing ($\Delta\upsilon_{OH}$) increases with annealing temperature between 170 °C and 200 °C in all blends of PVPh/7,9-copolyethers. Loss of hydrogen bonding signifies that in this temperature region the breaking and reforming of hydrogen bonds is irreversible. One possible explanation is that an irreversible process occurs that lowers the number of intermolecular contacts between two polymers, which in turn lowers the amount of intermolecular hydrogen bonding between PVPh and 7,9-copolyethers that can form as the blends cool to room temperature. This type of process could occur if the system undergoes a change in dispersion within the blend or phase separation. This also means that the stretching frequency of the hydrogen bonded hydroxyl band (υ_{OH}) is not reproducible in PVPh/7,9-copolyether blends upon heating or annealing at temperatures above 170 °C due to the irreversible process of breaking and reforming hydrogen bonds.

In Figure 26, $\Delta\upsilon_{OH}$ also decreases with increased flexibility of the 7,9-copolyether

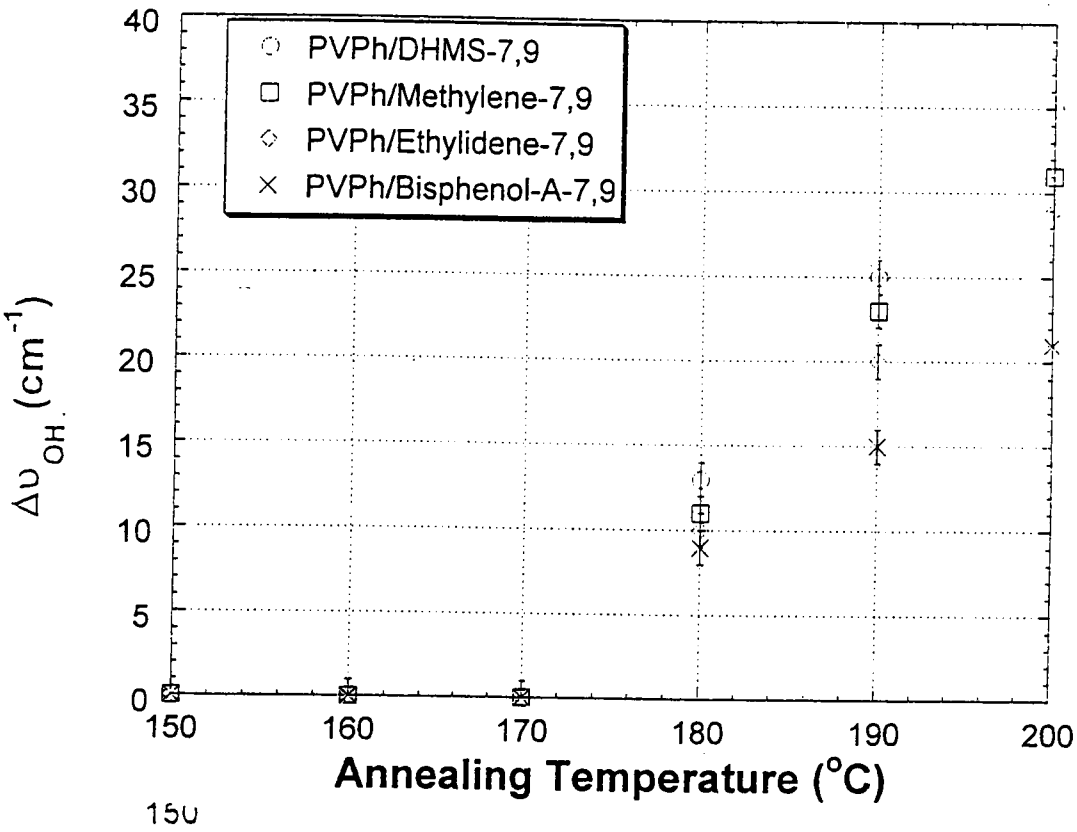

Figure 25. The plot of the difference in the stretching hydrogen bonded hydroxyl band in PVPh/7,9-copolyether blends (85/15, w/w%) before and after annealing ($\Delta\upsilon_{OH}$) at different temperatures for 8 hours.

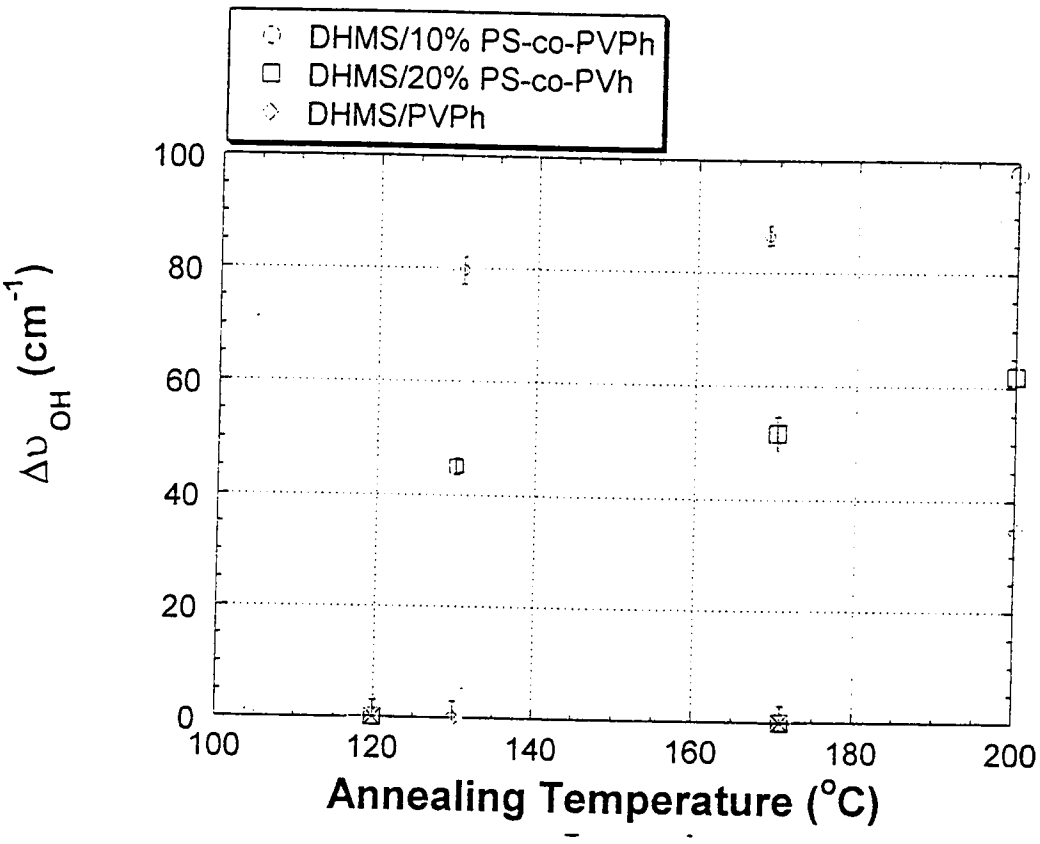

Figure 26. The plot of the difference in the stretching hydrogen bonded hydroxyl band before and after annealing ($\Delta\upsilon_{OH}$) at different temperatures for 8 hours in PS-*co*-PVPh/DHMS-7,9 blends (85/15, w/w%); (A)10% PVPh; (B) 20% PVPh; (C) 100% PVPh.

from PVPh/DHMS-7,9 blends to PVPh/bisphenol-A-7,9-copolyether blends. These results suggest that flexible polymer retains a better dispersion (mixing) in the blends than the more rigid 7,9-copolyether. Figure 26 shows the difference in the stretching frequency of the hydrogen bonded hydroxyl band ($\Delta\upsilon_{OH}$) before and after annealing in blends of PS-*co*-PVPh (10%, 20% and 100% PVPh) and DHMS-7,9 versus annealing temperature. This plot demonstrates that $\Delta\upsilon_{OH}$ goes up and thus the amount of hydrogen bonding decreases, as the annealing temperature increases in all blends regardless of the amount of PVPh content in PS-*co*-PVPh. This figure also shows that the stretching frequency of the hydrogen bonded hydroxyl band is equal before and after annealing at temperatures up to 130 °C in PS-*co*-PVPh (10% and 20% PVPh)/DHMS-7,9. Thus, the irreversible process that alters the hydrogen bonding occurs at a lower annealing temperature (130 °C) in PS-*co*-PVPh/DHMS-7,9 blends than for PVPh/DHMS-7,9 blend. One explanation may be that PS-*co*-PVPh (10% and 20% PVPh) have lower glass transitions (ca. 83 °C and ca. 91 °C, respectively) than pure PVPh (ca. 147 °C). This means that less thermal energy is needed to mobilize polymer chains in PS-*co*-PVPh (10% and 20% PVPh) blends than in PVPh blends. As a result, the irreversible process that alters the hydrogen bonding occurs in lower annealing temperatures in PS-*co*-PVPh blends (10% and 20% PVPh) than for PVPh blends.

1.12 Effect of Blend Composition on Intermolecular Hydrogen Bonding

The next parameter of interest is the effect of blend composition on the intermolecular hydrogen bonding in PS-*co*-PVPh/7,9-copolyethers blends. Figure 27 shows the IR spectra of PVPh and ethylidene-7,9-copolyether blends in the hydroxyl region for blends with

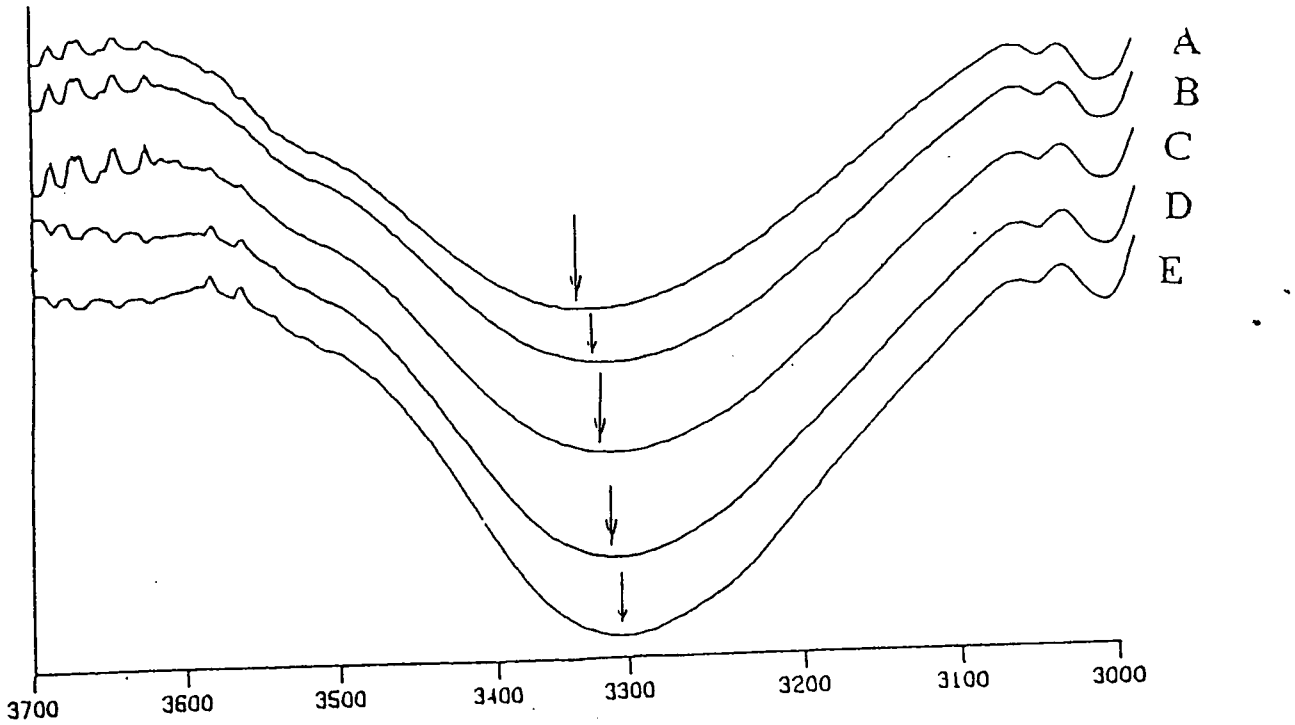

Figure 27 . IR spectra of the hydroxyl region in PVPh/ethylidene-7,9 copolyether with various compositions after annealing at 170 °C for 8 hours. (A) 15/85 (w/w%); (B) 35/65 (w/w%); (C) 50/50 (w/w%); (D) 65/35 (w/w%); (E) 85/15 (w/w%).

different blend compositions after annealing at 170 °C for 8 hours. Note that the PVPh content in PVPh/ethylidene-7,9-copolyether blends increases from curve A to curve E. Examination of this figure shows that the frequency of the hydrogen bonded hydroxyl band shifts towards lower frequency from curve A to E indicating that the amount of intermolecular hydrogen bonding increases as the amount of PVPh increases in the blend. The frequency of the stretching vibration of the hydrogen bonded hydroxyl group can be extracted from these plots using the fitting procedure described above. The result of curve fitting for the blends are also shown in Figure 28 and in appendix. Completion of this analysis for all blends provides the information required to produce Table 2 and Figure 29. Figure 29 shows a plot of the frequency of the stretching vibration of the hydrogen bonded hydroxyl group, ν_{OH},(tabulated in Table 2) versus the percentage of PVPh in the blends.

Interpretation of this plot shows that for each blend studied in this project, as the amount of PVPh increases, the amount of intermolecular hydrogen bonding increases. One would expect that if each -OH group could participate in intermolecular hydrogen bonding, the amount of intermolecular hydrogen bonding would reach a maximum in blends with equal concentrations of the hydroxyls of PVPh and the ethereal oxygens of 7,9-copolyethers. However, the continuous increase in intermolecular hydrogen bonding with PVPh concentration suggests that this is not the case. This is because not all hydroxyl groups of PVPh can participate in intermolecular hydrogen bonding with 7,9-copolyethers, which is not surprising. However, it is surprising that there is no turnover in this plot at high concentration of PVPh, as the amount of intermolecular hydrogen bonding must be zero at both ends of this plot. Therefore, all four spectra must connect to the pure PVPh data point at 3370 cm^{-1} on

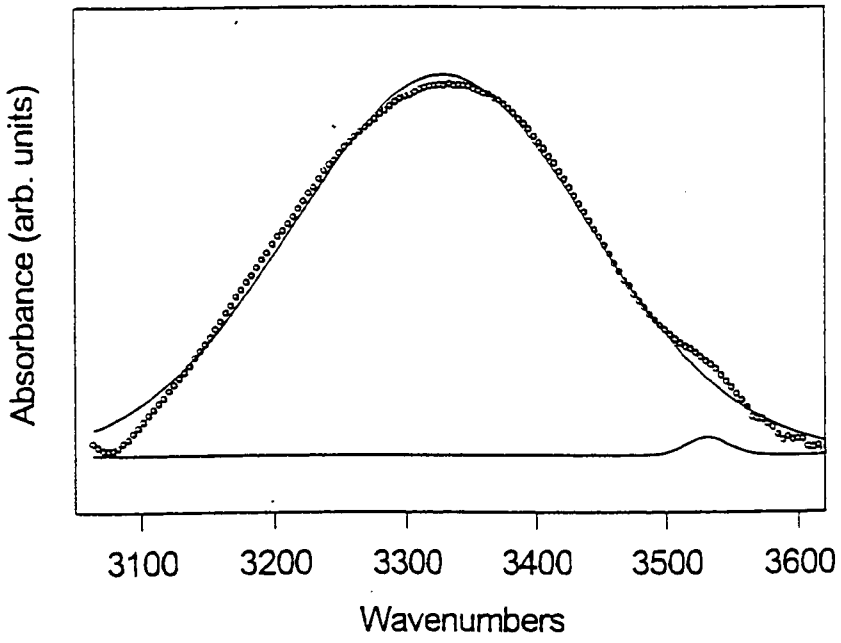

Curve-Fit Std Error= 0.000446408831 r2= 0.99864166

Curve-Fit Coefficients

Peak#	Type	Ampl	Ctr	Wid1	Wid2	Wid3
1	Gaussian	0.0296519	3327.7601	114.39938		
2	Gaussian	0.0013632	3525.9321	14.636983		

Measured Values

Peak#	Type	PkAmpl	PkCtr	Wid@HM	Area	%Area
1	Gaussian	0.0296519	3327.7601	269.38965	8.378642	99.406607
2	Gaussian	0.0013632	3525.9321	34.467262	0.0500151	0.593393
	Total				8.4286571	100

Figure 28. Curve-fitting of the hydroxyl region in PVPh/ethylidene-7,9 (50/50 w/w%) after annealing at 170 °C for 8 hours.

Table 2

Hydrogen Bonded Hydroxyl Frequency (υ_{OH}) in PVPh/7,9-copolyethers Blends with Different Compositions after Annealing at 170 °C for 8 hours.

Blend Composition*	7,9-DHMS blends (cm^{-1})	7,9-Methylene blends (cm^{-1})	7,9-Ethylidene blends (cm^{-1})	7,9-Bisphenol-A blends (cm^{-1})
15/85	3356	3354	3344	3342
35/65	3355	3351	3341	3332
50/50	3351	3343	3325	3330
65/35	3343	3329	3319	3326
85/15	3331	3324	3306	3319

* (PVPh/7,9-copolyether, w/w%)

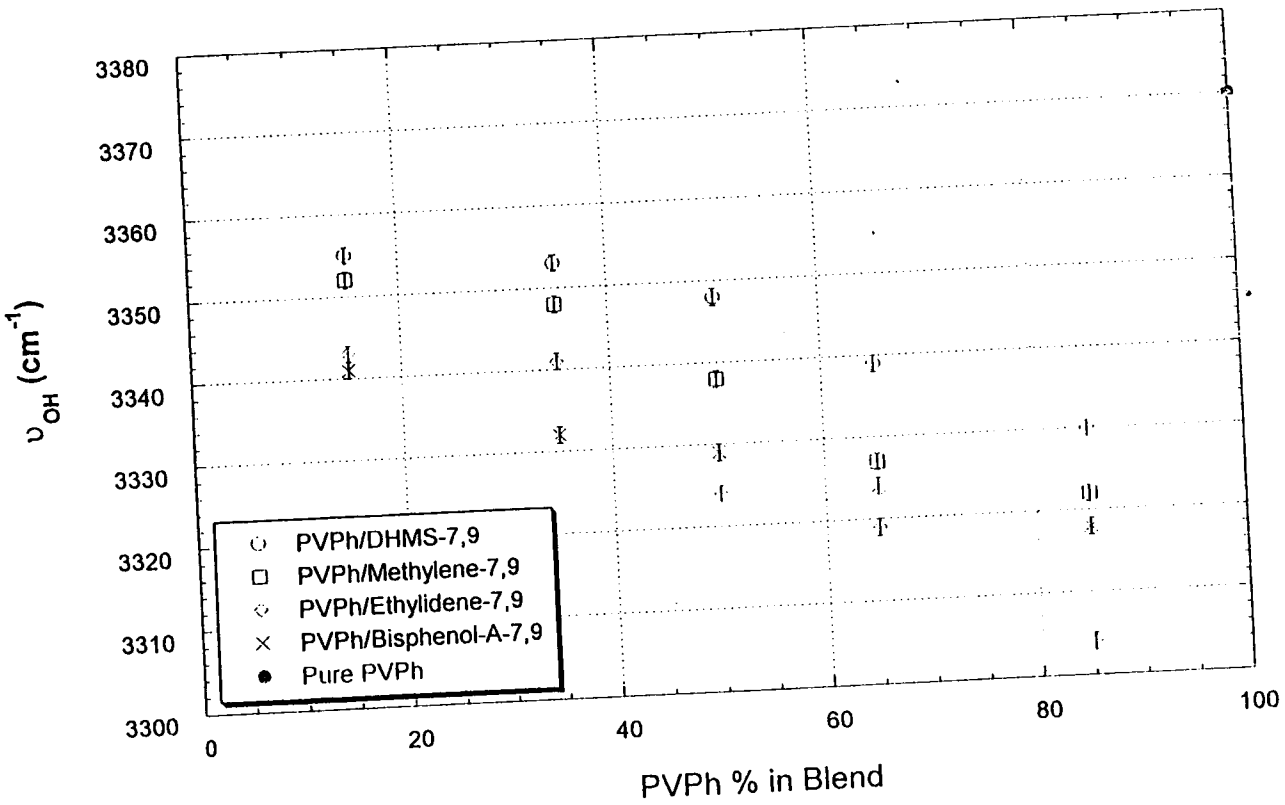

Figure 29. The plot of the frequency of the stretching hydrogen bonded hydroxyl band (υ_{OH}) in PVPh/7,9-copolyethers at various composition after annealing at 170 °C for 8 hours.

Figure 29. The plausible explanation for this behavior is that the 7,9-copolyethers are well dispersed in the PVPh at PVPh-rich blends, which in turn results in more intermolecular hydrogen bonding. Thus, a lower concentration of the polyether in the blend induces better mixing or a partial miscibility as a result of more intermolecular hydrogen bonding between the two polymers.

It must be emphasized that all the blends in this study are immiscible. However, there must exist a low concentration of LCP (Φ_{LCP}) where the polymers are miscible. In this system, υ_{OH} is less than υ_{OH} for pure PVPh due to the presence of intermolecular hydrogen bonds. As more LCP added at the system remains miscible, υ_{OH} will continue to decrease due to an increase in the number of intermolecular hydrogen bonds. However at some finite ΦLCP, the system will become immiscible. In the immiscible system, the amount of intermolecular hydrogen bonding will decrease and the number of hydrogen bonds will also decrease. This description explains the trend seen in Figure 29 and is corroborated by the work of Coleman and coworkers.[78] The FT-IR study of the blend of PS-*co*-PVPh (16% PVPh)/poly(*n*-octyl methacrylate) (POMA) also showed an increase in the amount of intermolecular hydrogen bonding as the PS-*co*-PVPh content was increased to turn an *immiscible* blend of PS-*co*-PVPh/POMA (20/80, w/w%) to a *miscible* blend of PS-*co*-PVPh/POMA (80/20, w/w%). Note that the stretching frequency of hydrogen bonded hydroxyl of PS-co-PVPh (16%) PVPh is observed at 3360 cm^{-1}. An increase in the stretching frequency of the hydroxyl group from 3370 cm^{-1} in *immiscible* blend of PS-*co*-PVPh (16% PVPh)/POMA (20/80, w/w%) to 3395 cm^{-1} for *immiscible* blend of PS-*co*-PVPh/POMA (50/50, w/w%) and eventually to 3450 cm^{-1} in *miscible* blend of PS-*co*-PVPh/POMA (80/20, w/w%) was reported. This shows that with

an increase in the amount of PS-*co*-PVPh, the blend of PS-*co*-PVPh/POMA becomes miscible. Accordingly, the stretching frequency of hydroxyl groups increases due to an increase in the intermolecular hydrogen bonding between the hydroxyl group of PS-co-PVPh and the carbonyl of POMA. These results were in agreements with theoretical calculations of the phase behavior for this blend system.

This information will be utilized in future studies of the phase behavior of these systems to try to find miscible blends. The Figure 29 also shows that the frequency of hydrogen bonded hydroxyl band (ν_{OH}) decreases from PVPh/DHMS-7,9 copolyether blends to PVPh/ethylidene-7,9 copolyether blends. This means that the extent of intermolecular hydrogen bonding between PVPh and 7,9-copolyether increases as the 7,9-copolyether becomes more flexible. Additionally, the results confirm that the rigidity of the 7,9-copolyethers inhibits the extent of intermolecular hydrogen bonding.

It is also important to note that the magnitude of the change in υ_{OH} as a result of a change in the rigidity of the 7,9-copolyether (for a given blend composition) is similar to the magnitude of the change in υ_{OH} induced by blend composition (for a given blend system). In other words, the difference between υ_{OH} for DHMS-7,9 and ethylidene-7,9 is ca. 20 cm^{-1} whereas the difference between υ_{OH} for a 15/85 and 85/15 blend is ca. 25 cm^{-1} for the DHMS-7,9 blends. Having said that the change in υ_{OH} is a result of change in the amount of intermolecular hydrogen bonding, we can conclude that the rigidity of DHMS-7,9 hinders the formation of intermolecular hydrogen bonds to the same extent as change in the blend composition. However, the hindrance in the formation of intermolecular hydrogen bonds may be overcome by choosing adequate blend compositions which are rich in PVPh. At this point,

we need to consider the effect of rigidity of an LCP on the formation of intermolecular interactions and the phase behavior in polymer mixtures. Most theoretical investigations of the phase behavior of liquid crystalline polymers and amorphous polymers assume that the LCP is a rigid rod.[79, 80, 81] There are many liquid crystalline polymers that are not rod-like, but are still anisotropic. DHMS-7,9 belongs to this category due to presence of the aliphatic spacer groups. Although DHMS-7,9 is anisotropic and fairly rigid to exhibit a liquid crystalline phase, it should not be considered a rod. This point must be realized in the interpretation of the results of this study. The above results show that the rigidity of a polymer chain does inhibit the formation of intermolecular hydrogen bonds. However, the effect of rigidity on intermolecular hydrogen bonding is not too dramatic and may not inhibit the formation of a miscible region. The results also show that the amount of intermolecular hydrogen bonding between two polymers improves at low LCP concentrations, suggesting the possibility of finding a miscible system in this region of the phase diagram. Future studies will examine this possibility.

1.13 The Effect of Spacing between Hydroxyl Groups on Intermolecular Hydrogen Bonding

The availability of hydroxyl groups for intermolecular hydrogen bonding is an important factor in the extent of intermolecular hydrogen bonding that can occur in blends. This effect has been recently examined by Coleman and Painter for poly (2,3-dimethyl butadiene-*stat*-4-vinylphenol) (24, 48 and 72 wt.%vinylphenol) and poly (*n*-alkyl methacrylates).[82] Their results show that the spacing between hydroxyl groups in poly(2,3-

dimethylbutadiene-*stat*-4-vinylphenol) can have an important impact on the extent of intermolecular hydrogen bonding between PS-*co*-PVPh with the other polymers. Coleman and Painter have also demonstrated that only a certain number of hydroxyl groups are available for hydrogen bonding. This limitation may be due to steric accessibility or a loss of internal degrees of rotational freedom in a chain where functional groups are hydrogen-bonded. For instance, in the case of PS-*co*-PVPh/polyether, a particular phenolic hydroxyl group may be adjacent to an ethereal group, but because one or more of its nearest same chain neighbors are already hydrogen-bonded to other groups, it may not be able to orient itself to form a hydrogen bond.

Therefore, the effect of spacing between hydroxyl groups on the intermolecular hydrogen bonds is examined in the blends of PS-*co*-PVPh (10%, 20% and 100% PVPh) and different 7,9-copolyethers. The IR spectra for the pure PS-*co*-PVPh and the blends of PS-*co*-PVPh/DHMS-7,9 (85/15, w/w%) are shown in Figure 30-32. The difference in the stretching frequency of the hydrogen bonded hydroxyl band in pure PS-*co*-PVPh (10, 20 and 100% PVPh) and the stretching frequency of the hydrogen bonded hydroxyl in PS-*co*-PVPh/7,9-copolyethers (85/15 w/w %) is defined as $\Delta\upsilon'$. The $\Delta\upsilon'$values are tabulated in Table 3. In a physical sense, the magnitude of $\Delta\upsilon'$ is related to the ratio of the number of hydroxyl groups involved in intermolecular hydrogen bonding with ethereal oxygen of 7,9-copolyethers to the total number of hydroxyl groups in PS-*co*-PVPh. For each studied blend, $\Delta\upsilon'$ value was extracted from the curve-fitting of corresponding IR spectra using the fitting procedure described above and are presented in Table 3.

The $\Delta\upsilon'$ values shown in Table 3 are plotted in Figure 33 as a function of the amount

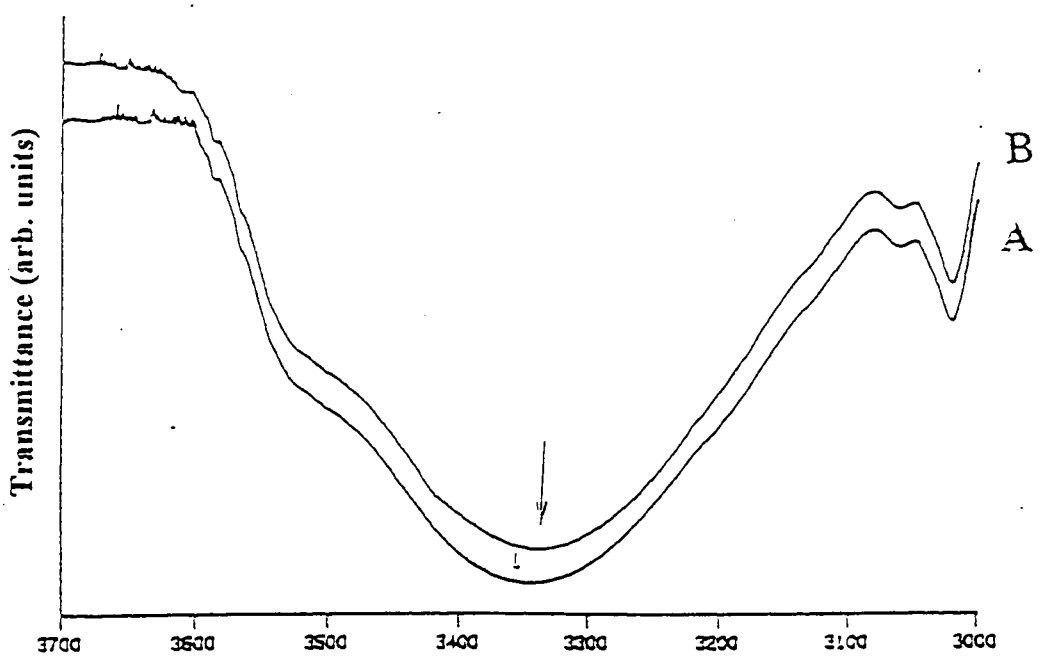

Figure 30. IR spectra of the hydroxyl region of (A) Pure PVPh; (B) PVPh/DHMS (85/15 w/w%).

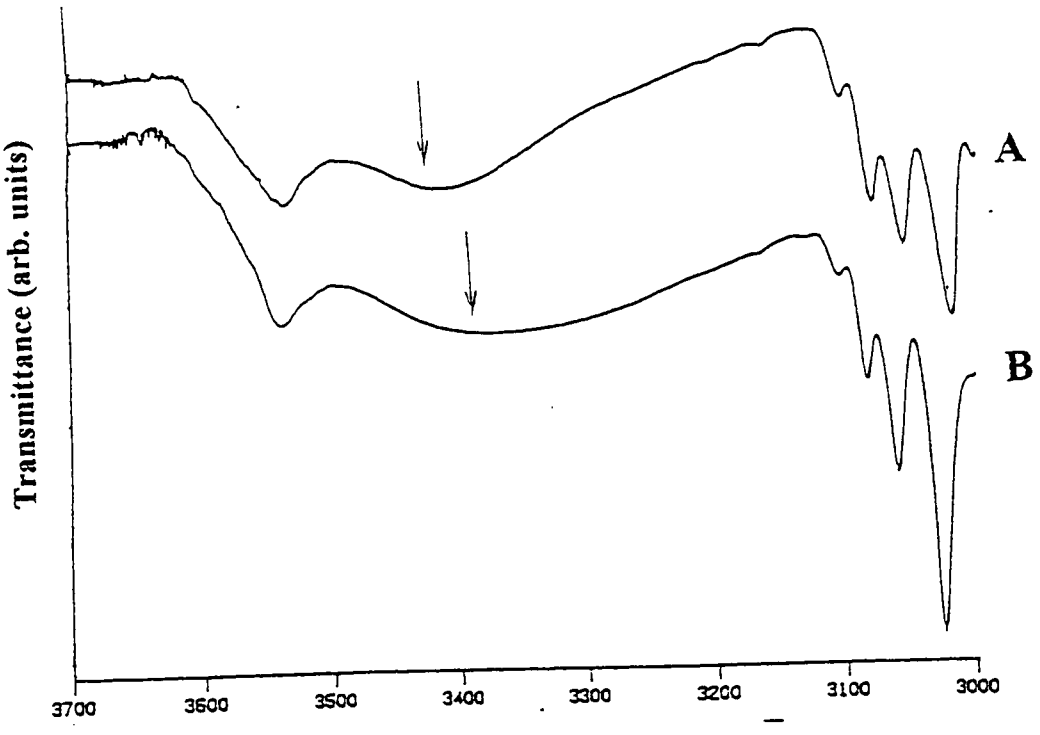

Figure 31. IR spectra of the hydroxyl region of (A) Pure PS-*co*-PVPh (20% PVPh); (B) PS-*co*-PVPh/DHMS (85/15 w/w%).

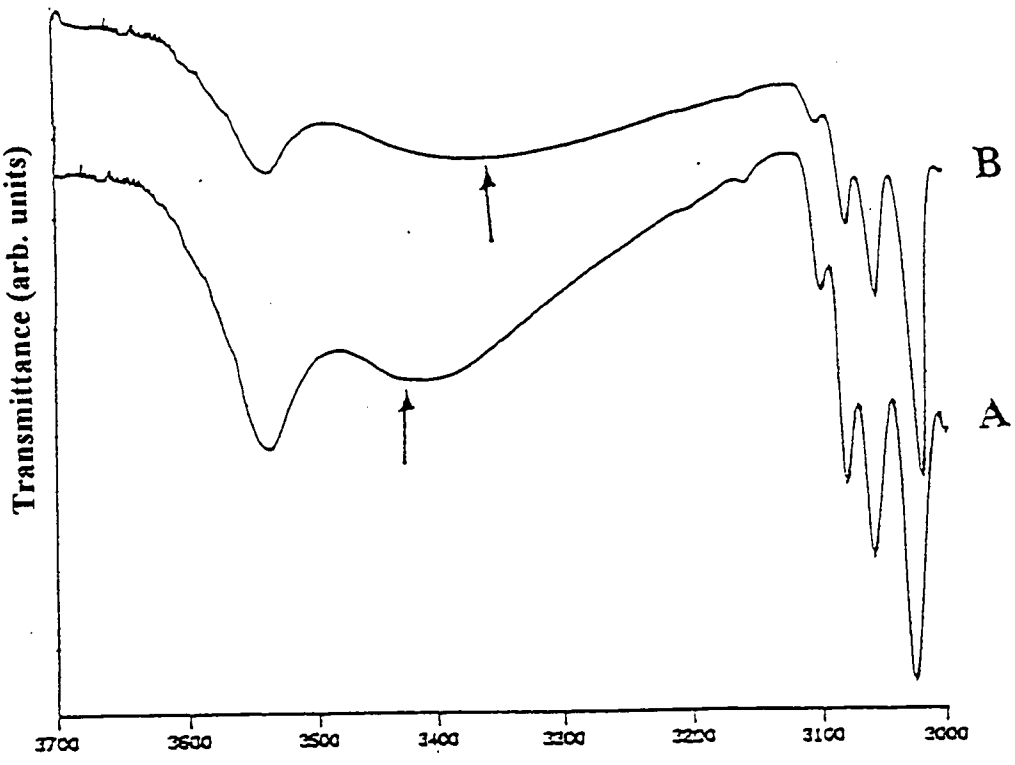

Figure 32. IR spectra of the hydroxyl region of (A) Pure PS-*co*-PVPh (10% PVPh); (B) PS-*co*-PVPh/DHMS (85/15 w/w%).

Table 3

Difference in Frequency of Hydrogen Bonded Hydroxyl Bands ($\Delta\upsilon'$) in Pure PS-*co*-PVPh (10, 20, 100% PVPh) and PS-*co*-PVPh/7,9-copolyethers Blends (85/15, w/w %) as Cast

PVPh% in PS-*co*-PVPh	DHMS-7,9 (cm^{-1})	Methylene-7,9 (cm^{-1})	Ethylidene-7,9 (cm^{-1})	Bisphenol-A-7,9 (cm^{-1})
10	79	83	91	93
20	44	66	73	80
100	39	46	64	51

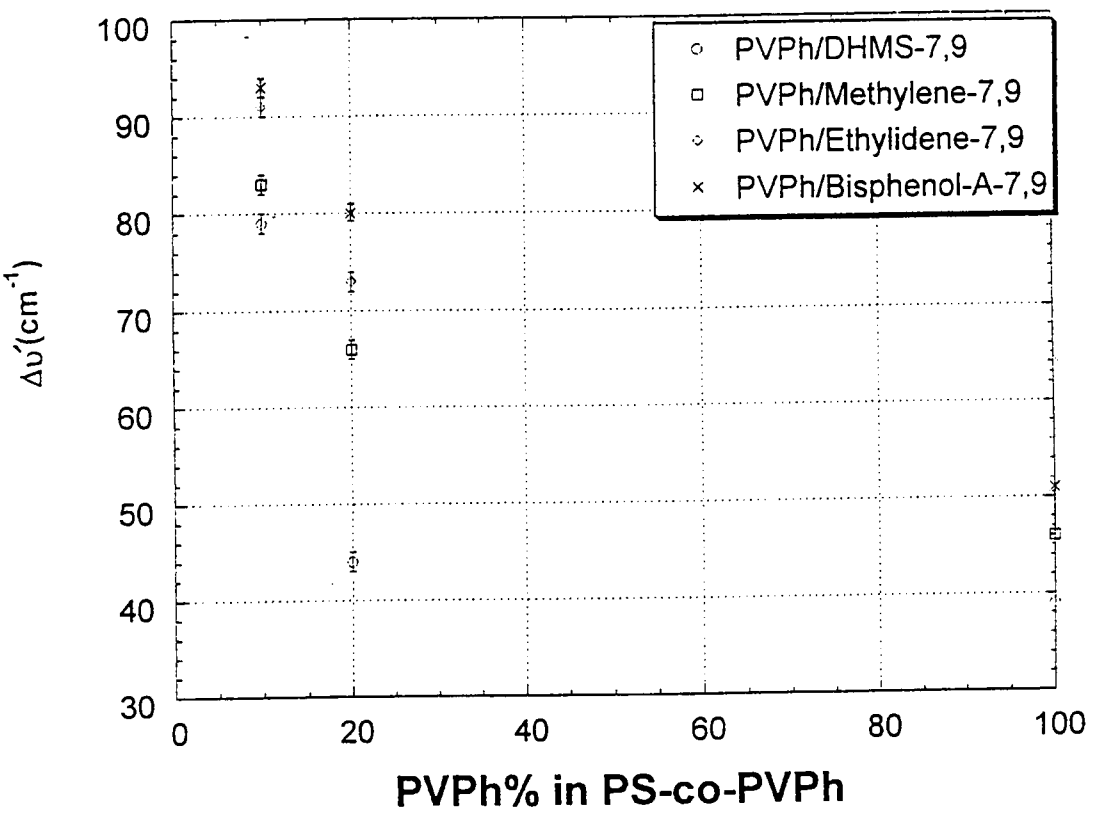

Figure 33. The plot of the difference of hydrogen bonded hydroxyl bands ($\Delta\upsilon_{OH}$) between pure PS-*co*-PVPh (10%, 20 and 100% PVPh) and PS-*co*-PVPh/7,9-copolyether blends (85/15 w/w%) as cast.

of PVPh in PS-*co*-PVPh. The plot shows that $\Delta\upsilon'$ increases as the PVPh content in PS-*co*-PVPh decreases indicating an increase in the extent intermolecular hydrogen bonding between PS-*co*-PVPh and 7,9-copolyethers. Note that the average distance between the hydroxyl groups in the phenolic copolymers increases, as the PVPh content in PS-*co*-PVPh decreases. As a result, increasing the distance between hydroxyl groups of PS-*co*-PVPh improves their rotational freedom with respect to each other . This results in an increase in the number of hydroxyl groups of PS-*co*-PVPh which can be involved in intermolecular hydrogen bonding with ethereal oxygen of 7,9-copolyether in the blends compared to total number of hydroxyl groups of pure PS-*co*-PVPh. It also should be realized that with increasing the distance between hydroxyl groups of PS-*co*-PVPh, the extent of intra molecular hydrogen bonding also decreases between the hydroxyl groups in PS-*co*-PVPh. This results in an increase in the number of the hydroxyl groups of PS-*co*-PVPh which can be involved in intermolecular hydrogen bonding in the blends compared to total number of hydroxyl groups of pure PS-*co*-PVPh. In turn, this increase in the amount of intermolecular hydrogen bonding can result in a larger $\Delta\upsilon'$ in PS-*co*-PVPh/7,9-copolyether blends. The same trend was observed in blends of PS-*co*-PVPh/7,9-copolyethers after annealing at 200 °C for 8 hours and PS-*co*-PVPh blends after annealing at 150 °C for 8 hours. These annealing temperatures were chosen for two reasons: (1) The polymers in blends are above their glass transition or crystalline melting point at these temperatures, so they can relax in to their equilibrium structures as they cool down to room temperature; (2) PS-*co*-PVPh (10% and 20% PVPh) and PVPh are approximately 30 °C above the annealing temperatures at which a change in a dispersion in

blend (or reduction in amount of intermolecular hydrogen bonding) is observed in the results described above. Table 4 represents $\Delta\upsilon'$ values for these annealed blends. The tabulated values in Table 4 is plotted in Figure 34. There are similar trends in both Figure 33 and 34. Figure 34 shows that $\Delta\upsilon'$ values of PS-*co*-PVPh (10%) /7,9-copolyether blend are closer to each other than those of PS-*co*-PVPh (20% and 100% PVPh)/7,9-copolyether blends. This data can be interpreted that the rigidity of 7,9-copolyethers becomes less important factor on the extent of intermolecular hydrogen bonding for PS-*co*-PVPh (10% PVPh) blends where the average distance between hydroxyl groups of PS-*co*-PVPh and their rotational freedom for the formation of intermolecular hydrogen bonds are the highest for the studied blends. The magnitude of $\Delta\upsilon'$ also becomes smaller in annealed blends than as cast blends due to the irreversible process that alters the intermolecular hydrogen bonding upon annealing. Again, both figures confirm that $\Delta\upsilon'$ becomes larger as one move from the more rigid DHMS-7,9 to ethylidene-7,9 which has a less rigid structure, indicating stronger intermolecular hydrogen bonding in ethylidene-7,9 blends. The data again confirms that the flexibility of 7,9-copolyethers promotes the extent of intermolecular hydrogen bonding in the blends.

Table 4

Difference in Stretching Frequency of Hydrogen Bonded Hydroxyl Bands ($\Delta\upsilon'$) in pure PS-*co*-PVPh (10%, 20% and 100% PVPh) and Annealed PS-*co*-PVPh/7,9-copolyether Blends (85/15, w/w%)

PVPh % in PS-co-PVPh	DHMS-7,9 (cm^{-1})	Methylene-7,9 (cm^{-1})	Ethylidene-7,9 (cm^{-1})	Bisphenol-A-7,9 (cm^{-1})
10	41	47	53	49
20	0	21	36	38
100	4	15	35	30

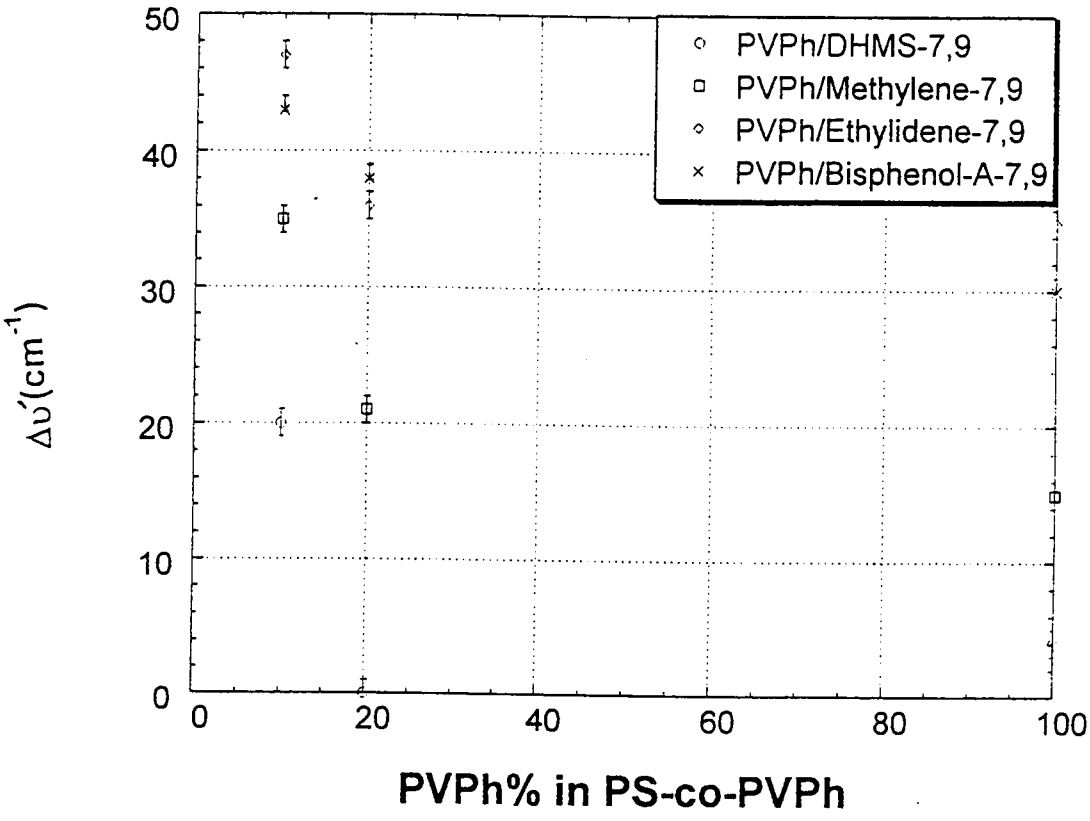

Figure 34. The plot of the difference of hydrogen bonded hydroxyl bands ($\Delta\upsilon_{OH}$) between pure PS-*co*-PVPh (10%, 20 and 100% PVPh) and PS-*co*-PVPh/7,9-copolyether blends (85/15 w/w%) versus the PVPh content of PS-*co*-PVPh after annealing at 200 °C (PVPh) for 8 hours and 150 °C (PS-*co*-PVPh, 10% and 20% PVPh) for 8 hours.

Chapter 2

Effect of Transesterification on the Properties of Polymer Blends containing a Liquid Crystal Polymer

2.1 Introduction

Liquid crystal polymers (LCPs) represent a technologically important class of polymers with unique characteristics.[83] These polymers possess a degree of structural order in solutions and/or melts, whereas semicrystalline polymers typically show structural order only upon solidification. The presence of this structural order in LCPs is responsible for their ability to form highly oriented fibers, films, and moldings which results in a material with both high modulus and high strength.

The "structurally ordered" or anisotropic state in LCP results from the presence of a rigid main chain backbone consisting of phenyl or other aromatic ring structures or a semiflexible main chain that is sterically restricted to rigid rod-like and/or extended chain conformations.[84] The anisotropic nature of liquid crystals on a molecular level translates to unusual physical properties including mechanical, optical, electrical, and rheological or flow properties. LCPs also exhibit a high degree of chemical resistance to most solvents, acids and bases even at elevated temperatures.[85] Due to their high length/diameter (L/D) ratio, LCPs exhibit a high degree of alignment.[86] The high degree of alignment in LCPs can result in their excellent mechanical strength and exceptional stiffness. Another consequence of the high L/D ratio in LCPs is that they exhibit a low melt viscosity. LCP chains are able to flow easily due to their low chain entanglement.

Thermoplastic polymers (TPs) such as polyethylene make up a large portion of the total consumption of plastics in consumer products.[87] TPs are polymers that repeatedly soften when heated and harden when cooled. TPs typically form a random coil conformation in the melt. When TPs are extruded, injection molded or fiber spun, the polymer chains may partially align due to applied shear, but on the removal of the stress they partially lose the orientation and recoil again. In contrast, LCPs under appropriate processing conditions have the tendency to align and to remain oriented.

The extents of fiber formation and orientation that occurs during processing are very important parameters that influence the final properties of an LCP material. [88] The oriented structure of LCPs is responsible for their high strength, low coefficient thermal expansion and dimensional stability. Even at higher temperatures, LCPs usually exhibit stiffness and strength comparable to some engineering plastics at room temperature, whereas typical TPs exhibit a substantial decline in their mechanical properties with increasing temperature. Such interesting properties have led to a substantial amount of research and development in the area of thermoplastic LCPs which can be used in the pure or blended state as a replacement for existing high performance materials as well as materials in new applications.

In spite of the unique combination of properties of LCPs that allow their potential application in different areas, LCP's prices are a serious hindrance to their major market influence.[89] Therefore, blending of LCP with other matrices may represent a convenient way for exploiting some of outstanding properties of LCP but at a moderate cost. During the last few decades polymer blends have become of prime commercial importance. Currently they constitute over 30% of the polymer market. Thus, the development of polymer blends

containing a LCP and a TP has recently attracted considerable attention both in industry and academia.

The addition of even a relatively small amount of LCP may induce a reduction in the melt viscosity, due to the low entanglement of LCP. [90] The decrease in melt viscosity of such blend improves its processibility. Thus, LCPs can also be utilized as a processing aid to reduce the melt viscosity of TP and also to improve the stiffness of the flexible polymers in the blends of LCP/flexible-coil polymer. The high mechanical strength of LCPs has led to the prediction that LCPs may act as a reinforcement phase when blended with TPs. In most cases, the addition of a LCP increases the mechanical strength and the stiffness of a TP matrix. As a result, a LCP/TP blend can be considered as an *in situ* composite with oriented LCP fibrils in the TP matrix. Because of the interfacial tension between the two phases, the interfacial region between the LCP and the TP is very important in the ultimate mechanical properties of the blend. The phase boundary can be a weak point in the blend and bulk mechanical properties of blend will depend heavily on the nature of the interface and its ability to respond to stress. Both the morphology and alignment of the LCP at the interface is also important in improving the interfacial adhesion between a LCP and TP in a blend.

Additionally, the correlation between the mechanical properties and the morphology of LCP/TP blends is an important aspect in LCP/TP blends.[91] The primary factors determining the morphologies of the LCP domains are the LCP content, processing conditions and rheological characteristics of the blend components. When the LCP is the minor component in the blend, it may form highly elongated domains parallel to the flow direction which appear as fibrils. LCPs tend initially to form spherical droplets within the

matrix polymer during processing. As the blend melt containing droplets begins to flow the droplet domains can deform into fibrous domains. The fibrous domains can also break up in to smaller droplets or the domains can coalesce. Spherical domains with weak interfacial adhesion will result in a brittle material with poor mechanical properties while a fibrous domain with good interfacial adhesion will display toughness and strength in mechanical properties.

To achieve the optimal properties in LCP/TP blends, the formation of a fibrous reinforcing LCP phase in the TP matrix is required.[92] Thus, extensional flow of the blend during processing rather than shear flow is preferred to facilitate formation of the fibrous reinforcing phase. The formation of the fibrous morphology also depends on the mixing flow which deforms the LCP droplets into fibrous domains.[93] In the melt-drawing processing of LCP/TP blends, the drawing condition is also a factor in the formation of LCP fibrils in the blend. A higher draw ratio causes a higher extensional deformation and, as a result, fibrils are formed. Thus, under these optimal conditions, the higher degree of molecular orientation and improved mechanical strength, as well as a reinforcing effect by the LCP phase can be achieved.

The resultant properties of LCP blends also depend on the interfacial adhesion between phases. Most polymers paris are immiscible and form multi-phase domains in mixing.[94] The homogeneity of polymer blends depends on the compatibility or interactions between polymers. The degree of interaction between two polymers is best described by the free energy of mixing, ΔG, which contains enthalpic (ΔH) and entropic (ΔS) contributions. For a blend to be single phase, the necessary condition is $\Delta G < 0$. The entropy terms are

usually small for polymers and thus the enthalpy terms dominates the free energy of mixing in polymer blends. A favorable heat of mixing may result from a preferred interaction between polymers. Therefore, the introduction of specific interactions can result in a negative contribution to the enthalpy of mixing and may improve the miscibility of two polymers. These specific interactions can be in the form of strong covalent interactions such as transreactions and ionic bonding or non-bonding weak interactions such as hydrogen bonding, ion-dipole, dipole-dipole, and donor-acceptor interactions.[95]

Of particular interest, in our study is that transreactions such as transesterification have the potential to induce miscibility in blends containing LCP polyesters. In particular, polyester blends are able to undergo interchange reaction between ester functional groups.[96] Interchange reactions will occur in the molten state under appropriate conditions. There are many factors that influence the progress of transesterification reactions in blends including their initial compatibility of the two polymers and blending conditions.

One of the consequences of transesterification reactions in polyesters is the alteration of the ester groups in polyesters.[97] This is shown in Figure 36 for the initial transesterification reaction between poly carbonate (PC) and poly(ethylene terephthalate) (PET). Note that the ester group of PC (indicated by star in Figure 35) is incorporated into PET structure upon transesterification.

The initial reaction between two homopolymers results in the formation of two block copolymers at the biphasic interface. Further transreactions results in the formation of more block copolymers as well as the scrambling of the block copolymers to form random copolymers at the interface.[87] The compatibilizing effect associated with the formation of

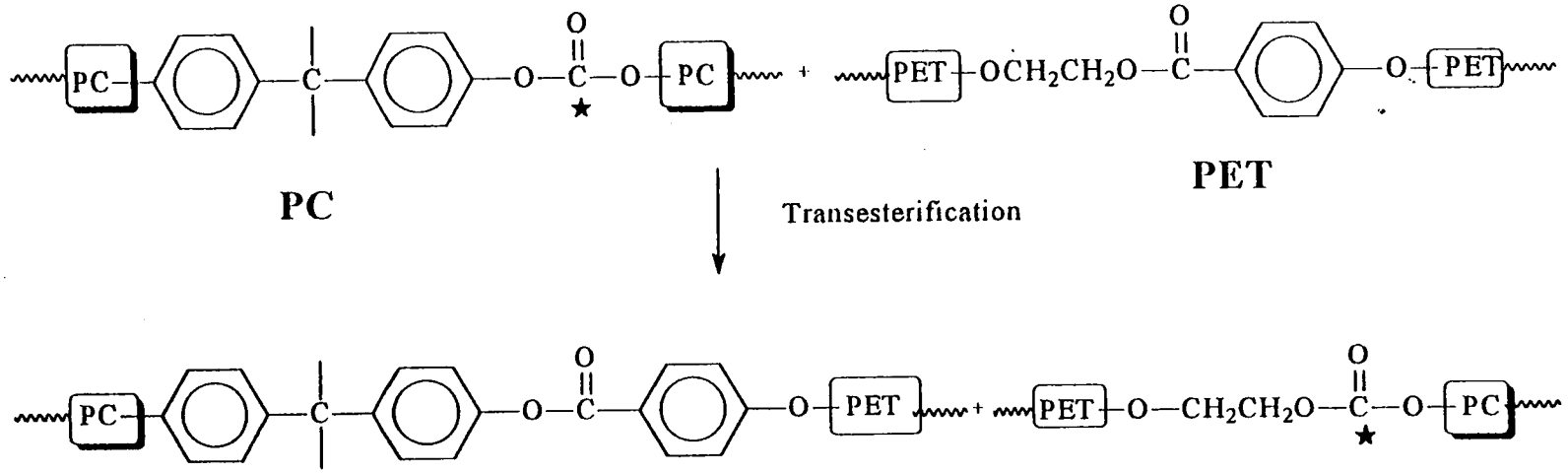

Figure 35. The transesterification between PC and PET

these different type of copolymers may transform a two phase blend into a miscible system.[98] Therefore, these interchange reactions will modify the phase behavior and the overall properties of the polyester blend.

2.2 Literature Review

Nuclear magnetic resonance spectroscopy (NMR) and infrared spectroscopy (IR) provide powerful tools for acquiring information on the miscibility of polymer blends by identifying interacting groups and to gain a molecular-level understanding of the components of the blend.[99] This is an advantage for NMR and IR spectroscopy over other methods such DSC, DMA and scattering techniques which are not directly able to identify the individual structures in distinct regions of a blend. IR, ^{1}H NMR and ^{13}C NMR have been utilized by researchers in the analysis of the micro structure of ester-containing polymer blends to provide information on the kinetics and mechanism of transreactions upon annealing.[100,101,102] The thermodynamics of the interaction and mechanical properties of the blend components can also be changed by transesterification reactions. Thus, methods such as DSC and DMA have also been utilized as complimentary methods to study the transreactions in polymer blends.[103]

The transesterification process in the melt-mixed blend of poly carbonate (PC) and polyethylene terephthalate (PET) has been studied by Porter, *et al.*[104], utilizing NMR. The copolymers formed by transesterification were isolated by TLC because they had different traveling distance from PC and PET on TLC plates. The study showed that the amount of copolymer formed increased with the temperature and duration of melt mixing. Copolymers

formed by transesterification were identified in the blend after 10 minutes at 270 °C by both ^{1}H and ^{13}C NMR spectroscopy. The intensity of the peak at 131.22 ppm corresponding to the bisphenolA-terephthalic diad increased as the transesterification proceeded. The miscibility of the PC/PET blend improved with as little as 2% of copolymers formed by transesterification, as shown by DSC.

Solid-state NMR and diffuse-reflectance FT-IR have also been utilized to study the transesterification in a blend of PC/poly(butylene terephthalate) (PBT) after annealing at 270 °C.[105] For the blend prepared from solution, transesterification was observed after annealing above the melting temperature of PBT. The structural analysis of the products of the transesterification reactions between PC and PBT was performed using IR and ^{1}H- NMR spectroscopy. As the transesterification proceeded, the degree of randomness of the copolymers increased, due to cross transreactions between copolymer chains. Applying a statistical method, the main chain length of the various sequences and the degree of randomness were calculated. The formation of block copolymers at the initial stages of transesterification was confirmed. Devaux[106] described a statistical method for the determination of the mean sequence length of formed copolymers diads upon transesterification using the peak areas in ^{13}C- NMR. Devaux, *et al.*[107] also reported the kinetics and mechanism of transesterification reactions between PC and PBT. The extent of transesterification was monitored by ^{13}C NMR peak areas of the bisphenol-A terephthalate diad at 133.4 ppm and 167.5 ppm, corresponding to the aromatic and carbonyl carbons of the terephthalate unit, respectively. They reported rate constants and activation energies of the transesterification reaction in PC/PBT blends. A few years later, Godard, *et al.*[108] studied the

kinetics of the transesterification in a molten PC/PET blend using NMR spectroscopy. They found that the transesterification in a PC/PET blend is a second order reaction (first order with respect to PC or PET). Kinetic parameters such as rate constants and activation energies were identical to those of PC/PBT blend reported by Devaux and coworkers in reference 100.

Miscibility and transesterification in a blend of a liquid crystalline poly (hydroxybenzoate)-poly(ethylene terephthalate) (PHB-PET) and poly arylate at 270 °C has been examined by Tyan and coworkers.[109] The poly arylate was a bisphenol-A -terphthaloyl-isophthaloyl (molar ratio: 2:1:1) copolyester with trade name of U-100®, supplied by Unitika Corp. DSC and NMR studies confirmed partial miscibility in this blend after 15 minutes annealing at 290 °C and NMR showed the formation of four different diads, which resulted from the transesterification between PHB-PET and the poly arylate. The miscibility between PHB-PET and the poly arylate increased with the formation of these diads as a function of annealing time, as shown by DSC and polarized optical microscopy. The kinetics of the transesterification reaction and corresponding activation energy were also obtained for this blend.

In a similar study[110], the miscibility of a liquid crystalline poly (oxybenzoate-phenyleneisophthalate) (POP) with PC was also investigated. A single glass transition was observed for transesterified blend in all compositions. Annealing of PC/POP blends at 310 °C, which is above the melting point of POP, induced transesterification after 12 minutes as confirmed by DSC, IR and NMR spectroscopy. FT-IR spectroscopy of the annealed blend after 4 minutes revealed the appearance of IR absorptions at 1740 cm^{-1} and 1070 cm^{-1}. These bands were attributed to carbonyl and C–O bonds of the ester group of PC attached to POP.

New ^1H NMR peaks at 8.25 ppm and 7.58 ppm, corresponding to the attachment of PC to oxybenzoate and phenyleneisophthalate units of POP, were also observed in these blends after 12 minutes of annealing. The transesterification resulted in an amorphous blend with a single T_g as PC reacted with isophthalate and oxybenzoate groups in POP. Additionally, as a result of transesterification between PC and POP, the development of an isotropic phase was observed by optical microscopy. This was explained by the formation of amorphous regions and the loss of birefringence of the liquid crystalline phase of POP.

The melt-mixed blends of PHB-PET/PET with different compositions were studied by Ou and Lin.[111] Shown by NMR, the extent of transesterification at 275 °C increased as a function of time. The growth of a signal at 7.4 ppm assigned to PHB-PET diads was observed as the annealing time was increased. They attributed the growth of the PHB-PET diad peak as a result of transesterification between PET and PHB-PET. The extent of transesterification reactions increased with blending time. The presence of the new copolymers also hindered the crystallization of PET resulting in a decrease in T_m of PET in blends. Paci, *et al.*[112] reported that a the blend of PBT with a liquid crystalline poly (biphenyl-4, 4'-xylene sebacate) (PBS) were miscible in the isotropic state above 290 °C. Evidence of transesterification was observed at 290 °C after 2 minutes annealing by DSC measurements. The melting and crystallization temperature of PBT decreased with the amount of PBS in the blend. As a consequence of transesterification between PBT and PBS, the enthalpy of isotropization of PBS showed a 16% reduction after 2 minutes annealing, which increased to a 70% reduction after 20 minutes annealing at 290 °C. This reduction was explained as the result of the disruption of the smectic phase of PBS as the transesterification proceeded.

Nobile, *et al.* [113] studied the possibility of transesterification in a PC/PHB-PET blend, using FT-IR spectroscopy. Blends of PC and PHB-PET were compounded using a single screw extruder. FT-IR was used to find any evidence of ester-exchange between PC and PHB-PET. No change in absorption bands were found at characteristic ester group frequencies. Based on their observations, they concluded that no transesterification had occurred on processing of the blends. The blend of PC/PHB-PET was also investigated by Jung and Kim[114]. The blend of PC and PET/PHB was extruded at 260 °C. They confirmed that the glass transition of PC is decreased by a small addition of PHB-PET, although the glass transitions of the LCP remain unchanged. This was interpreted as due to the possible exclusion of PC from the LCP phase while there was some partial mixing in the PC phase due to transesterification. Moreover, a quite good interphase adhesion was observed from an SEM analysis of the blend.

The transesterification between PC and PHB-PET and its impact on the miscibility of the blend was also studied by Wei *et al.*[115] A single glass transition for PC/PHB-PET blend (40/60 wt.%) was observed after annealing at 260 °C for 60 minutes. This was attributed to transesterification between PC and PHB-PET. ^{13}C NMR spectroscopy was used to characterize the extent of transesterification and the formed copolymers. New peaks at 120.9 ppm and 148.3 ppm corresponding to the bisphenol-A-terephthalate diad as well as at 165.9 ppm corresponding to a bisphenol-A-oxybenzoate diad were identified upon annealing and transesterification in the blend.

Hopfe and coworkers also studied PC/PBT melt blends by DSC and NMR spectroscopy. They found evidence for transesterification in this blend upon annealing at 250

°C.[116] It was found that the transesterification rate depends upon the catalyst content used in the PBT synthesis. The rate of crystallization of PBT in the blend decreases with increasing amount of PC and amount of formed copolymer. Homogenization and improved compatibility due to progressive transesterification was observed by polarized light microscopy.

The transreactions in poly(2-ethyl-2-methyl-1,3-propylene terephthalate) (PEMPT)/PC blend has been reported by Kollodge, *et al.*[117] The blend showed partial miscibility after annealing at 240 °C for 128 minutes, monitored by a shift of T_g using DSC. Proton NMR provided information about the transesterification between PEMPT and PC. The appearance of a peak at 4.19 ppm was observed corresponding to methylene groups of PEMPT attached to the bisphenol-A unit of PC. It was found that transreaction of approximately 4% of the terephthalate groups was required to shift the phase behavior from two phase to single phase in a PEMPT/PC 50/50 wt. % blend.

As reported by Wei and Tyan[118], addition of a small amount of PHB-PET to originally immiscible blends of LC copoly (oxybenzoate-naphthalate) (73/27), known as Vectra® and poly (etherimide) (PEI) resulted in a system with higher ultimate tensile and impact strength as well as better interfacial adhesion between Vectra® and PEI. DSC measurement of a 50/50 (w/w%) PHB-PET/PEI blend after annealing at 300 °C did not show any change in the T_g of the blend components. However, a shift in the glass transitions of PHB-PET and PEI was observed for a blend with a composition of 40/60 wt.% after annealing at 280 °C. This indicates that the miscibility of the blend improved as the amount of PEI increased. Polarized optical microscopy of the blend also showed a partial miscibility as the birefringence of the PHB-PET/PEI (40/60 wt.%) was decreased with annealing time due to transesterification

between PHB-PET and PEI and disruption of the LC phase. Andresen and Zachmann investigated transesterification reactions in a PET and poly (ethylene-2,6-naphthalene dicarboxylate) (PEN) blend upon melt pressing of the components.[119] They reported that transesterification between PET and PEN occurred at 280 °C in the blend after two minutes. DSC measurements showed a decrease in the melting point of the blend and a single glass transition temperature was observed upon annealing for the 30/70 (PET/PEN)wt.% blend. Wide angle X-ray scattering measurements also showed the formation of a single phase blend and partial miscibility of the blend after transesterification.

2.3 The Goals of this study

We are interested in investigating the transesterification in a blend of PC/PHB-PET and its consequences on the blend morphology and mechanical properties of the blend. ^{13}C-NMR spectroscopy is utilized to characterize the formation of copolymers and quantification of the transesterification process in the blend. The transesterification in the polymer blends can change the chemical structure of the blend components by the formation of copolymers at the biphasic interface. As mentioned above, transreactions can also alter the morphology and the mechanical properties of the blend. Therefore, it is desirable to examine the effect of transesterification on the loss of the liquid crystalline character of the blend components. The final mechanical properties of the blend are also examined to correlate the micro structure changes that occur in the blend due to transesterification to the macroscopic properties.

2.4 Experimental

Polycarbonate (PC) (M_w = 64,000 g/mole), phenol, methanol and tetra cholroethane (TCE) were purchased from Aldrich Chemical Company. Poly (hydroxy benzoate)-*co*-poly-(ethylene terephthalate) (PHB-PET) (40/60 molar ratio) (M_w = 50,000 g/mole) was provided by Eastman Chemical Company. PC was dissolved in toluene and was precipitated in methanol to remove any impurities. The blend of PC and PHB-PET (40/60, w/w%) was prepared by dissolving the polymers in a mixture of phenol and TCE 50/50 (w/w%) and then precipitated in methanol. The blends was kept *in vacuo* for four days at 100 °C to remove any residual solvent. The annealing of the blends was carried out under nitrogen at 260 °C for different times. The characterization of the blends was carried out by ^{13}C NMR spectroscopy using a 400 MHz Bruker NMR spectrometer. A 10% (w/v%) solution of the annealed blend in a mixture of $CDCl_3$/ CF_3COOD (85/15, v/v%) was prepared for ^{13}C NMR studies. The optical microscopy of the blends was performed using an Olympus BH-2 microscope. The image analysis was completed using NIH image software. Tensile measurement was performed by an Instron instrument with a 2,000 g load cell and a crosshead speed of 50 mm/min. The samples were prepared by melt pressing of unannealed and annealed blends at different annealing time. The specimen were cut in 2.5 cm x 2.5 mm strips for tensile measurements. Five samples of each blend were analyzed for the tensile measurements.

2.5 Results and Discussion

It is well established that polyesters can undergo ester-ester interchange reactions or transesterification with itself or with other polymers at high temperatures.[120] Though the blend

of thermoplastic LC polyesters and flexible-coil polymers are usually immiscible due to the low entropy of mixing, transesterification can be sought as a means to improve the miscibility of such a blend. Here, we monitor the extent of transesterification between PHB-PET, which is a liquid crystalline copolyester and amorphous PC in the PC/PHB-PET (40/60 w/w%) blend. The blends are annealed at 260 °C by NMR spectroscopy as a function of time. ^{13}C NMR spectroscopy is utilized as a suitable tool to provide the chemical verification of transesterification between PHB-PET and PC in the blend. The chemical structures of the repeating units of PC and PHB-PET are shown in Figure 36.

The ^{13}C NMR spectra of PC/PHB-PET blend (40/60, w/w%) upon annealing at 260 °C are shown in Figure 37-39. The examination of these spectra shows the appearance of new resonance signals at 120.9 ppm, 148.4 ppm and 165.9 ppm after 30 minutes of annealing. These new signals can be attributed to the formation of bisphenol-A oxybenzoate and bisphenol-A terephthalate diads resulting from transesterification between PC and PET-PHB.[121] The chemical structures of these diads are shown in Figure 40.

As reported by Wei *et al.*[115], the assignments of these peaks was verified by model compound studies of PC with hydroxy benzoic acid and terephthalic acid (monomeric units of PHB-PET) after heating of each mixture at 300 °C . After heating, the NMR analysis of PC/hydroxybenzoic acid and PC/terephthalic acid mixtures showed the appearance of new peaks at 120.9 ppm, 148.3 ppm and 165.9 ppm at the same chemical shifts seen for PC and PHB-PET blend. They confirmed that bisphenol-A oxybenzoate and bisphenol-A terephthalate diads were also produced by the reaction of PC with hydroxy benzoic acid and terephthalic acid in the model compound study.

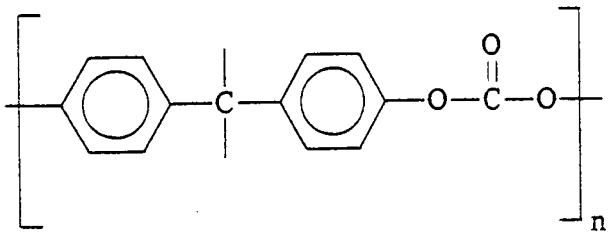

Poly Carbonate (PC)

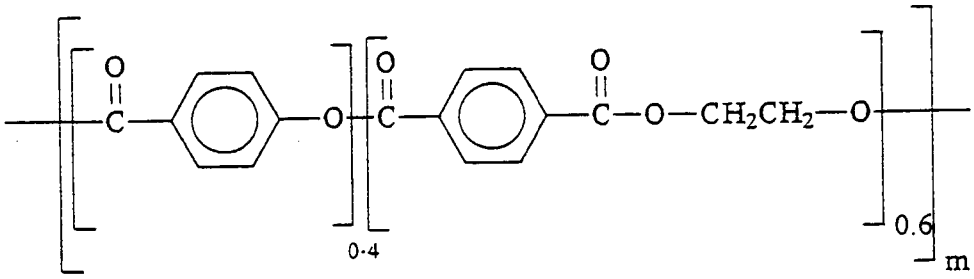

PHB-PET

Figure 36. The chemical structures of PC and PHB-PET

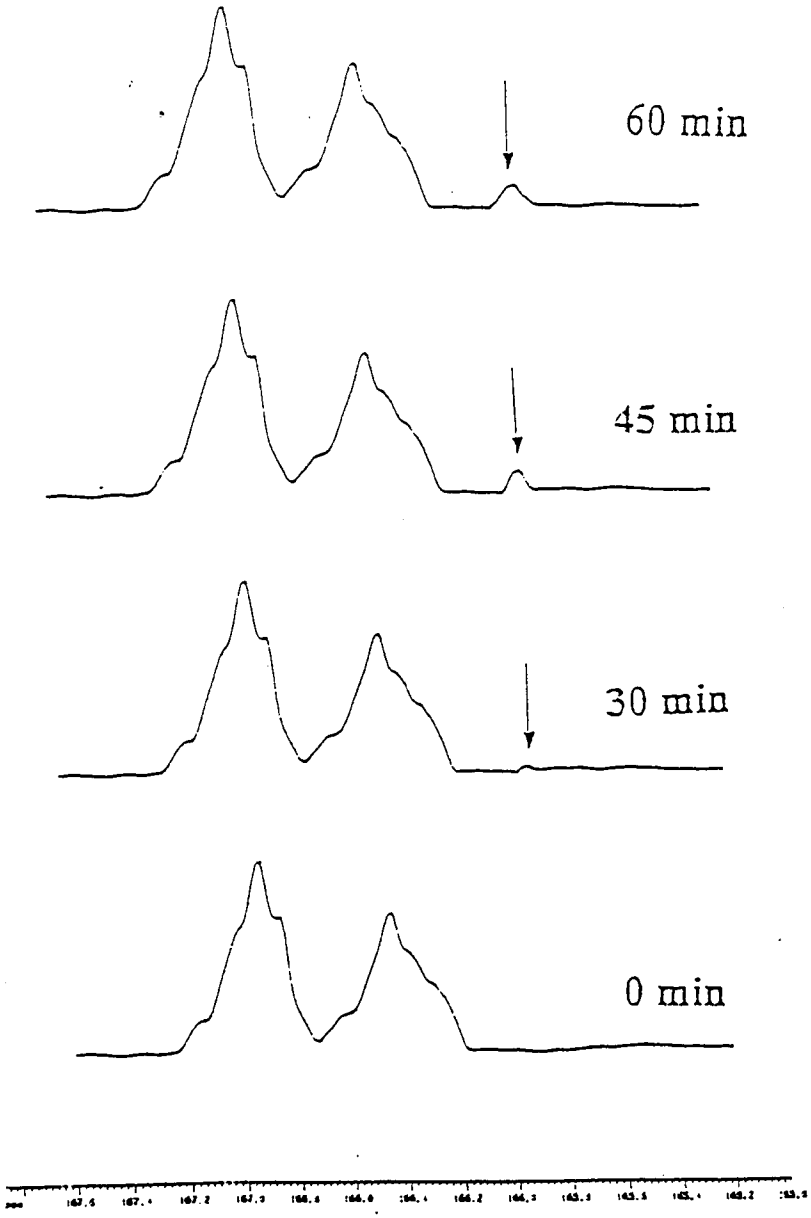

Figure 37. ^{13}C NMR spectra of PC/PHB-PET blend annealed at different times at 165 ppm region.

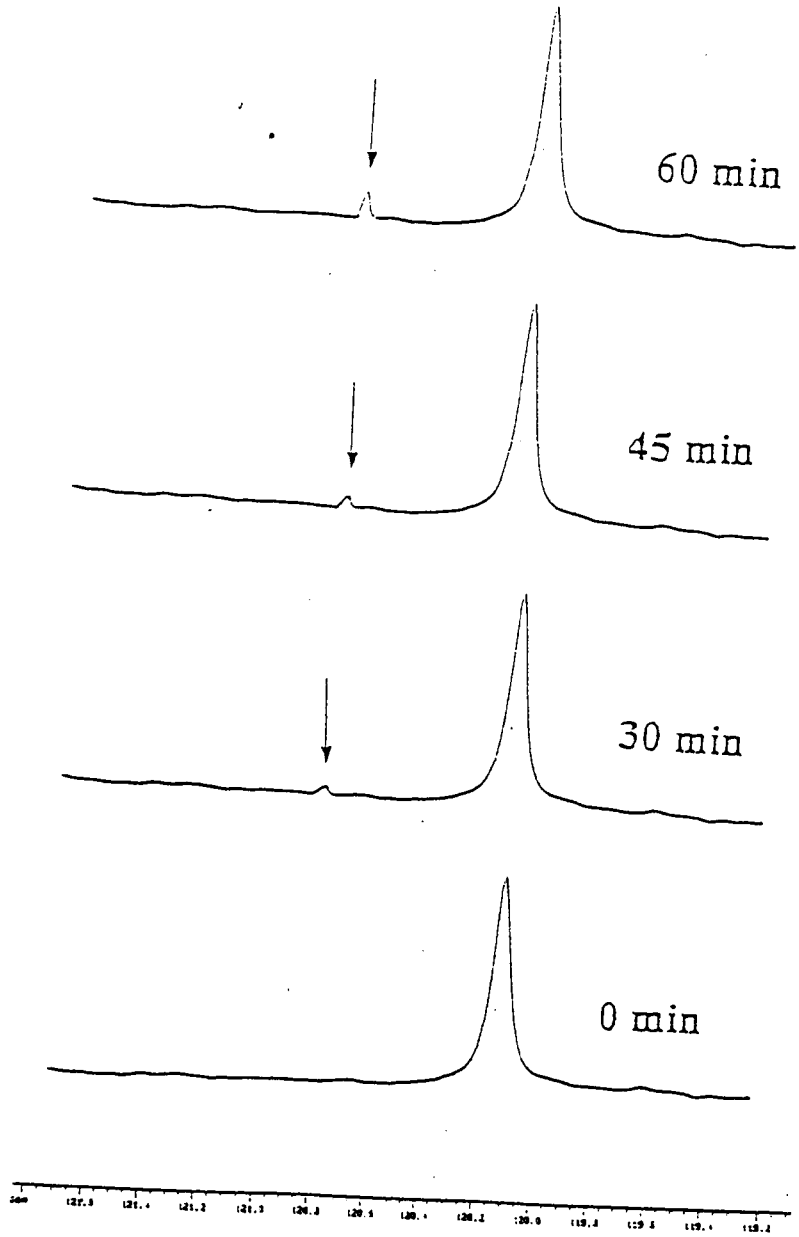

Figure 38. ^{13}C NMR spectra of PC/PHB-PET blend annealed at different times at 120 ppm region.

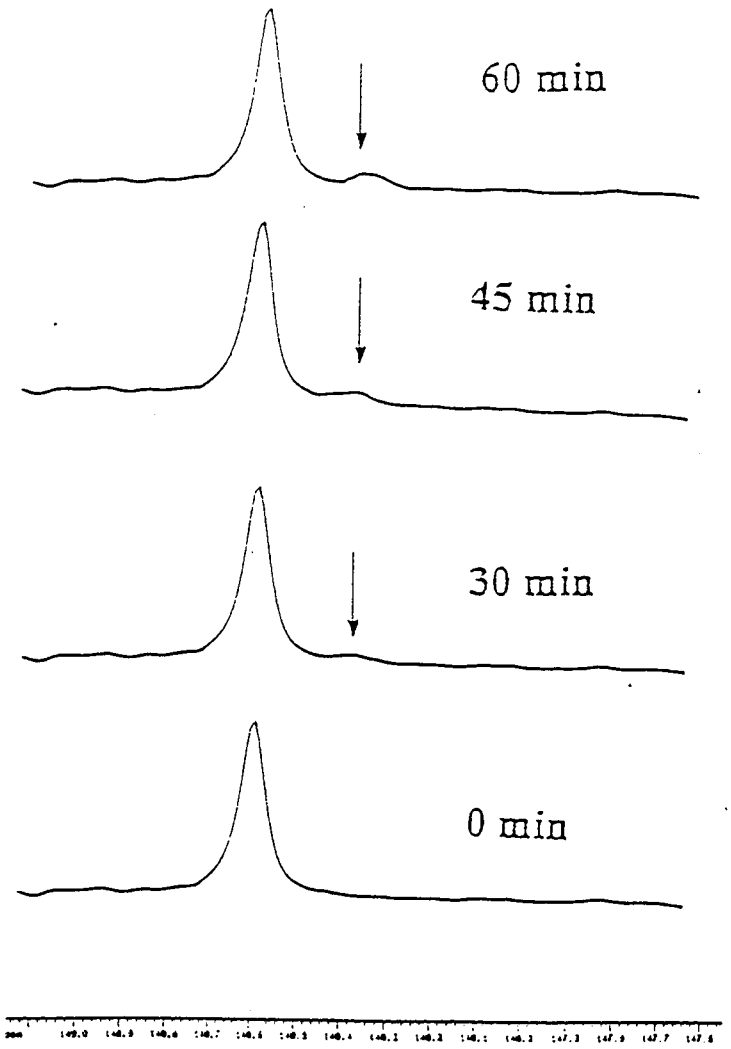

Figure 39. ^{13}C NMR spectra of PC/PHB-PET blend annealed at different times at 148 ppm region.

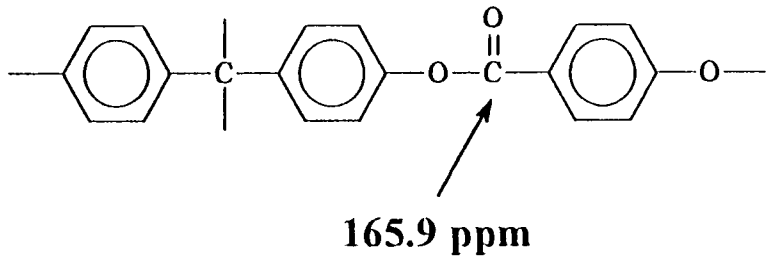

Bisphenol-A-Oxybenzoate Diad

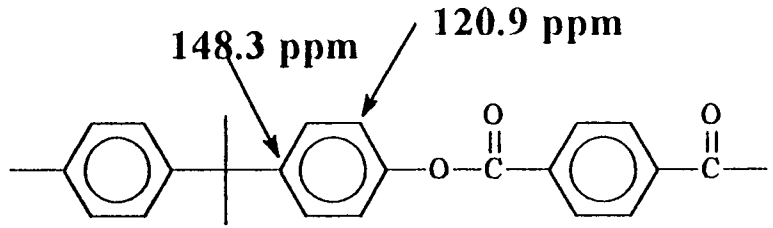

Bisphenol-A-Terephthalate Diad

Figure 40. Structures of bisphenol-A oxybenzoate and bisphenol-A-terephthalate diads

Generally, the carbon of a carbonyl group is more deshielded than the carbon of an aromatic ring. As a result, the carbonyl group shows up at a higher chemical shift (or more down-field) than an aromatic carbon in ^{13}C NMR spectrum. By the same reason, the resonance peak for the carbon of the carbonyl group in bisphenol-A oxybenzoate diad shows up at 165.9 ppm (more down-field at higher chemical shift) whereas the resonance peak for the aromatic carbons in bisphenol-A terephthalate diad show up at 120.9 and 148.4 ppm (more up-field at lower chemical shifts). Note that the area under these peaks increases with annealing time up to 60 minutes, as shown in Figures 37-39. This is expected because the amount of these diads as transesterification products increases with reaction time. However, the integration results of these peaks suggest no significant growth in the area under these peaks after 60 minutes annealing of blend. This is because the amount of formed bisphenol-A oxybenzoate and bisphenol-A terephthalate diads produced by transesterification and the amount of bisphenol-A oxybenzoate and bisphenol-A terephthalate diads undergoing further transesterification have reached a steady state. Therefore a saturation in transient mole fraction of bisphenol-A oxybenzoate and bisphenol-A terephthalate diads is observed.

Furthermore, a quantitative analysis of the formed copolymers in PC/PHB-PET blend was also completed to quantify the amount of each transesterification product. An analysis of formed diads based on a method developed by Yamadera and Devaux was utilized.[122, 123] One can divide PHB/PET structure into three components noted as $(AB)_1$, B_1 and A_1 for oxybenzoate, terephthalate, and ethylene in PHB-PET, respectively (see Figure 41). The bisphenol-A and carbonate groups in PC are also noted as A_2 and B_2.

Before staring the transesterification, we have A_1B_1, $A_1(AB)_1$, A_2B_2 and $(AB)_1(AB)_1$

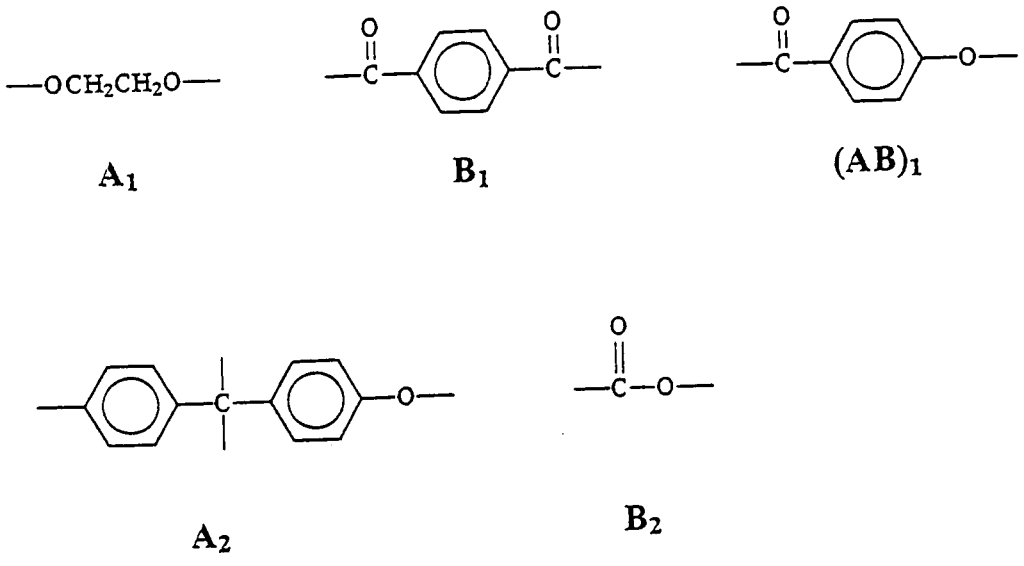

Figure 41. The chemical structures of different components of PC and PHB-PET.

diads in the blend. The mole fraction of A_1, F_{A_1}, in the blend can be obtained as:

$$F_{A_1} = \frac{[A_1(AB)_1]+[A_1B_1]}{[A_1(AB)_1]+[A_1B_1]+[(AB)_1B_1]+[(AB)_1(AB)_1]+[A_2B_2]} \quad (2.1)$$

Considering :

$[A_1]_{total} = [A_1(AB)_1] + [A_1B_1]$, $[A_2]_{total} = [A_2B_2]$, and $[(AB)_1]_{total} = [(AB)_1B_1] + [(AB)_1(AB)_1]$

one can write equation (2.1) as:

$$F_{A_1} = \frac{[A_1]_{total}}{[A_1]_{total}+[A_2]_{total}+[(AB)_1]_{total}} \quad (2.2)$$

in the same manner for A_2 and $(AB)_1$, we can write:

$$F_{A_2} = \frac{[A_2]_{total}}{[A_1]_{total}+[A_2]_{total}+[(AB)_1]_{total}} \quad (2.3)$$

$$F_{(AB)_1} = \frac{[(AB)_1]_{total}}{[A_1]_{total}+[A_2]_{total}+[(AB)_1]_{total}} \quad (2.4)$$

As the transesterification between PC and PHB-PET occurs, we have the formation of new diads A_2B_1, A_1B_2, $A_2(AB)_1$ and $(AB)_1B_2$ in the blend. The mole fraction of these new diads can be obtained from the concentration of starting components in the blend. For instance, the mole fraction of A_1B_2 diad, $F_{A_1B_2}$, can be written as:

$$F_{A_1B_2} = \frac{[A_1B_2]}{[A_1(AB)_1]+[A_1B_1]+[(AB)_1B_1]+[(AB)_1(AB)_1]+[A_2B_2]+[A_2B_1]} \times \frac{1}{[A_2(AB)_1]+[A_1B_2]+[(AB)_1B_2]} \quad (2.5)$$

Considering $[A_1]_{total} = [A_1B_1] + [A_1(AB)_1] + [A_1B_2]$; $[A_2]_{total} = [A_2B_2] + [A_2B_1] + [A_2(AB)_1]$, and $[(AB)_1]_{total} = [(AB)_1B_1] + [(AB)_1(AB)_1] + [(AB)_1B_2]$, one can rewrite equation (2.5) as:

$$F_{A_1B_2} = \frac{[A_1B_2]}{[A_1]_{total} + [A_2]_{total} + [(AB)_1]_{total}} \qquad (2.6)$$

Accordingly, we can also obtain:

$$F_{(AB)_1(AB)_1} = \frac{[(AB)_1(AB)_1]}{[A_1]_{total} + [A_2]_{total} + [(AB)_1]_{total}} \qquad (2.7)$$

$$F_{(AB)_1B_1} = \frac{[(AB)_1B_1]}{[A_1]_{total} + [A_2]_{total} + [(AB)_1]_{total}} \qquad (2.8)$$

The formation of the new copolymer diads is a result of the random occurrence of transesterification between the starting components in the blend. Therefore, the probability of the formation of different new diads is not equal for all of them. For example, the probability of finding an A_1 group followed by B_2, $P_{A_1B_2}$,can be calculated by:

$$P_{A_1B_2} = \frac{[A_1B_2]}{[A_1B_1] + [A_1B_2] + [A_1(AB)_1]} = \frac{[A_1B_2]}{[A_1]_{total}} \qquad (2.9)$$

In the same manner, one can write:

$$P_{A_1(AB)_1} = \frac{[A_1(AB)_1]}{[A_1]_{total}} \qquad (2.10)$$

$$P_{(AB)_1(AB)_1} = \frac{[(AB)_1(AB)_1]}{[(AB)_1]_{total}} \qquad (2.11)$$

The probability values will be utilized in the determination of the amount of the formed

copolymer diads as described below. From equation (2.2), one can write:

$$[A_1]_{total} + [A_2]_{total} + [(AB)_1]_{total} = \frac{[A_1]_{total}}{F_{A_1}} \qquad (2.12)$$

Replacement of the denominator in (2.6) from equation (2.12), followed by using equation (2.9) gives:

$$F_{A_1B_2} = \frac{F_{A_1}[A_1B_2]}{[A_1]_{total}} = F_{A_1} . P_{A_1B_2} \qquad (1.13)$$

In a similar manner, we can write:

$$F_{A_2(AB)_1} = F_{A_2} . P_{A_2(AB)_1} \qquad (2.14)$$

$$F_{(AB)_1B_1} = F_{(AB)_1} . P_{(AB)_1B_1} \qquad (2.15)$$

$$F_{A_2B_1} = F_{A_2B_1} . P_{A_2B_1} \qquad (2.16)$$

Therefore, one can obtain the mole fractions of the formed diads from the above equations if the mole fractions of starting components in the blend and the probabilities of the formation of the diads in the blend are known. In practice, the integrals under the peaks calculated from the NMR analysis are used as the probability values of respective diads . This is because the higher the peak area of a formed copolymer diad , the higher the amount of diad is produced as a result of transesterification. This also means that the higher the peak area of a formed copolymer diad, the higher probability for formation of that copolymer diad during transesterification reaction. Thus, the areas under the peaks of formed copolymer

diads are directly proportional to the probability of the formation for copolymer diads.

Knowing the initial amount of PC and PHB-PET (or the initial amount of starting components) in the blend , the mole fraction of bisphenol-A terephthalate and bisphenol-A oxybenzoate diads in PC/PHB-PET blends can be calculated using equations (2.14) and (2.16). The integral values under the peaks at 120.9 ppm, 148.3 ppm, and 165.9 ppm at different times are directly used as the probability values ($P_{A_2B_1}$ and $P_{A_2(AB)_1}$) in equations (2.14) and (2.16). Table 5 shows the calculated mole fractions of bisphenol-A oxybenzoate and bisphenol-A terephthalate diads (error within ± 5%) in PC/PHB-PET blends after 30, 45 and 60 minutes of annealing at 260 °C.

The tabulated values of mole fractions of bisphenol-A oxybenzoate and bisphenol-A terephthalate diads are plotted in Figure 42. The data indicates that as the time of annealing of the blend increases, the mole fraction of the diads produced from the transesterification between PC and PHB-PET increases. A steeper increase was observed for 165.9 ppm peak corresponding to the carbonyl group of bisphenol-A oxybenzoate diads, especially after 45 minutes annealing. This shows that the rate of formation of bisphenol-A oxybenzoate diad is faster than that of bisphenol-A terephthalate at the annealing temperature of 260 °C. This may be explained due to the rigid structure of PHB segments in PHB-PET. The more rigid PHB segment has a larger size compared to that of flexible PET segment. Based on simple collision theory, the collision frequency in chemical reactions is proportional to the square of the size of the reacting species.[124] Therefore, the more rigid PHB segments have higher probability of collision with PC to form bisphenol-A-oxybenzoate diads than that of PET segments.

Table 5

The Mole Fraction of Bisphenol-A Oxybenzoate and Bisphenol-A Terephthalate Diads in PC/PHB-PET Blends Upon Annealing at 260 °C.

Annealing Time (min)	Diad Mole Fraction at 120.9 ppm (mole)	Diad Mole Fraction at 148.39 ppm (mole)	Diad Mole Fraction at 165.9 ppm (mole)
0	0.000	0.000	0.000
30	0.003442	0.010614	0.006844
45	0.007720	0.018038	0.029348
60	0.011136	0.025781	0.033524

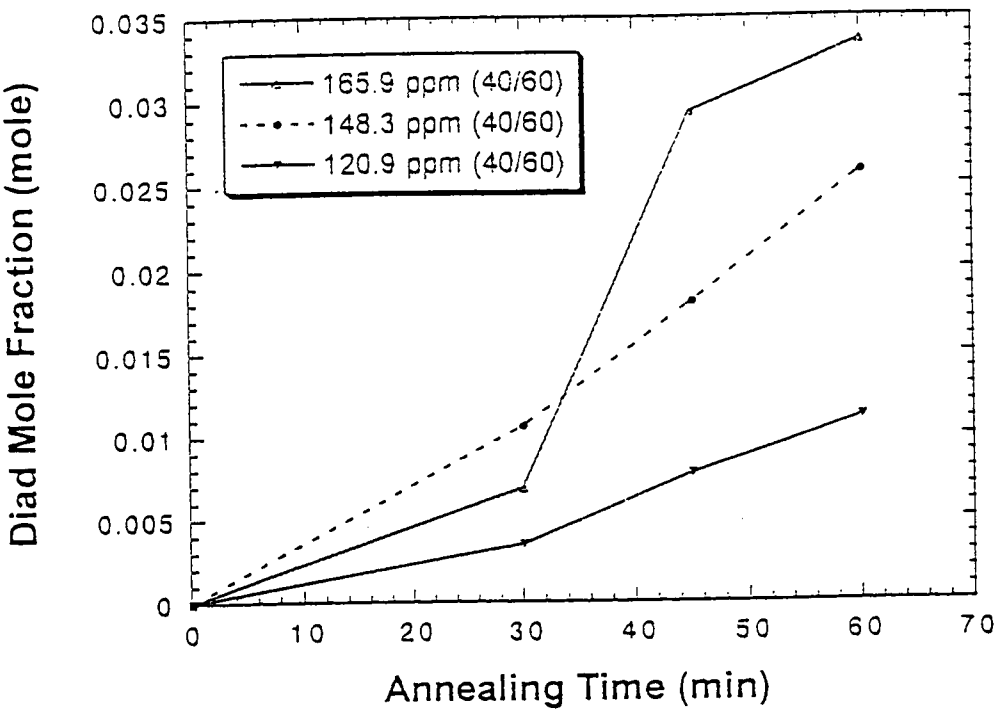

Figure 42. The plot of transient diad mole fraction in PC/PHB-PET blends as a function of annealing time.

Thus, the progressive formation of transient bisphenol-A oxybenzoate and bisphenol-A terephthalate diads up to 60 minutes of annealing was confirmed and quantified by ^{13}C NMR spectroscopy. However, our objective of this study is to correlate the changes in the micro structure of the PC/PHB-PET blend to the macroscopic properties of the blend such as morphology and mechanical properties. It is known that transesterification can alter the morphology of polymer blends. In the case of PC/PHB-PET, the chemical structure of the liquid crystalline PHB-PET is severely deteriorated as transesterification proceeds. Consecutive transreactions between PC and PHB or PET form random copolymers in the blend. Thus, a loss of liquid crystalline character in the blend is expected as a result of the transesterification in blend. The disruption of liquid crystalline structure of PHB-PET is shown in Figure 43.

The liquid crystalline domains in the blend typically exhibit birefringence under cross polarized light. However, the birefringence emanating from liquid crystalline domains under cross polarized light in the blend diminishes as PC undergoes consecutive transesterification with PHB-PET upon annealing. This is due to the breakdown of the liquid crystalline PHB-PET structure and the formation of amorphous random copolymers as the transesterification proceeds. The loss of liquid crystallinity in PC/PHB-PET upon annealing of the blend can be quantified using polarized optical microscopy and image analysis. The parameter of integrated density in the blend images is utilized to quantify amount of liquid crystallinity in the blend and is defined as the pixel intensity of birefringent LC domains in the image after the pixel intensity of the isotropic background is subtracted. The integrated density is measured for the annealed blends at different times. Figure 44 shows a plot of the measured integrated density

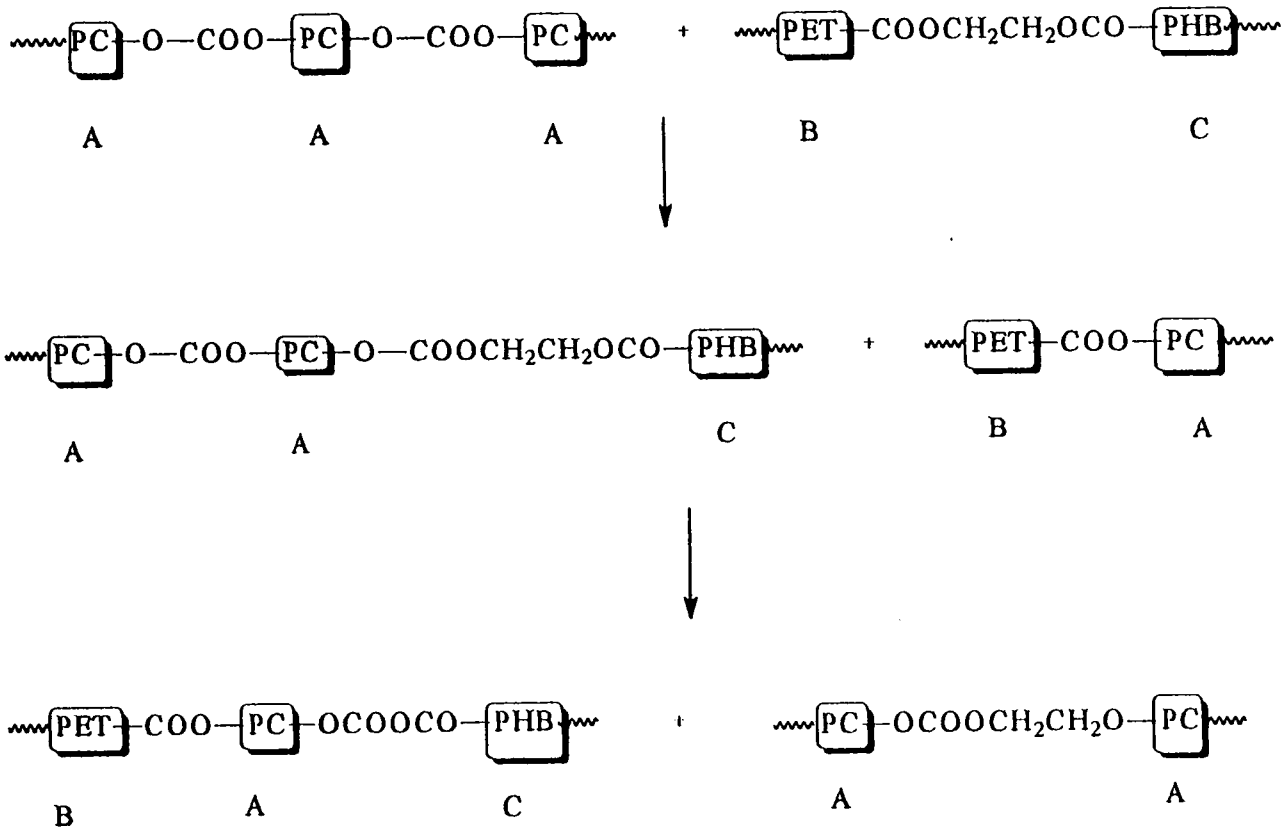

Figure 43. A schematic path for transesterification between PC and PHB-PET

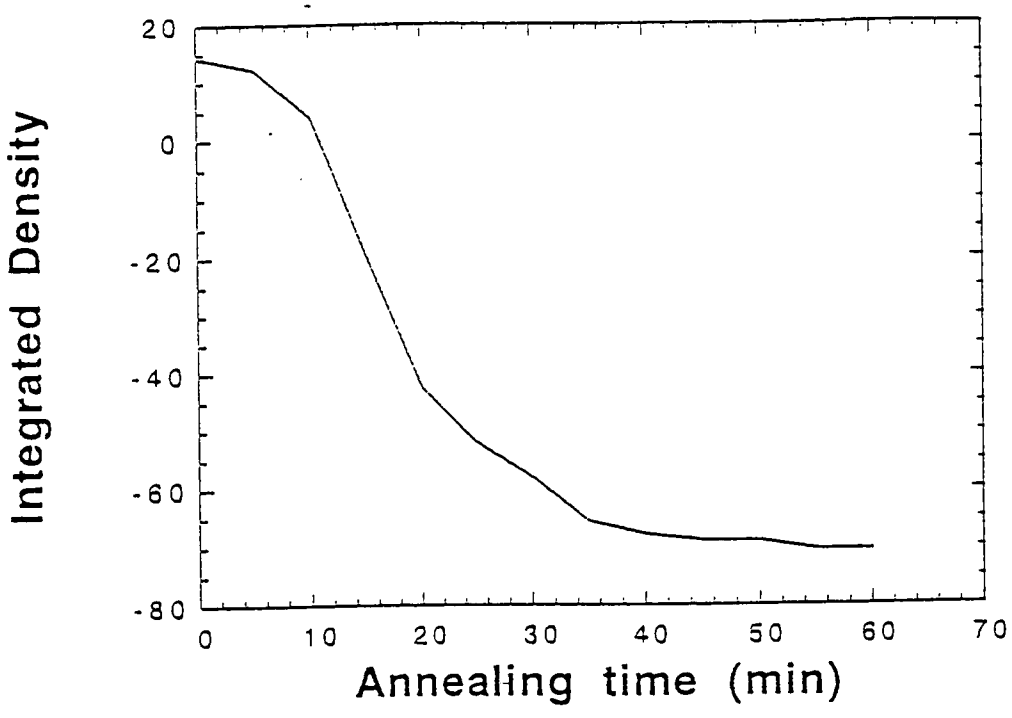

Figure 44. The plot of integrated density of annealed PC/PHB-PET images as function of annealing time.

of annealed PC/PET-PHB blends at different annealing times. As seen in Figure 44, the measured integrated density values becomes more negative as annealing time increases due to the expansion of isotropic domains at longer annealing times. Note that the darker isotropic regions have lower pixel intensity than the brighter LC domains. This plot also shows that the integrated density sharply declines at early stages of annealing indicating a sharp decrease in the birefringence of the liquid crystalline domain up to 30 minutes of annealing. This is presumably due to rapid destruction of liquid crystalline structure of PHB-PET and the formation of new random copolymers during consecutive transesterification reactions in the blend during this time period. However, the integrated density value levels off after that up to 60 minutes. This may be because the supply of liquid crystalline PHB-PET is depleted as a result of the formation random copolymers.

Lastly, the effect of transesterification on the mechanical properties of PC/PET-PHB is discussed. Generally, the formation of copolymers at the interface by transesterification reactions promotes interfacial adhesion and enhances compatibility in the blend. As a result, an improvement in mechanical properties in the blend is expected due to improved interfacial adhesion between blend components. To examine this in our system, the Young's modulus of PC/PHB-PET blend was measured as a function of annealing time. Figure 45 shows a plot of Young's modulus of the blend as a function of annealing time. The data can be interpreted in the following way.

This data shows that an initial decrease in the Young's modulus of the blend is observed after 30 minutes of annealing due to disruption of the liquid crystalline and rigid structure of PHB-PET upon transesterification between PC and PHB-PET. However, as the

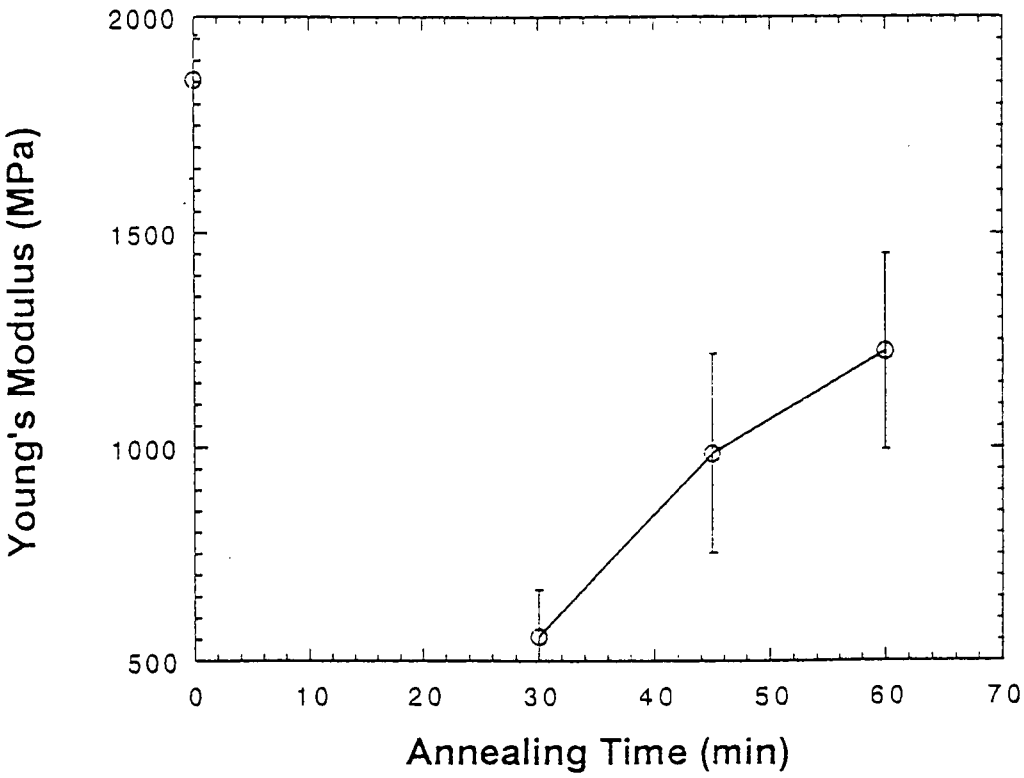

Figure 45. Young's Modulus of PC/PHB-PHB blend as a function of annealing temperature.

transesterification proceeds for more than 30 minutes, the interfacial adhesion between PC and PHB-PET increases due to increased formation of copolymers at interface and as a result a recovery trend in Young's modulus is observed up to 60 minutes annealing time. Note that the overall Young's modulus of the blend after 60 minutes of annealing is still lower than that of the unannealed sample. This may be due to the loss of the liquid crystallinity (rigidity) of blend as a result of consecutive transesterification reactions. One might expect that there is a point during transesterification where the Young's modulus of blend can be optimized without a major destruction of liquid crystalline structure of PHB-PET. In other words, a compromise between the loss of liquid crystalline character and the interfacial modification of the annealed blends can be obtained. Optical microscopy and tensile measurements results suggest that this point can be reached in the annealed PC/PET-PHB blend with annealing time of less than 30 minutes.

Based on our ^{13}C NMR results, the first signatures of the formed bisphenol-A oxybenzoate and bisphenol-A terephthalate diads were observed in the blend that has been annealed for 30 minutes. Thus, it was difficult for us to verify the formation of bisphenol-A oxybenzoate and bisphenol-A terephthalate diads by NMR spectroscopy in the annealed blends for less than 30 minutes. This is presumably due to limited sensitivity (signal/noise ratio) of NMR instrument used in this study. The future study of these blends with more sensitive NMR instruments (600 MHz or higher) with a higher resolution will help in the determination of the optimal point in these blends.

Conclusion and Future work

FT-IR spectroscopy is utilized to investigate the effect of polymer chain rigidity on the formation of intermolecular hydrogen bonds in the blends .The results of this study indicate that increasing the rigidity of polymer chain lowers its ability to form intermolecular hydrogen bonds with a coiled polymer. However, the rigidity effect was not dramatic for the polymers examined in this study. The results showed that the amount of intermolecular hydrogen is higher in the blends with low concentration of LCP due to better dispersion of LCP, suggesting that a one-phase blend may be reachable for mixtures of non-rigid LCP and an amorphous polymer, where the composition of blend is rich in amorphous polymer.

The results of this study also indicated that the extent of intermolecular hydrogen bonding in the blend lowers at higher temperatures due to increased local and global mobilities of the polymers. The high- temperature annealing of the blends also revealed an irreversible process of breaking and reforming of hydrogen bonds which may correspond to a change in the dispersion of the blend components. The results of this study also showed that the extent of intermolecular hydrogen bonds increases with an increase in spacing between the functional groups along the polymer chain and their rotational freedom.

Future work will be focused in the following directions:

1) The effect of spacing of hydroxyl functional groups on the formation of hydrogen bonds to maximize the intermolecular hydrogen bonding will be studied by FT-IR spectroscopy.

2) The phase behavior of PS-*co*-PVPh/7,9-copolyether blends with low concentration of LCP and the possibility of finding an one-phase system will be studied.

3) NMR spectroscopy can be utilized to measure the spin-spin relaxation times in blends of

PS-*co*-PVPh and 7,9-copolyether. These experiments will provide information on the molecular motions and mobility of polymers at different temperatures in these blends. The information on the domain size of components in the blends can also be obtained by spin diffusion experiments.

The formation of copolymers at the interface of PC/PHB-PET blends was characterized using ^{13}C NMR spectroscopy and was quantified by diad analysis of bisphenol-A oxybenzoate and bisphenol-A terephthalate. The mole fraction of these diads increases with annealing time up to 60 minutes, due to transesterification reactions between PC and PHB-PET. The formation of copolymers at interface was correlated to the changes in blend morphology. A loss of liquid crystalline character was also observed as a result of disruption of liquid crystalline structure of PHB-PET in blend and quantified by polarized optical microscopy. The mechanical properties of the blend were also correlated to the micro structure changes in the blends due to the formation of copolymers at interface. The results of Young's modulus measurements supported the loss of liquid crystallinity of PC/PHB-PET blend through a decrease in Young's modulus. The results tensile measurements exemplify a trade-off between the loss of liquid crystalline character of the blend and its strength and presumably better interfacial adhesion resulting from transesterification upon annealing.

The future work will be focused on the diad analysis of PC/PHB-PET with more powerful NMR instrument in search of finding an optimal condition between loss of liquid crystallinity of the blends and its interfacial adhesion. The effect of transesterification on interfacial adhesion in the blend will also be studied. In order to do so, the fracture toughness of the interface will be measured using an asymmetric double cantilever beam fracture test.

LIST OF REFERENCES

1. Folkes, M. J.; Hope, P.S., In *"Polymer Blends and Alloys"*, Blackie Academic and Professional; London, **1993**.

2. Sweeny, F. M., *In "Polymer Blends and Alloys Guide Book to Commercial Products"*; Technomic Publishing, Inc., Lancaster. PA, **1988**.

3. Utracki, L. A., In *"Polymer Alloys and Blends, Thermodynamics and Rheology"*, Oxford University Press, Hanser, NY, **1990**.

4. Kaempf, G. *Polymer J.*, **1987**, *19*, 257.

5. Xanthos, M., *Polym. Eng. Sci.*, **1988**, *28*, 1392.

6. Flory, P. J., In *"Principles of Polymer Chemistry"*, Cornell University Press, Ithaca, NY, **1953**.

7. Porter, R. S.; Wang, L. -H., *Polymer*, **1992**, *33*, 2019.

8. Huggins, M. L., *J. Chem. Phys.*, **1941**, *9*, 440.

9. Freeman, P. I.; Rowlinson, J. S., *Polymer*, **1959**, *1*, 201.

10. Siow, K. S.; Delma, G.; Patterson, D., *Macromolecules*, **1972**, *5*, 29.

11. Flory, P. J.; Orwoll, R. A., Vrij, A., *J. Am. Chem. Soc.*, **1964**, *86*, 3507.

12. Flory, P. J.; Orwoll, R. A.; Vrij, A., *J. Am. Chem. Soc.*, **1964**, *86*, 3515.

13. Flory, P. J., *J. Am. Chem. Soc.*, **1965**, *87*, 1833.

14. Lacomble, R. H.; Sanchez, I. C., *Macromolecules*, **1978**, *11*, 1145.

15. Painter, P. C.; Graf, J. F.; Coleman, M. M., *J. Chem. Phys.*, **1990**, *92*, 6166.

16. Graf, J. F.; Coleman, M. M.; Painter, P. C., *J. Phys. Chem.*, **1991**, *95*, 6710.

17. Coleman, M. M.; Painter, P.C., *Prog. Polym. Sci.*, **1995**, *20*, 1.

18. Coleman, M. M.; Serman, C. J.; Bhagwager, D. E.; Painter, P. C., *Polymer*, *31*, 1187.

19. Coleman, M. M.; Serman, C. J.; Bhagwagar, D. E.; Painter, P., *Polymer*, **1990**, *31*, 1187.

20. Painter, P. C.; Coleman, M. M., In *"Fundamentals of Polymer Science"*, 2nd Ed., Technomic Publishing Company; Lancaster, PA, **1992**.

21. Coleman, M. M.; Painter, P. C., *Appl. Spect. Rev.*, **1984**, *20*, 255.

22. Coleman, M. M.; Graf, J. F.; Painter, P. C., eds., In "*Specific Interactions and the Miscibility of Polymer Blends*", Technomic Publishing Company, Lancaster, **1991**.

23. Coleman, M. M.; Lichkus, A. M.; Painter, P. C., *Macromolecules*, **1989**, *22*, 586.

24. Lu, F. J.; Benedetti, E.; Hus, S. L., *Macromolecules*, **1983**, *16*, 1525.

25. (A) Olabisi, O.; Robeson, L. M.; Shaw, M. T., In "*Polymer-Polymer Miscibility*", Academic Press, New York, **1979**. (B) Paul, D. R.; Newman, S., eds., In "*Polymer Blends*", Academic Press, New York, **1978**. (C) Manson, A.; Sperling, L. H., In "*Polymer Blends and Composites*", Plenum Press, New York, **1976**. (D) Sperling, L. H. ed., In "*Recent Advances in Polymer Blends, Grafts and Blocks*", Plenum Press, New York, **1974**. (E) Platzer, N. A. J., ed., In "*Multi-component Polymer systems*", Adv. Chem. Ser., No. 99, Am.Chem. Soc., Washington, D.C., **1971**.

26. (A) Kelmpner, D.; Frisch,K. C., In "*Polymer Alloys, Blends, Blocks, Grafts and Interpenetrating Networks*", Plenum Press, New York, **1979**. (B) Walsh, D. J.; Higgins, J. S.; Maconnachie, A., eds., In "*Polymer Blends and Mixtures*", NATO ASI Series E: Applied Sciences No. 89, Mitinus Nijhoff Publishers Dordrech/Boston/Lancaster, **1985**. (C)Ottenbrite, R. M.; Utracki, L. A.; T. Inoue, eds., In "*Current Topics in Polymer Science*, Vol. II, Rheology and Polymer Processing/Multiphase Systems", Hanser Publishers, New York,**1987**. (D) Paul, D. R.; Sperling, L. H., eds., "*Multicomponent Polymer Materials*", *Adv. Chem. Ser.*, No.211, Am. Chem. Soc., Washington, D.C., **1986**.

27. Olabisi. O., *Macromolecules, 1975, 8*, 316.

28. Allard, D.; Prud'homme, R. E., *J. Appl. Polym. Sci.*, **1982**, *27*, 559.

29. Prud'homme, R. E., *Polym. Eng. Sci.*, **1982**, *22*, 90.

30. Robeson, L. M.; Furtek, A. B., *Am. Chem. Soc.,Div. Org. Coat. Plast. Chem., Pap.*, **1977**, *37*, 136.

31. Robeson, L. M.; Hale, W. F.; Merriam, C. N., *Macromolecules*, **1981**, *14*, 1644.

32. Harris, J. E.; Goh, S. H.; Paul, D. R.; Barlow, J. W., *J. Appl. Polym. Sci.*, **1982**, *27*, 839.

33. Robeson, L. M., In "*Polymer compatibility and Incompatibility: Principles and Practice*", ed. By Solc, K., MMI Press Sym. Series, Vol 2, Harwood Academic Publishers, New York, **1982**.

34. U.S. Patent No.4,678,833, **1987**.

35. Coleman, M. M.; Moskala, E. J., *Polymer*, **1983**, *24*, 253.

36. Coleman, M. M.; Moskala, E. J., *Poly. Commun.*, **1983**, *24*, 207.

37. Tang, S. P.; Pearce, E. M.; Kwei, T. K., *J. Polym. Sci., Polym. Lett. Ed.*, **1980**, *18*, 201.

38. Kwei, T. K.; Pearce, E. M.; Min, B. Y., *Macromolecules*, **1985**, **18**, 2326.

39. Smith, K. L.; Winslow, A. E.; Peterson, D. E., *Ind. Eng. Chem.*, **1959**, *51*, 1361.

40. Osada, Y.; Sato, M., *J. Polym. Sci., Polym. Letts. Ed.*, **1976**, *14*, 129.

41. Lysaght, M. J., In "*Ionic Polymers*", L. Holiday, ed., Wiley, New York, **1975**.

42. Michaels, A. S., *Ind. Eng. Chem.*, **1965**, *57*, 32.

43. Plans, J.; MacKnight, W. J.; Karasz, F. E., *Macromolecules*, **1984**, *17*, 810.

44. Wellinghoff, S. T.; Koenig, J. L.; Baer, E., *J. Polym. Sci., Polym. Phys. Ed.*, **1977**, *15*, 1913.

45. Djordjevic, M. B.; Porter, R. S., *Polym. Eng. Sci.*, **1983**, *23*, 650.

46. Wahrmund, D. C.;Bernstein, R. B.; Barlow, J. W.; Paul, D. R., *Polym. Eng. Sci.*, **1978**, *18*, 677.

47. Noland, J. S.; Hsu, N. N. -C.; Saxon, R.; Schmitt, J. M., *Adv. Chem. Ser.* **1971**, *99*, 15.

48. Bernstein, R. E.; Wahrmund, D. C.; Barlow, J. W.; Paul, D. R., *Polym. Eng. Sci.*, **1978**, *18*, 1220.

49. Yun, Xu, Y.; Painter, P. C.; Coleman, M. M., *Makromol. Chem. Macromol. Symp.*, **1991**, *52*, 91.

50. Coleman, M. M.; Yun, Xu, Y.; Harrell, J. R.; Painter, P. C., *Makromol. Chem. Macromol. Symp.*, **1991**, *52*, 89.

51. Zhang, H.; Bhagwagar; Graf, J. F.; Painter, P. C.; Coleman, M. M., *Polymer*, **1994**, *35*, 5379.

52. Le Menestrel, C.; Bhagwagar, D. E.; Painter, P. C.; Coleman, M. M.; Graf, J. F., *Macromolecules*, **1992**, *25*, 7101.

53. Yun, Xu; Painter, P. C.; Coleman, M. M., *Makromol. Chem., Macromol. Symp.*, **1991**, *51*, 61.

54. Sermon, C. J.; Painter, P. C.; Coleman, M. M., *Polymer*, **1991**, *32*, 1049.

55. Yun, Xu, Y.; Graf, J.; Painter, P. C.; Coleman, M. M., *Polymer*, **1991**, *32*, 3103.

56. Moskala, E. J.; Howe, S. E.; Painter, P. C.; Coleman, M. M., *Macromolecules*, **1984**, *17*, 1671.

57. Moskala, E. J.; Varnell, D. F.; Coleman, M. M., *Polymer*, **1985**, *26, 228.*

58. Helminiak, F. E.; Arnold, F. E.; Bener, C. L., *Am. Chem. Soc. Polym. Preprints*, **1975**, *16*, 659.

59. Flory, P. J., In *"Principles of Polymer Chemistry"*, Cornell University Press, Ithaca, NY, **1953**.

60. Flory, P. J., *Macromolecules*, **1978**, *11*, 1138.

61. Ballauf, M., *Mol. Cryst. Liq. Cryst.*, **1986**, *136*, 175.

62. Tang, W. -L.; Coleman, M. C.; Painter, P. C., *Makromol. Chem., Macromol. Symp.*, **1994**, *54*, 315.

63. Painter, P.C.; Tang, W., -L.; Graf, J. F.; Thomas, B.; Coleman, M. M., *Macromolecules*, **1991**, *24*, 3929.

64. Coleman, M. M.; Pehlert, G. J.; Painter, P. C., *Macromolecules*, **1996**, *29*, 6820.

65. Pehlert, G. J.; Painter, P. C.; Veytsman, B.; Coleman, M. M., *Macromolecules*, **1997**, *30*, 3671.

66. Hu, Y.; Painter, P. C.; Coleman, M. M., *Macromolecules*, **1998**, *31*, 3394.

67. Khatri, C. A.; Vaidya, M. M.; Levon, K.; Jha, S. K.; Green, M. M., *Macromolecules*, **1995**, *28*, 4719.

68. Ledwidth, A.; Rahnema, M.; Sengupta, P. K., *J. Polym. Sci., Polym. Chem. Ed.*, **1980**, *8*, 2239.

69. Percec, V.; Nava, H.; Jonsson, H., *J. Polym. Sci., Polym. Chem., Ed.*, **1987**, *25*, 1943.

70. Hall, E.; Ober, C. K.; Kramer, E. J.; Colby, R. H.; Gilmor, J. R., *Macromolecules*, **1992**, *26*, 3764.

71. Coleman, M. M.; Painter, P. C., *Appl. Spect. Rev.*, **1984**, *20*, 255.

72. Le Menestrel, C.; Bhagwagar, D. E.; Painter, P.C.; Coleman, M. M.; Graf, J. F., *Macromolecules*, **1992**, *25*, 7101.

73. March, J., In "*Advanced Organic chemistry*", John Wiley & Sons; New York; **1992**.

74. Lowry, T. H.; Richardson, K. S., In "*Mechanism and Theory in Organic chemistry*", Harper Collins Publishers; New York; **1987**.

75. Sperling, H. L.; In "*Introduction to Physical Polymer Chemistry*", Wiley-Interscience; New York; Second Edition, **1992.**

76. Coleman, M. M.; Painter, P. C., *Appl. Spect. Rev.*, **1984**, *20*, 255.

77. Dadmun, M. D.; Clingman, S.; Ober, C. K.; Nakatani, A. I., *J. Polym. Sci. Polym. Phys. Ed.*, **1998**, *36*, 3017.

78. Yun, X.; Painter, P.C.; Coleman; M. M., *Makromol. Chem., Macromol. Symp.*, **1991**, *51*, 61.

79. Ballauf, M., *Mol. Cryst. Liq. Cryst.*, **1986**, *136*, 175.

80. Flory, P. J., *Macromolecules*, **1978**, *11*, 1138.

81. Tang, W.-L; Coleman, M. M.; Painter, P. C., *Macromol. Symp*, **1994**, *84*, 313.

82. Coleman, M. M.; Pehlert, G. J.; Painter, P.C., *Macromolecules*, **1996**, *29*, 6820.

83. Collyer, A. A., In "*Materials Science and Technology*", **1989**, *5*, 309.

84. Dobb, M. G.; McIntyre, J. E., *Adv. Polym. Sci.*, **1984**, *60/61*, 61.

85. Collyer, A. A., In "*Rheology and Processing of Liquid Crystal Polymers*", Acierno, D.; Collyer, A. A. Eds., Chapman & Hall, New York, **1996**.

86. Baird, D. G.; Ramanathan, R., *Contemporary Topics in Polymer Science*, **1990**, *6*, 73.

87. Cox M. K., *Mol. Cryst. Liq. Cryst.*, **1987**, *153*, 415.

88. Dole, J. R., *ChemTech*, **1987**, No. 9, 546.

89. Annon, T., *Modern Plastics*, **1991**, *68*, 115.

90. Weiss, R. A.; Huh, W.; Nicolais, L. *Polym. Eng. Sci.*, **1987**, *27*, 684.

91. Williams, D. J., *Adv. Polym. Technol.*, **1990**, *10*, 173.

92. Beery, D.; Kenig, S.; Siegman, A., *Polym. Eng. Sci.*, **1991**, *31*, 459.

93. Utracki, L. A., In "*Polymer Alloys and Blends*", Oxford University Press, New York, **1990**.

94. Flory, P. J., In *"Principles of Polymer Chemistry"*, Cornell University Press, Ithaca, NY, **1953**.

95. Porter, R. S.; Wang, L.-H., *Polymer*, **1992**, *33*, 2019.

96. Fakirov. S., In "*Solid State Behavior of Linear Polyesters and Polyamides*", Schultz, J. M.; Fakirov, S., Eds., Prentice Hall, Englewood, NJ, **1990**.

97. Henrichs, P. M.; Tribone, J.; Mass, D. J., *Macromolecules*, **1988**, *21*, 1282.

98. Kotliar, A. M.; *J. Polym. Sci., Polym. Chem. Ed.*, **1973**, *11*, 1157.

99. Yu, T.; Guo, M., *prog. Polym. Sci.*, **1990**, *15*, 825.

100. Devaux, J.; Godard, P.; Mercier, J. P., *J. Polym. Sci., Polym. Phys. Ed.*, **1982**, *20*, 1881.

101. Henrichs, P.; Tribone, J.; Massa, D.; Hewitt, *Macromolecules*, **1988**, *21*, 1282.

102. Godard, P.; Dekoninck, J.; Devlesaver, V.; Devaux, J., *J. Polym. Sci. Polym. Chem. Ed.*, **1986**, *24*, 3301.

103. Kimura, M.; Porter, R. S.; Salee, G., *J. Polym. Sci., Poly. Phys. Ed.*, **1983**, *21*, 367.

104. Wang, L. -H.; Lu, M.; Yang, X.; Porter, R. S., *J. Macromol. Sci. -Phys.*, **1990**, *B29*, 171.

105. Velden, G. v. d.; Kolfschoten-Smitsmans, G.; Veermans, A., *Polym. Commun.* **1987**, *28*, 169.

106. Devaux, J.; Godard, P.; Mercier, J. P., *J. Polym. Sci. Polym. Phys. Ed.*, **1982**, *20*, 1875.

107. Devaux, J.; Godard, P.; Mercier, J. P., *J. Polym. Sci., Polym. Phys. Ed.*, **1982**, *20*, 1901.

108. Godard, P.; Dekoninck, J. M.; Devlesaver, V., *J. Polym. Sci., Polym. Chem. Ed.*, **1986**, *24*, 3315.

109. Tyan, H.; Wei, K. -H.; Wei, K. -H., *J. Polym. Sci.*, **1998**, *36*, 1959.

110. Wei, K.-H.; Jang, H. -C; Ho, J. -C., *Polymer*, **1997**, *38*, 21.

111. Ou, C.-F.; Lin, C. -C, *J. Appl. Polym. Sci.*, **1996**, *61*, 1455.

112. Paci, M.; Barone, C.; Magagnini, P. L., *J. Polym. Sci., Polym. Phys.*, **1987**, *25*, 1595.

113. Nobile, M. R.; Amendola, E.; Nicolais, L.; Acerno, D.; Carfagna, C., *Polym. Eng. Sci.*, **1989**, *29*, 244.

114. Jung, S. H.; Kim, S. C., *Polymer J.*, **1988**, *20*, 73.

115. Wei, K.-H; Ho, J. -C.; *Macromolecules*, **1997**, *30*, 1587.

116. Hopfe, I.; Pompe, G.; Eichhorn, K. -J., *Polymer*, **1997**, *38*, 2321.

117. Kollodge, J. S.; Porter, R.S., *Macromolecules*, **1995**, *28*, 4106.

118. Wei, K.-H.; Tyan, H. -L., *Polymer*, **1998**, *39*, 2103.

119. Andresen, E.; Zachmann, H. G., *Colloid Polym. Sci.*, **1994**, *272*, 1352.

120. Porter, R. S.; Wang, L.-H., *Polymer*, **1992**, *33*, 2019.

121. Wei, K.-H; Ho, J.-C, *Macromolecules*, **1997**, *30*, 1587.

122. Yamadera, R.; Murano, M. J., *J. Polym. Sci.; Polym. Chem. Ed.*, **1967**, *5*, 2259.

123. Devaux, P.; Goddard, P.; Mercier, J. P., *J. Polym. Sci.; Polym. Phys. Ed.*, **1982**, *20*, 1875.

124. Noggle, J. H., In "*Physical Chemistry*", 3rd Ed., Harper Collins College Publishers; New York, **1996**.

APPENDIX

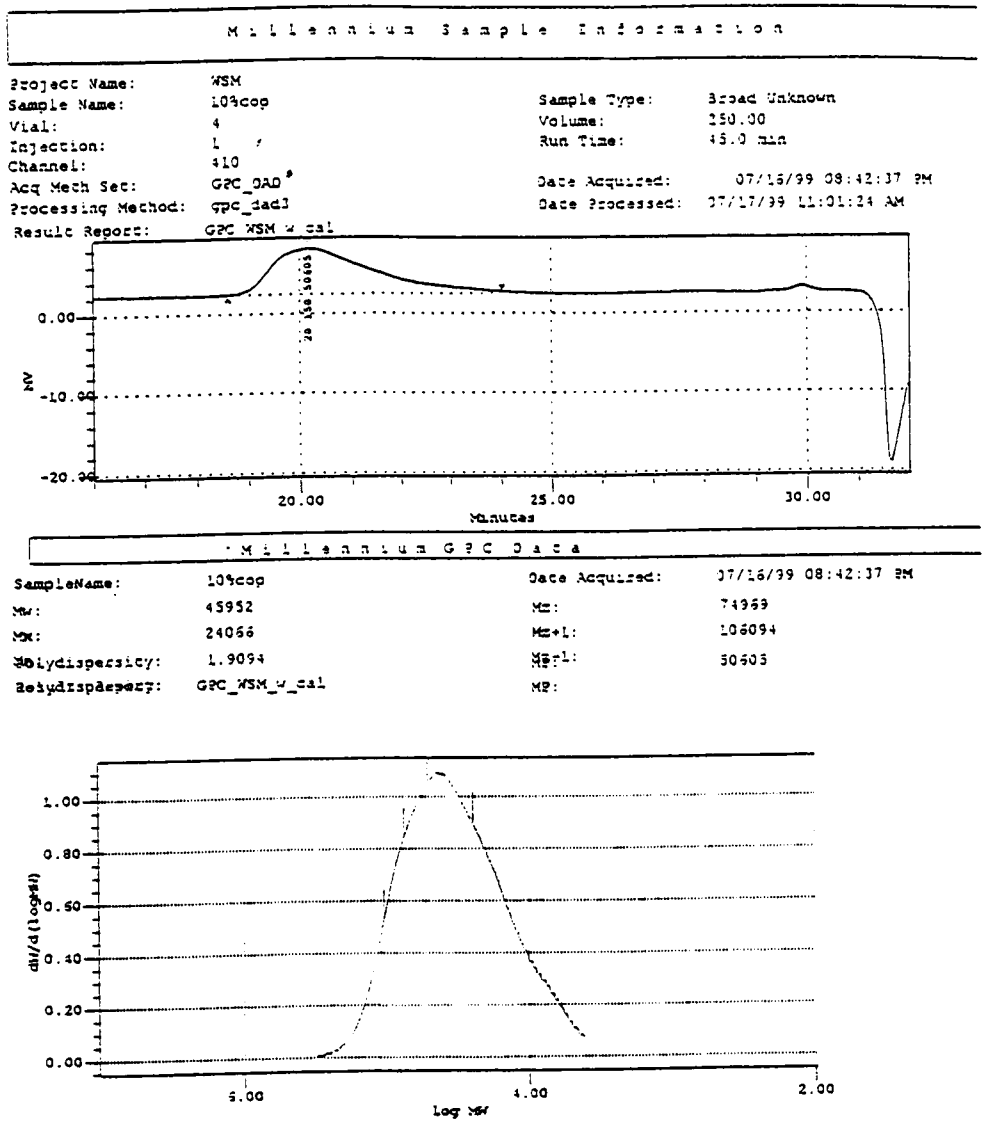

Figure 46. GPC data of PS-*co*-PVPh (10% PVPh)

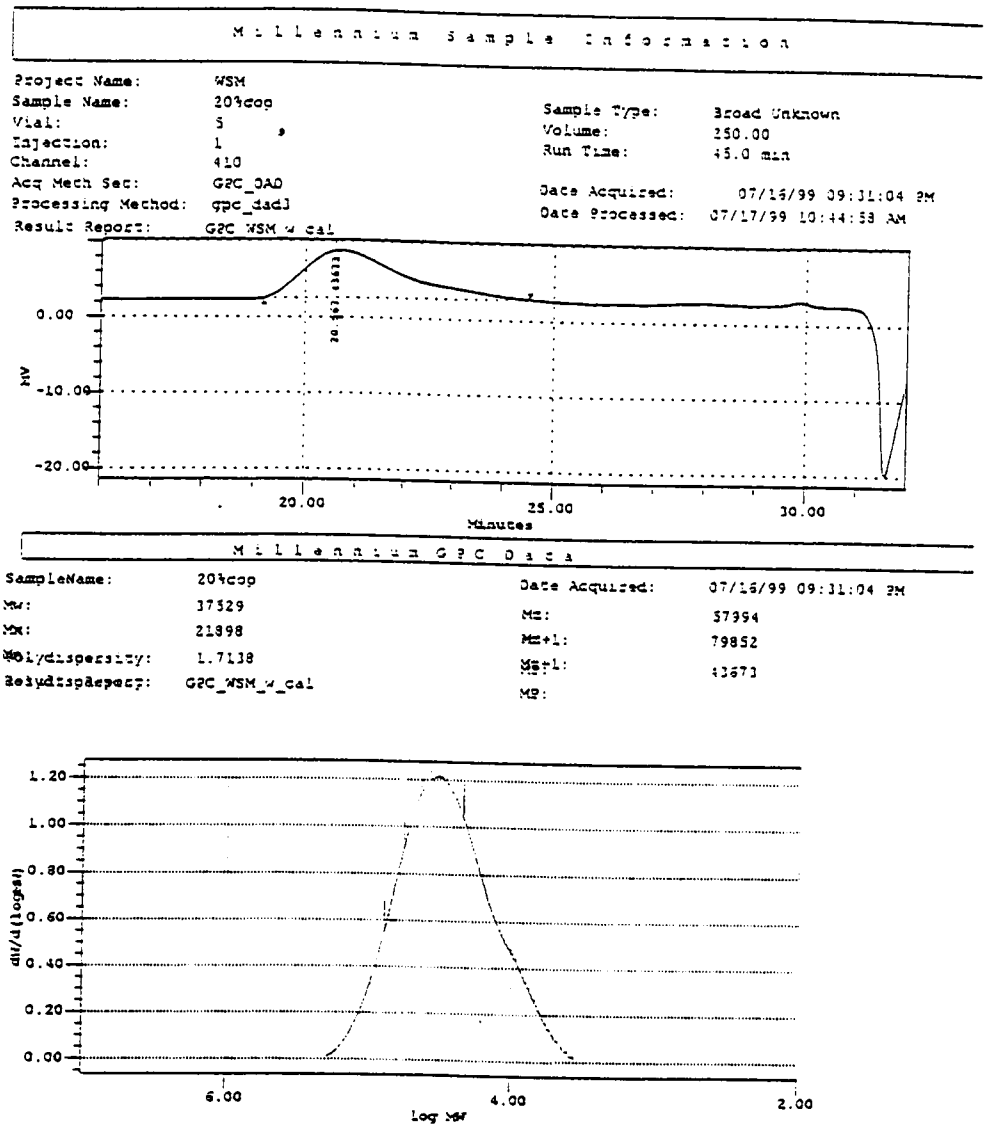

Figure 47. GPC data of PS-*co*-PVPh (20% PVPh)

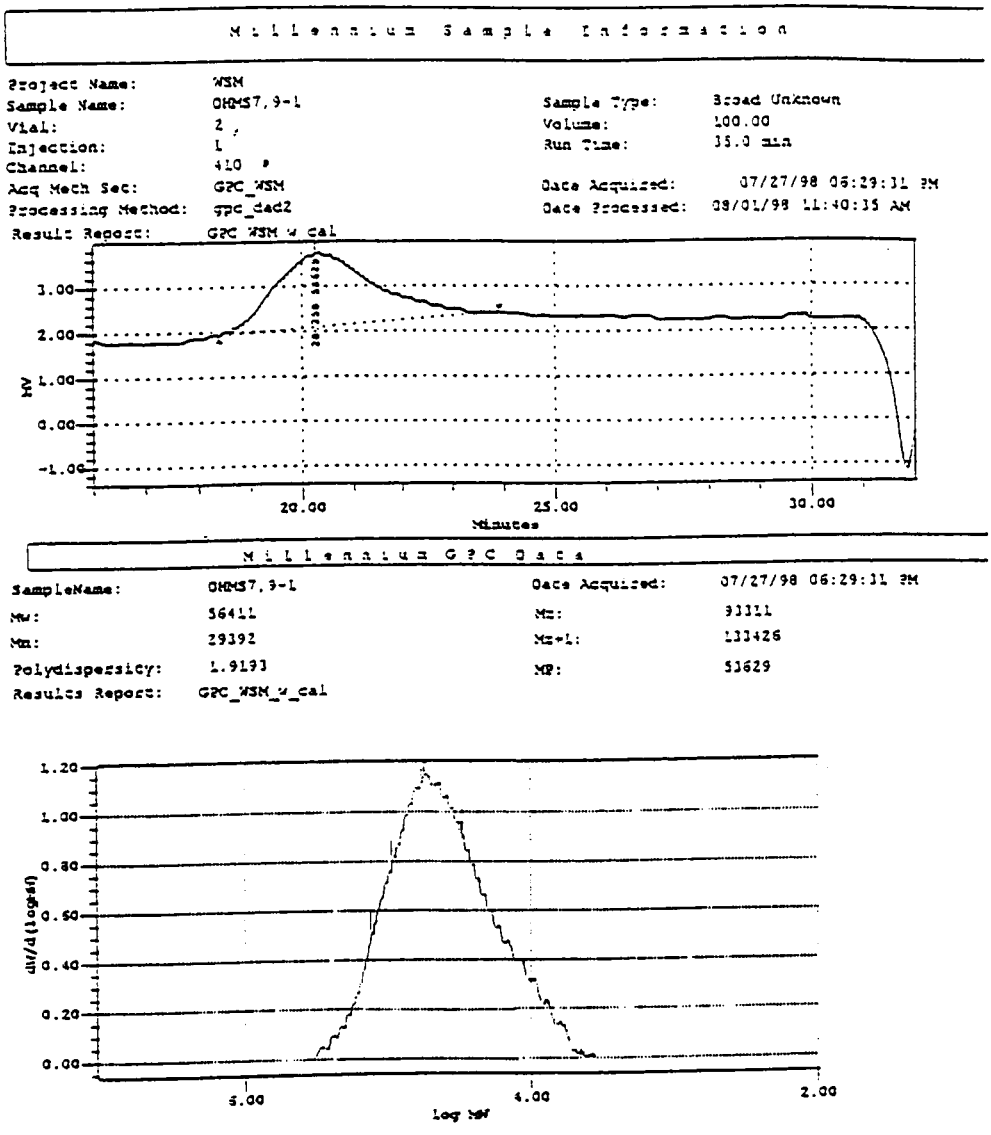

Figure 48 . GPC data of DHMS-7,9

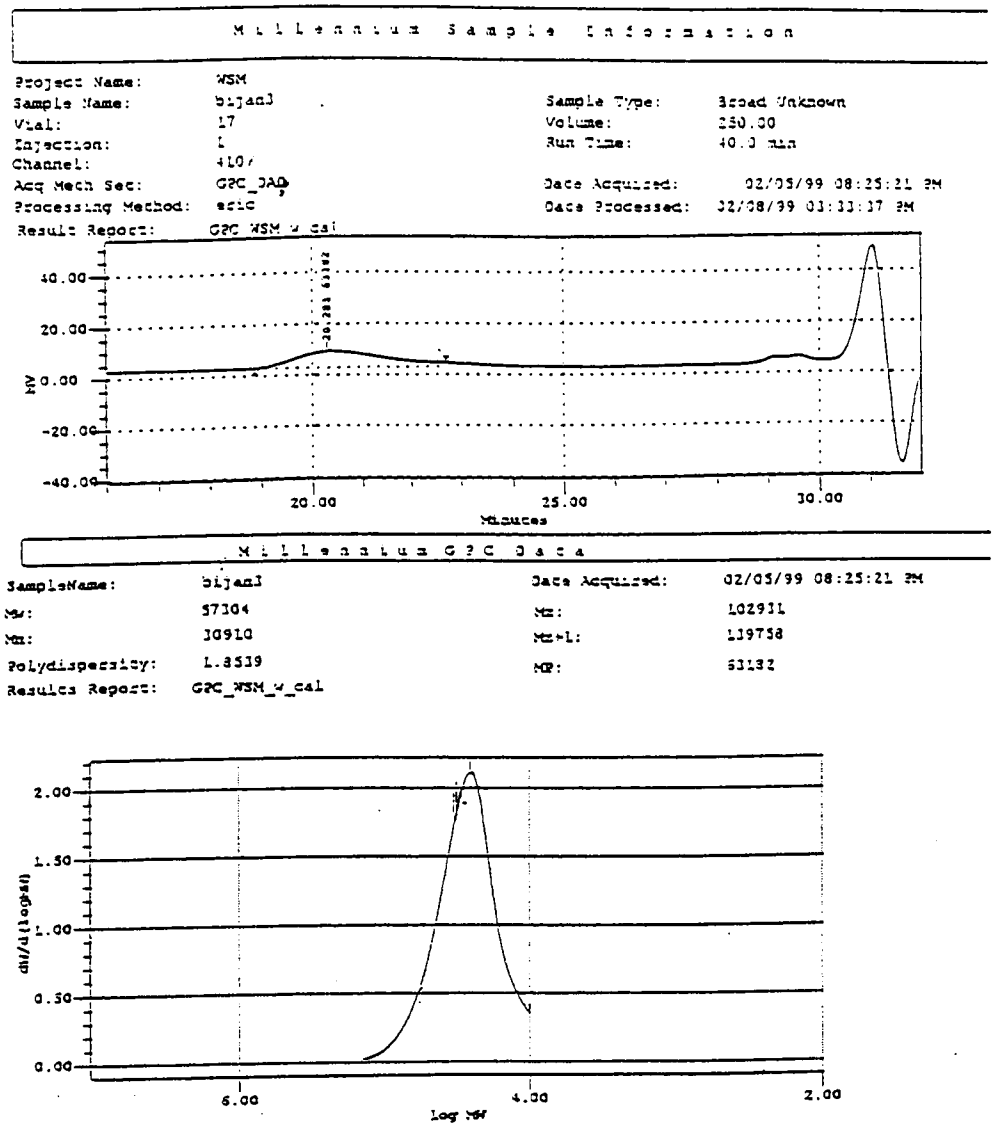

Figure 49. GPC data of Methylene-7,9 copolyether

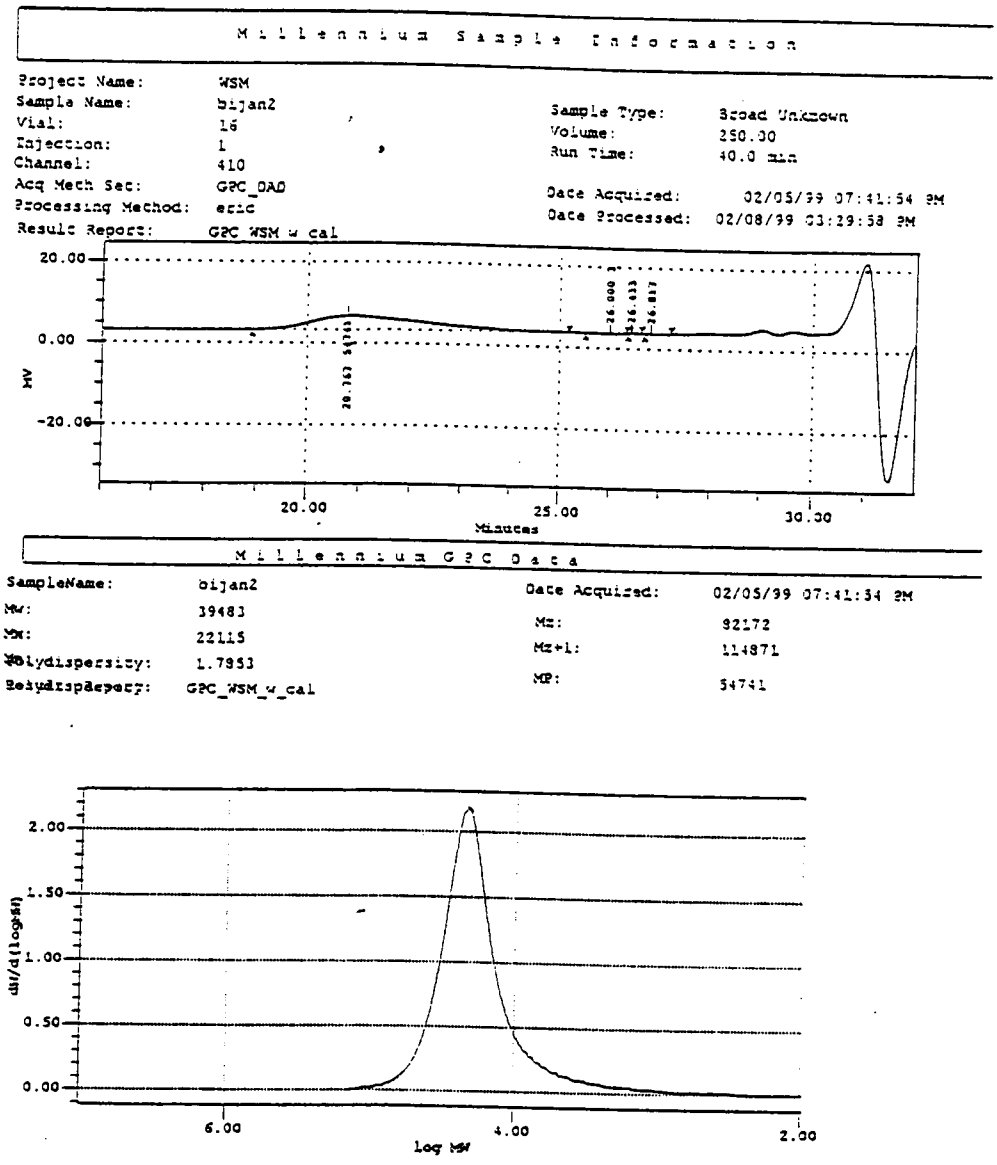

Figure 50. GPC data of Ethylidene-7,9 copolyether

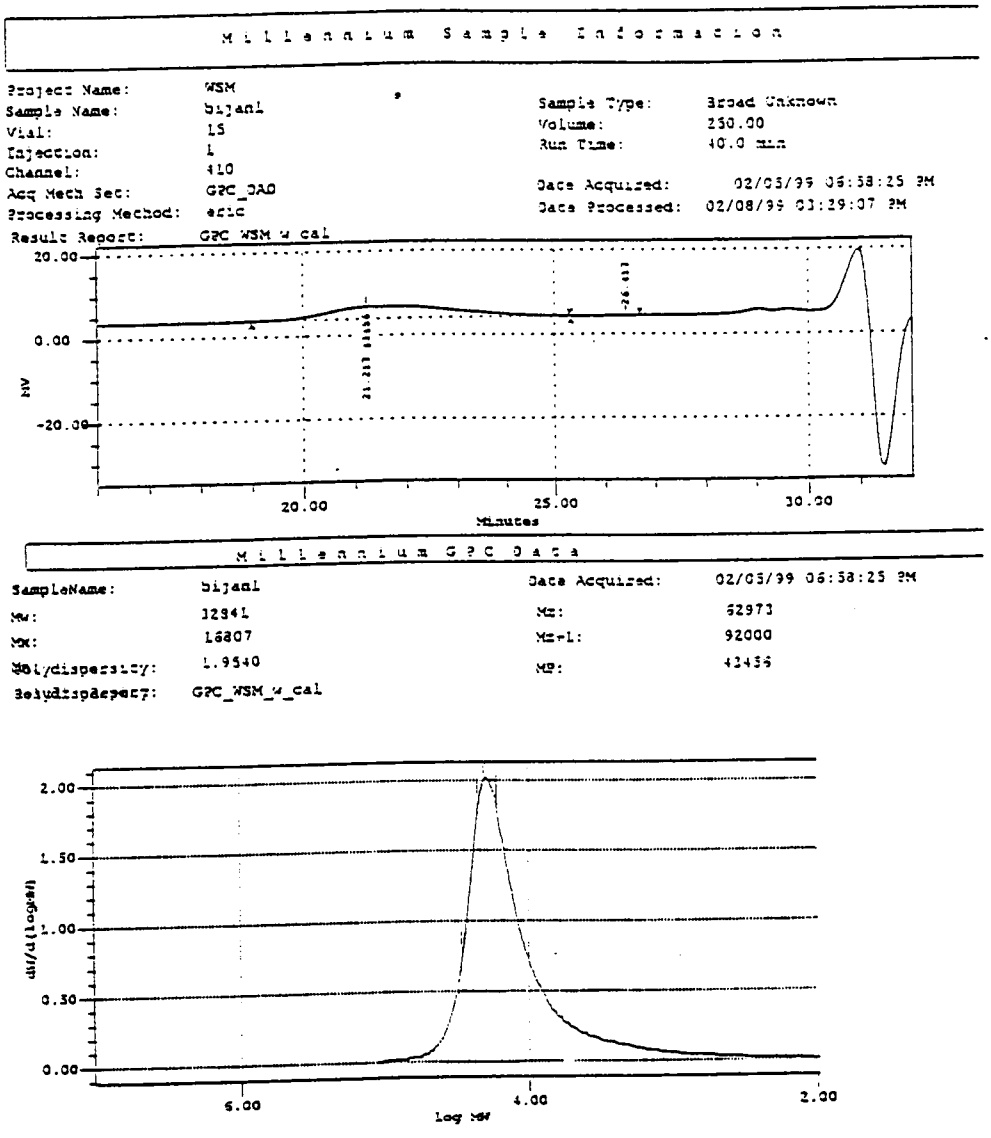

Figure 51. GPC data of Bisphenol-A-7,9 copolyether

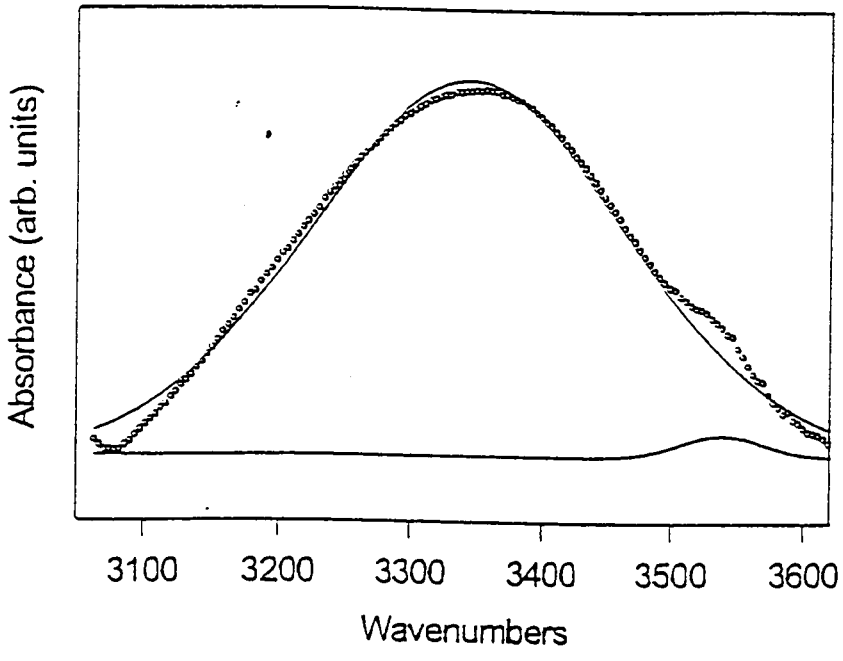

Curve-Fit Std Error= 0.00212914889 r2= 0.997876757

Curve-Fit Coefficients

Peak#	Type	Ampl	Ctr	Wid1	Wid2	Wid3
1	Gaussian	0.0250865	3344.4615	120.25182		
2	Gaussian	0.0019257	3525.0737	17.252333		

Measured Values

Peak#	Type	PkAmpl	PkCtr	Wid@HM	Area	%Area
1	Gaussian	0.0250865	3344.4615	283.17101	7.4353401	98.702271
2	Gaussian	0.0019257	3525.0737	47.690538	0.0977592	1.2977293
	Total				7.5330994	100

Figure 52. Curve-fitting of the hydroxyl region in PVPh/ethylidene-7,9 (15/85 w/w%) after annealing at 170 °C for 8 hours.

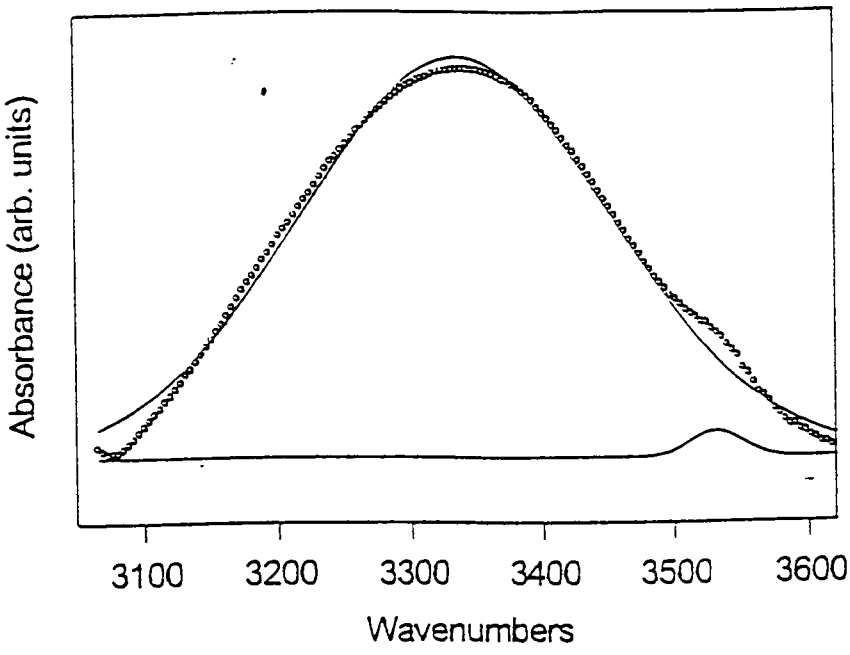

Curve-Fit Std Error= 0.00131603427 r2= 0.996018233

Curve-Fit Coefficients

Peak#	Type	Ampl	Ctr	Wid1	Wid2	Wid3
1	Gaussian	0.0267784	3341.5603	118.03076		
2	Gaussian	0.0017116	3525.0778	18.076857		

Measured Values

Peak#	Type	PkAmpl	PkCtr	Wid@HM	Area	%Area
1	Gaussian	0.0267784	3341.5603	277.94085	7.7910742	99.014345
2	Gaussian	0.0017116	3525.0778	42.567559	0.0775576	0.9856555
	Total				7.8686318	100

Figure 53 . Curve-fitting of the hydroxyl region in PVPh/ethylidene-7,9 (35/65 w/w%) after annealing at 170 °C for 8 hours.

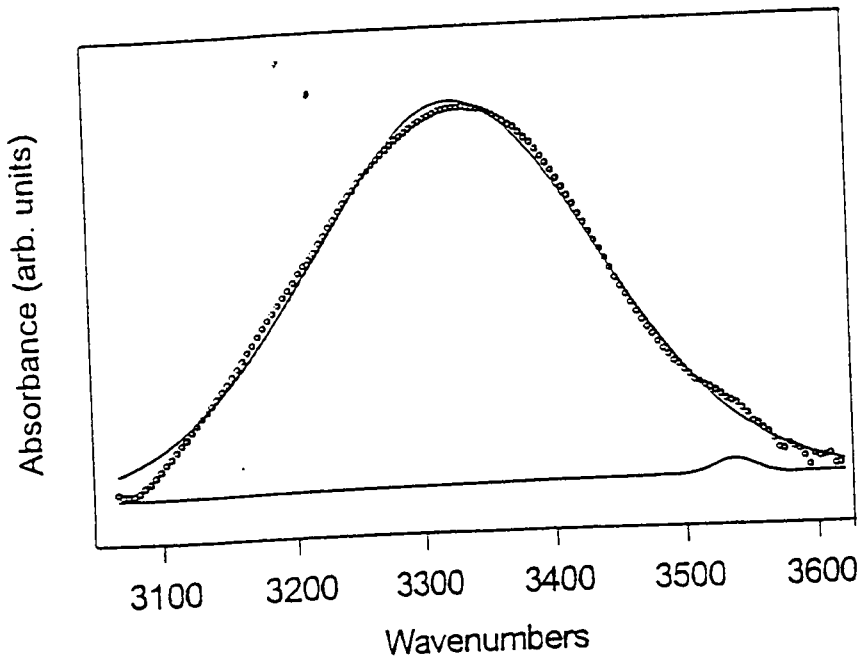

Curve-Fit Std Error= 0.00127176366 r2= 0.996558509

Curve-Fit Coefficients					
Peak# Type	Ampl	Ctr	Wid1	Wid2	Wid3
1 Gaussian	0.0334137	3319.7869	109.11404		
2 Gaussian	0.0008812	3525.7329	14.591491		

Measured Values					
Peak# Type	PkAmpl	PkCtr	Wid@HM	Area	%Area
1 Gaussian	0.0334137	3319.7869	256.94354	9.0189849	99.741266
2 Gaussian	0.0008812	3525.7329	24.940914	0.0233957	0.2587335
Total				9.0423806	100

Figure 54 . Curve-fitting of the hydroxyl region in PVPh/ethylidene-7,9 (65/35 w/w%) after annealing at 170 °C for 8 hours.

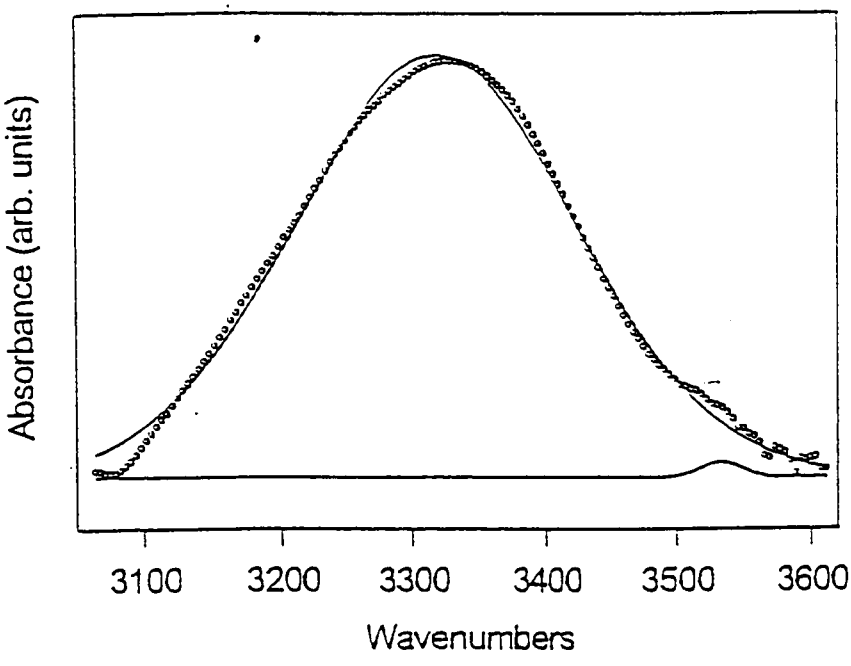

Curve-Fit Std Error= 0.00170751011 r2= 0.992341919

Curve-Fit Coefficients

Peak#	Type	Ampl	Ctr	Wid1	Wid2	Wid3
1	Gaussian	0.0334137	3306.7869	109.11404		
2	Gaussian	0.0008812	3525.7329	10.591491		

Measured Values

Peak#	Type	PkAmpl	PkCtr	Wid@HM	Area	%Area
1	Gaussian	0.0334137	3306.7869	256.94354	9.0189849	99.741266
2	Gaussian	0.0008812	3525.7329	24.940914	0.0233957	0.2587335
	Total				9.0423806	100

Figure 55. Curve-fitting of the hydroxyl region in PVPh/ethylidene-7,9 (85/15 w/w%) after annealing at 170 °C for 8 hours.

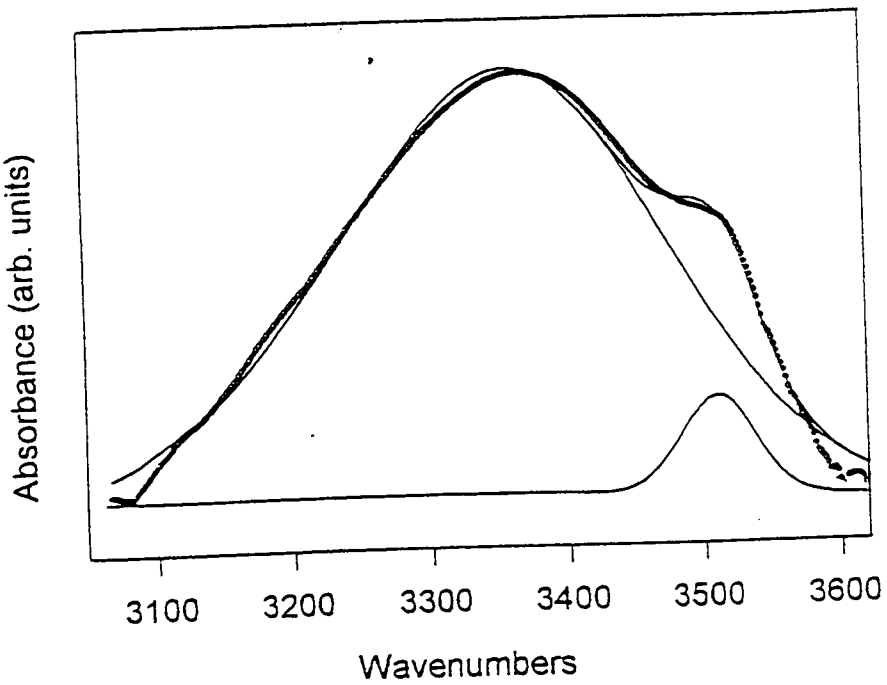

Curve-Fit Std Error= 0.000782339954 r2= 0.992893403

Curve-Fit Coefficients						
Peak#	Type	Ampl	Ctr	Wid1	Wid2	Wid3
1	Gaussian	0.1405667	3370.6421	130.50048		
2	Gaussian	0.0300917	3525.8025	28.04814		

Measured Values						
Peak#	Type	PkAmpl	PkCtr	Wid@HM	Area	%Area
1	Gaussian	0.1405667	3370.6421	307.30474	44.27092	95.440593
2	Gaussian	0.0300917	3525.8025	66.047945	2.1149191	4.5594068
	Total				46.385839	100

Figure 56 . Curve-fitting of the hydroxyl region in PVPh.

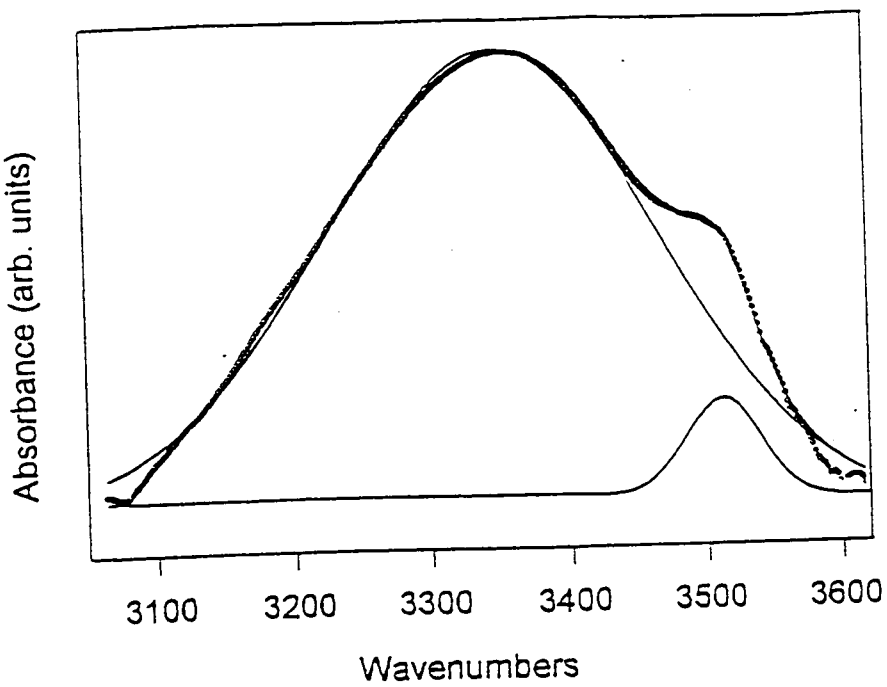

Curve-Fit Std Error= 0.00212914889 r2= 0.997876757

Curve-Fit Coefficients

Peak#	Type	Ampl	Ctr	Wid1	Wid2	Wid3
1	Gaussian	0.1505517	3331.4738	131.87498		
2	Gaussian	0.0286561	3525.2129	26.230452		

Measured Values

Peak#	Type	PkAmpl	PkCtr	Wid@HM	Area	%Area
1	Gaussian	0.1505517	3331.4738	310.54169	47.816209	96.20947
2	Gaussian	0.0286561	3525.2129	61.767524	1.8838977	3.7905304
	Total				49.700107	100

Figure 57 . Curve-fitting of the hydroxyl region in PVPh/DHMS-7,9 (85/15 w/w%).

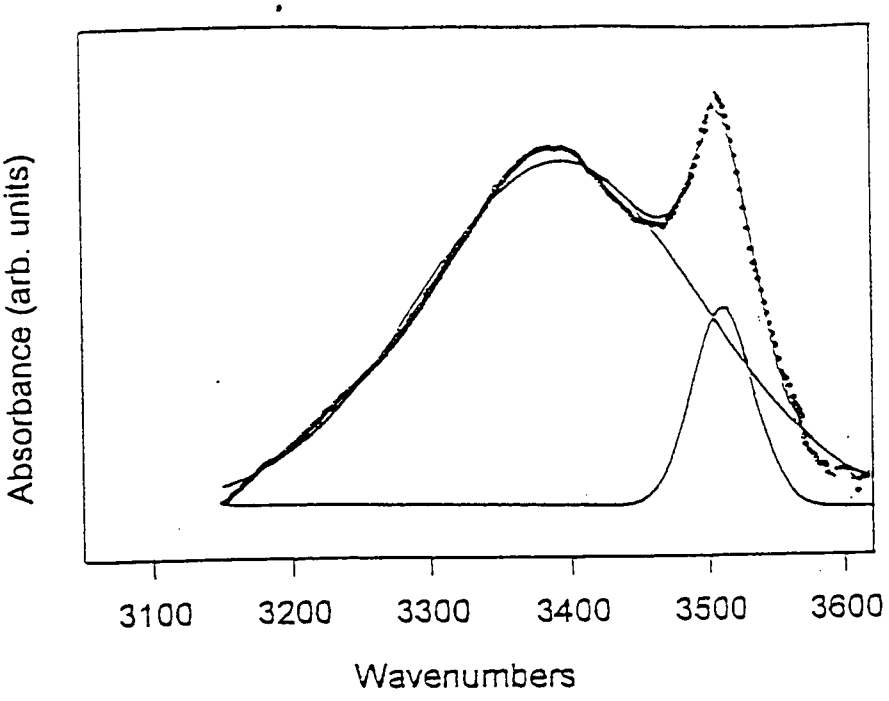

Curve-Fit Std Error= 0.0012162594 r2= 0.990808965

Curve-Fit Coefficients

Peak#	Type	Ampl	Ctr	Wid1	Wid2	Wid3
1	Gaussian	0.0554656	3391.4578	115.49934		
2	Gaussian	0.0296923	3525.8733	19.020766		

Measured Values

Peak#	Type	PkAmpl	PkCtr	Wid@HM	Area	%Area
1	Gaussian	0.0554656	3391.4578	271.97984	15.238052	91.500146
2	Gaussian	0.0296923	3525.8733	44.790179	1.4134938	8.4998539
	Total				16.651546	100

Figure 58 : Curve-fitting of the hydroxyl region in PS-*co*-PVPh (20% PVPh).

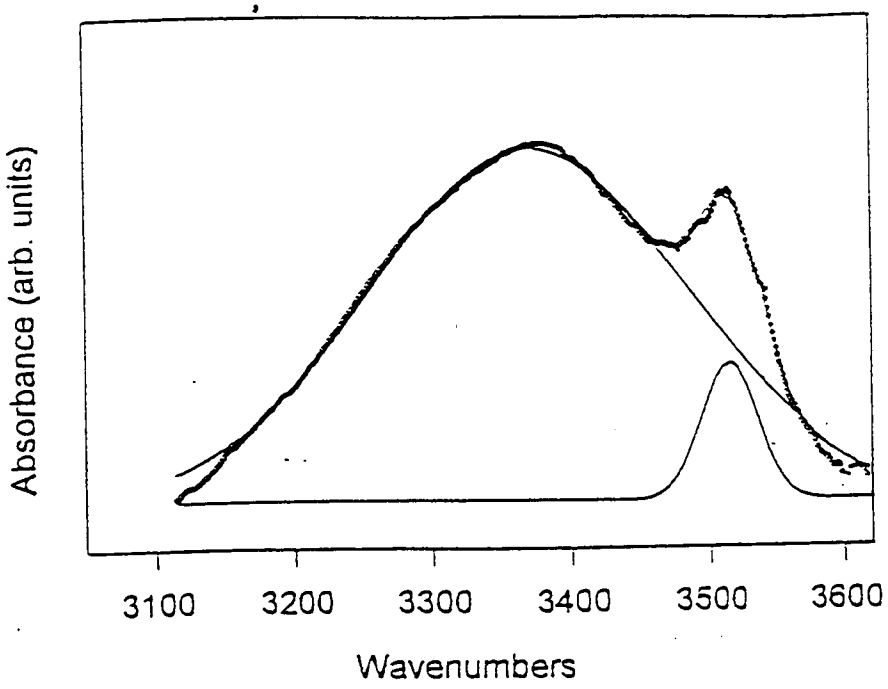

Curve-Fit Std Error= 0.00250078079 r2= 0.970885356

Curve-Fit Coefficients

Peak#	Type	Ampl	Ctr	Wid1	Wid2	Wid3
1	Gaussian	0.0187835	3347.9473	142.35345		
2	Gaussian	0.0459182	3525.0651	20.817466		

Measured Values

Peak#	Type	PkAmpl	PkCtr	Wid@HM	Area	%Area
1	Gaussian	0.0187835	3347.9473	335.21654	5.975189	71.378319
2	Gaussian	0.0459182	3525.0651	49.020989	2.395965	28.621681
	Total				8.3711541	100

Figure 59. Curve-fitting of the hydroxyl region in PS-*co*-PVPh (20% PVPh)/DHMS-7,9.

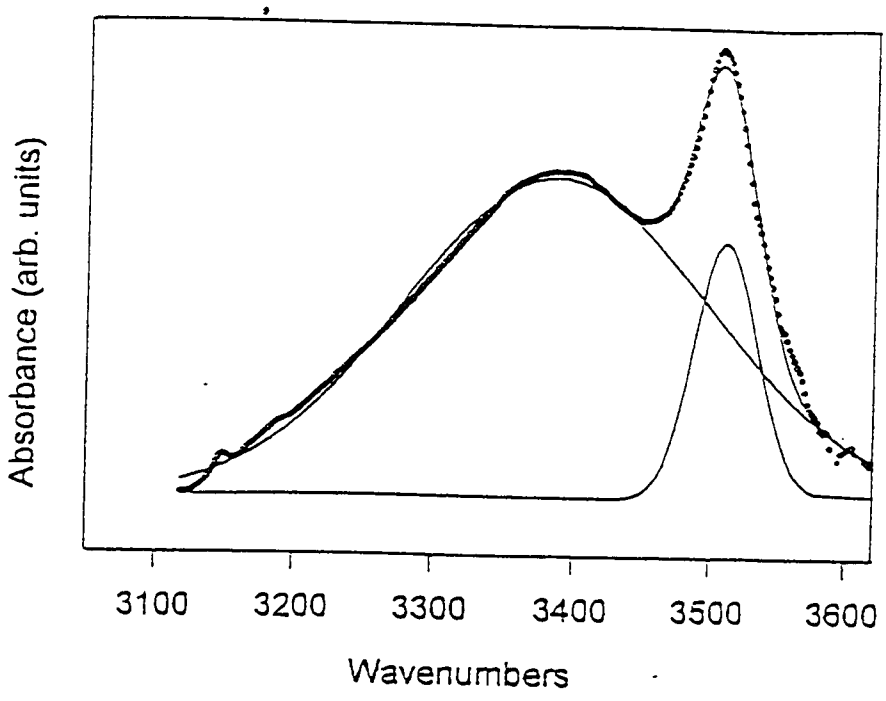

Curve-Fit Std Error= 0.000711052955 r2= 0.995298232

Curve-Fit Coefficients

Peak#	Type	Ampl	Ctr	Wid1	Wid2	Wid3
1	Gaussian	0.094385	3398.3614	119.96829		
2	Gaussian	0.0731455	3525.8308	23.225675		

Measured Values

Peak#	Type	PkAmpl	PkCtr	Wid@HM	Area	%Area
1	Gaussian	0.094385	3398.3614	282.50333	27.890152	86.754005
2	Gaussian	0.0731455	3525.8308	54.692012	4.2583949	13.245995
	Total				32.148547	100

Figure 60. Curve-fitting of the hydroxyl region in PS-*co*-PVPh (10% PVPh).

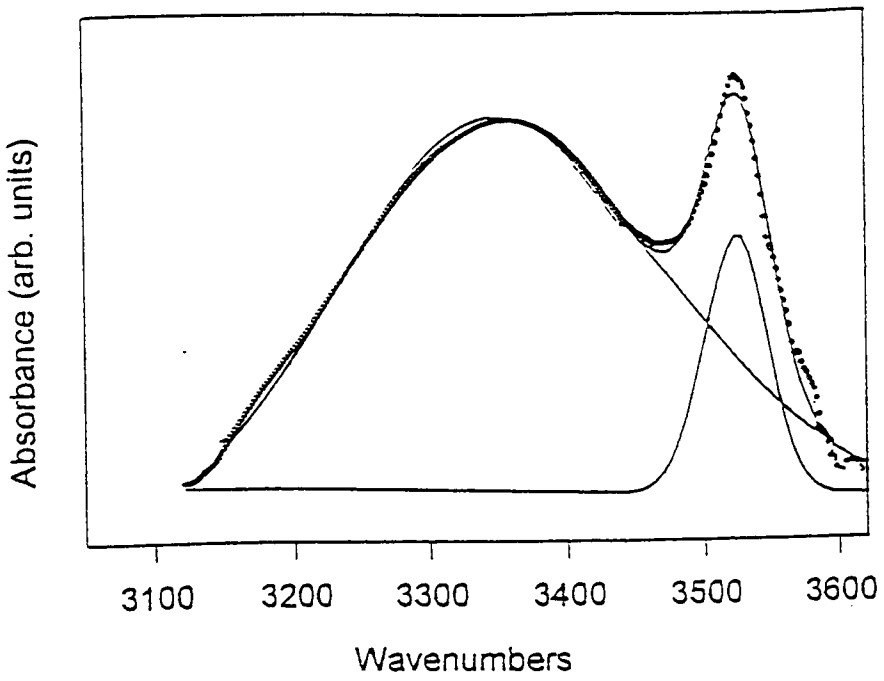

Curve-Fit Std Error= 0.00192896338 r2= 0.975965765

Curve-Fit Coefficients

Peak#	Type	Ampl	Ctr	Wid1	Wid2	Wid3
1	Gaussian	0.0923337	3319.1291	121.47915		
2	Gaussian	0.0872477	3525.0637	21.819159		

Measured Values

Peak#	Type	PkAmpl	PkCtr	Wid@HM	Area	%Area
1	Gaussian	0.0923337	3319.1291	233.58139	7.9570488	91.020295
2	Gaussian	0.0872477	3525.0637	51.379796	0.7850112	8.9797049
	Total				8.74206	100

Figure 61. Curve-fitting of the hydroxyl region in PS-*co*-PVPh (10% PVPh)/DHMS-7,9.

VITA

Bijan Radmard was born on February 26, 1966 in Tehran, Iran. He received B.S. degree in chemistry from National University of Iran in 1989. Then he came to the United states in December 1992 to complete his graduate education. He received his M.S. degree in organic chemistry from Western Kentucky University in December 1994. Then, he pursued a Ph.D. degree in polymer chemistry at the University of Tennessee in Knoxville.